

Dear editor, dear reviewers,

We sincerely thank you for your constructive comments, which will certainly help to improve the manuscript in terms of clarity and readability. We have modified the manuscript taking into account your suggested revisions. Please find below a point-by-point response to your review comments and the revised manuscript.

With kind regards,

Christian Halla on behalf of all authors

Our following author's response is structured as followed:

1 Anonymous Referee #1

Comments of Referee #1 are in blue.

The author's point-by-point response has been inserted in grey.

In case of major adjustments the changed text was inserted in black.

2 Referee #2: Masaki Hayashi

Comments of Referee #2 are in blue font

The author's point-by-point response has been inserted in grey.

In case of major adjustments the changed text was inserted in black.

3 Manuscript

All changes made in the manuscript are a marked-up **in red**.

1 Anonymous Referee #1

General comments:

Introduction: Most of the information in the introduction is relevant and important to include. However, the introduction could be significantly improved if all the information presented contributed directly towards 1) highlighting the importance of studying rock glaciers in the dry Andes or 2) discussing the knowledge gaps in the current literature that will be filled by completing the study objectives. If structured in this way, all of the information in the introduction builds towards the objectives and a strong argument is created for carrying out the study. The first two paragraphs are good. The third paragraph (climate change and impacts on the cryosphere) could be modified to highlight the importance of calculating changes in rock glacier volume over time and mention the lack of studies available. Information that does not directly build toward this end could be removed (e.g. sentence starting on L47, L54). The third paragraph could also be used to highlight the importance of understanding rock glacier hydrology and lack of studies available, or information related to hydrology could be moved to the fifth paragraph. The fourth paragraph (velocities) could highlight the knowledge gaps related to surface velocities of rock glaciers in the dry Andes since surface velocity fields are one of the results for this paper. This paragraph could be made more concise and some information removed. It is not clear from reading the fifth paragraph (hydrology) how your third objective (hydrological structure of the rock glacier) will provide a new contribution to the literature. Please modify this paragraph so that it provides the reader with a clear understanding of the importance of this objective.

I have reviewed the introduction in detail for sentence structure, grammar and to make the text more concise. Please complete the same exercise for the rest of the publication before re-submitting (a native English speaker should do this). I have suggested some changes, but have not thoroughly reviewed the document in this context. A copy of the paper is attached in which I have highlighted text that I noticed should be reviewed and likely modified while reading through the text.

Thank you very much for the suggested improvements. We carefully revised the Introduction according to your suggestions and further went over the whole manuscript to strengthen its red line and argumentation. The details of these changes are listed below.

Minor grammatical comments:

Note: If a point pertains to a particular sentence, I have referenced the line number the sentence begins on.

Thank you for the straightforward suggestions and corrections for our manuscript. A reply to each specific review comment is given below each suggestion. If only single words were changed during the revision, the revisions made are given within the specific reply. If the sentence structure or sections were rewritten, the revised text is given below the reply.

Change “contents” to “content” here and throughout the paper

“Contents” were changed to “content” throughout the paper.

L20 Suggest removing “rates” since it is the precipitation that is stored, not the precipitation rate.

“rates” was removed.

L21 Suggest explicitly stating that these results are derived from the geophysical data and modify the sentence so it is a bit more intuitive to read as follows (or something similar): "Geophysical results show heterogeneous ice and water content with ice-rich permafrost and supra-, intra- and sub-permafrost aquifers in the subsurface."

The sentence was modified to:

Geophysical results show heterogeneous ice and water content with ice-rich permafrost and supra-, intra- and sub-permafrost water pathways at the end of the thaw period.

L24 In this sentence the author is trying to stress the importance of the water reserve stored in Dos Lenguas rock glacier. However, the statement is not very strong because a volume estimate is compared to a % area covered so it is not possible to evaluate the importance of the reservoir with the information in the sentence. Is there data available to report an approximate value for the ice volume (.e.g in kg) in the mountain catchment?

We are aware that the argument is not very strong and cannot be since the ground ice content of permafrost remains unknown in the whole basin. There are values for the ice volumes potentially contained in the rock glaciers and the Aqua Negra glaciers. The values are based on assumed ice content and thicknesses of the landforms and therefore speculative (see table in Schrott (1996). However, there is no data for the 90 % of the catchment area, which is likely underlain by permafrost. But since it has not been investigated and the amount of ground ice in the catchment remains unknown, we stay with the reserved argument.

L27 Suggest removal of "that are". It is unnecessary.

"that are" was removed in L27

L33 Suggest removing "Besides storing large amounts of sediment" since this takes up space and does not add to the discussion here.

"Besides storing large amounts of sediment" was removed in L33

L37 This sentence seems out of place and disrupts the flow of the introduction. It would make more sense to incorporate this into the final two paragraphs of the introduction or delete it. If it is retained, I would suggest rewriting the latter part of the sentence as "whose material source is derived from periglacial talus slopes." The term slope already implies that the material is coming from a valley slope, so there is no need to specify this.

The above and the following sentence were inserted because the editor had asked for a discussion of the genesis of rock glaciers at the beginning of the introduction. In this context, it is important to mention the source of rock glaciers. The sentence was shortened as suggested:

In this study we investigate the water storage capacities of a tongue-shaped rock glacier, whose material source is derived from periglacial talus slopes.

L41 It is not clear what the author means by "higher" and it does not seem necessary to include this. I would suggest rewriting the latter part of the sentence as follows ".predicted to increase at a faster rate compared to lowland areas."

The sentence has been rewritten accordingly:

Under a changing climate, temperatures in the semi-arid to arid Andes are predicted to increase at a faster rate compared to their lowlands (Bradley et al., 2006).

L42. Concomitant is not a commonly used word. I would suggest changing it to a synonym such as “associated.”

The synonyms have been exchanged accordingly:

Associated changes in the mountain cryosphere, [...]

L46 Change “discharges” to “discharge”.

In L46 “discharges” was corrected to “discharge”.

L59 Change “sings” to “signs”

In L59 “sings” was corrected to “signs”.

L59 Change “manifested in” to “manifested as”

In L59 “manifested in” was corrected to “manifested as”.

L60 Change “showed” to “shows”

In L60 “showed” was corrected to “shows”.

L63 Change “indicating increased” to “which increase”

In L63 “indicating increased” was changed to “which increase”.

L64 Suggest changing this sentence to “Thus, rock glacier movement is impacted by hydrology and ground temperatures.”

The sentence has been changed accordingly:

Thus, rock glacier movement is impacted by hydrology and ground temperatures (Kenner et al., 2019).

L65 I think this sentence would read better if it was divided into two and written in a more concise way. For example “Interannual vertical variations of the surface topography are mostly related to the mass balance of rock glaciers (Kääb et al., 1998; Konrad et al., 1999). Annual mass balance and discharge are significantly lower for rock glaciers compared to glaciers (Krainer and Mostler, 2002).”

The sentence has been divided into two like suggested:

Interannual vertical variations of the surface topography are mostly related to the mass balance of rock glaciers (Kääb et al., 1998; Konrad et al., 1999). Annual mass balance and discharge are significantly lower for rock glaciers compared to glaciers (Kääb et al., 1997; Krainer and Mostler, 2002)

L72 Suggest removing “on the temporal scale” as it is unnecessary.

The sentence was revised.

Ice-rich permafrost functions as long-term water storage while the active layer functions as seasonal reservoir (Jones et al., 2018b).

L76 Suggest removing “add significant amounts of” to make the sentence more concise.

In L76 “add significant amounts of” was removed

L77 This sentence does not make sense and should be reworded. I would suggest “Active layer and permafrost (e.g.rock glaciers) regulate shallow ground water drainage and throughputs functioning as an aquifer, aquitard, and/or aquiclude (Jones et al., 2019).”

The sentence has been reworded. Due to the revision of the term aquifer throughout the manuscript (suggested by reviewer 2) the terminology used in the sentence has been additionally changed to:

Shallow groundwater drainage in rock glaciers is regulated by unfrozen and frozen conditions with supra-, sub- and intra- permafrost flow (Jones et al., 2019).

L80 Here it is not clear what depends on the water input and different hydraulic properties. Do you mean to say the buffering capacity depends on water input and different hydraulic properties? Please specify.

That is right. It was meant to say that both, water input and different hydraulic properties, regulate the buffering capacity. For instance, high and fast input during summer storm and groundwater channel would have a low buffering capacity compared to snowmelt percolating slowly into frozen ground. The sentence has been reformulated:

The water input and different hydraulic properties of hydrological flowpaths of frozen and unfrozen ground delay and buffer the water release of rock glaciers (Harrington et al., 2018; Jones et al., 2019; Rogger et al., 2017) which impacts the runoff generation in mountain catchments (Geiger et al., 2014; Krainer and Mostler, 2002).

L84 Please add "have" to the sentence. ": :studies have investigated"

In L84, "have" has been added to the sentence.

L87-103. These two paragraphs describe the objectives of the study and place these objectives in the context of previous studies in the area and knowledge gaps. The information presented is good, but there is repetition of information in the two paragraphs so I would like to suggest merging these two paragraphs, removing any repetitive information, and making the text more concise.

The repetitions were removed. The paragraphs were merged.

The hydrologic importance of water storage capacities in rock glaciers compared to glaciers (Croce and Milana, 2002; Milana and Maturano, 1999) as well as river discharge (Schrott, 1996) and chemistry during summer months due to the melt of frozen ground (Lecomte et al., 2008) has been previously investigated in the Upper Agua Negra catchment in the dry Andes of Argentina. The present study of the talus rock glacier 'Dos Lenguas' builds upon this earlier research and presents results of high-resolution surface detections and extensive hydro-geophysical subsurface measurements in the data-scarce region of the dry Andes. In spite of speculations on their hydrological significance (Azocar and Brenning, 2010; Corte, 1976; Jones et al., 2018a), almost no quantitative and measurement-based estimates about water storage capacities of Andean rock glaciers and their changes over different time-scales exist. With the present study, we try to fill this gap and aim to: (1) quantify long-term ice storage capacities and water content at the end of the thaw period by estimating the current material composition, (2) analyse surface deformations and gain quantitative estimates of interannual storage changes and (3) infer the internal hydrologic structure from the spatial distribution of ice and water content in different geomorphological areas of the active rock glacier.

L92 Please change "an" to "a"

In L92, "an" has been changed to "a".

L102 Change "contents" to "content".

"Contents" were changed to "content" throughout the paper.

L109 Suggest removing "few" and "different" as these are unnecessary.

"Few" and "different" have been removed.

L12 Suggest changing to “...discontinuous permafrost extends to ~4000 m a.s.l. potentially covering large areas within the basin and includes active rock glaciers...”

The sentence has been changed accordingly.

The lower limit of discontinuous permafrost extends to ~4000 m a.s.l. potentially covering large areas in the basin, including active rock glaciers (0.88 km²) (Schrott, 1994; Tapia-Baldis and Trombotto-Liaudat, 2020).

L125 Please indicate the subject matter of these previous studies briefly

Previous studies at Dos Lenguas have investigated hydrological-geomorphological aspects such as the active layer and the discharge and its geochemical influence on the Upper Aqua Negra stream. In order to avoid repetition the geochemical matter of Dos Lenguas was added to the sentence in L120 and the sentence in L125 has been revised.

Hydrochemical analysis of melt water indicates significant internal recycling by sublimation and evaporation and delayed meltwater throughputs from Dos Lenguas and other rock glaciers in the Upper Aqua Negra basin (Lecomte et al., 2008).

Previous studies at Dos Lenguas have investigated hydrological-geomorphological aspects such as the active layer and the discharge of 5-8 l s⁻¹ during the thaw period (Schrott, 1994; Schrott, 1996).

L188 In order to obtain a volume estimate it would have been necessary to multiply each raster value by the cell size, then sum all the raster pixels overlapping the rock glacier. Please specify this here so that it is clear.

Thanks for the comment. The section has been reworded and we added the information on the subdivision of the surface area of the rock glacier to be clearer on the spatial relation of the volume estimates. The different volume estimates were specified to be clearer on the differences between pixel wise volumetric changes, total volumetric changes, and net changes of the ice mass of the respective geomorphological units, i.e. their surface areas.

The vertical changes of the rock glacier surface area over the periods 2016–17 and 2017–18 were estimated by subtracting surface elevations of the 2016 DEM from the 2017 DEM and the 2017 DEM from the 2018 DEM, respectively. Then, the pixel wise volumetric change was derived by multiplying the vertical changes of each raster cell by cell size. The total positive and total negative volumetric changes (bar graphs in Fig. 4) for the different geomorphological units of Dos Lenguas (fig. 1b) were summed up to derive negative and positive volumetric changes of the respective surface areas. The total volumetric net changes of the geomorphological units are the sum of positive and negative volumetric changes in the respective surface areas. The density of ice (900 kg m⁻³) was used to estimate the corresponding net change of ground ice, which is given as water equivalent (1 mm yr⁻¹ represents 1 kg m⁻² yr⁻¹ or 1 l m⁻² yr⁻¹) for each geomorphological area except for the side and front slopes.

Therefore, it was assumed that the net changes in ground ice are mainly caused by volume expansion due to freezing of water and volume reduction due to melting of ground ice or thawing of ice-supersaturated permafrost. The net change in absolute ice content per year was interpreted as a first order estimate of the interannual water storage change. The assumption implies that spatial variations of the flow regime, bulk density changes of debris, and edge effects of surface areas of the rock glacier are included in total volumetric net changes, but potentially of minor importance for the considered time scale.

L189-191 This sentence could be improved and made more concise. For example “ First order estimates of interannual water storage changes are derived, assuming the volumetric changes are mainly caused by melting or gaining of ground ice at the active layer / ice-rich permafrost boundary.” Note that “changes that do not equal zero” is implied and does not need to be explicitly stated.

Has been changed also with regard to the comments L354 and L355, that the gains and losses of ice causing volumetric changes could not only occur at the active layer / ice-rich permafrost boundary, but everywhere where ground ice and ice-rich permafrost increases or decreases its mass.

Therefore, it was assumed that the net changes in ground ice are mainly caused by volume expansion due to freezing of water and volume reduction due to melting of ground ice or thawing of ice-supersaturated permafrost. The net change in ground ice content per year was interpreted as a first order estimate of the interannual water storage change.

L201 How was the standard deviation of the error of each DEM calculated? Did you use the 34 GCPs to calculate the standard deviation? Please specify here.

Indeed, we used average reprojection errors of the 34 GCPs to calculate the Limit of Detection in our analysis. We hope that our alteration of the sentences following Eq. 1 clarifies the error calculation:

“[...] where t is the critical value of a given confidence interval in a two-sided student's t-distribution and σ is the error associated with the DEM, calculated from the average reprojection error of 34 ground control points for epochs i and $i+1$.”

L203 Here it makes sense to say that you have masked out values less than the LoD (< LoD). However, I am not sure what masking out values > -LoD refers to. Could you be more explicit here?

Thanks for the comment and spotting the error (> -LoD). Masking out values (> \pm LoD) was referred to the terminology used in the context of mapping positive and negative volumetric changes based on DEMs of Difference (DoDs). We have corrected the sentence, since the editor had already suggested to remove the terminology related to DoDs, and as the LoDs increase with the higher confidence intervals and t-values.

Raster values less than the LoD were later excluded from the calculation of the total positive and total negative volumetric changes of the respective surface areas (Fig. 4, Table 5).

L207 It is not clear what these references refer to. Do you mean to say that you used the methodology of Hauck and Kneisel (2008) and Kneisel (2008)? If so, you could write (following Hauck and Kneisel, 2008: : :).

It was meant to refer to the general imaging of internal structures with ERT and SRT. We have removed the references, as the sentence refers directly to Dos Lenguas.

2-D Electrical resistivity tomography (ERT) and seismic refraction tomography (SRT) were conducted along identical long- and cross-profiles on the Dos Lenguas rock glacier (Fig. 1b) to image the internal structure and to quantify its material composition based on a petrophysical model, the so-called Four-Phase Model (4PM, see below) (Hauck et al., 2011).

L208-210 I think that this comment would fit better in the discussion section when you compare your results to other studies. Here, it distracts the flow of the methodology section and would be more useful in the discussion.

The comment has been removed.

L216 Please indicate somewhere in the methods how the y-axis depth scale was obtained for both the ERT and SRT.

The y-axis of ERT and SRT has been changed from depth to altitudes, like in Fig. 8. The surface topography was included for both inversions.

The penetration depth of the ERT depends on the layout geometry (length and spacing) and the array (electrode configurations). Generally, when the relative separation of current electrodes (A, B) and potential electrodes (M, N) is increased, the penetration depth of the configuration becomes deeper. Details of the multi-electrode gradient array are given by Dahlin and Zhou (2006) where penetration depths, geometry factors and relative signal to noise ratios are compared for Wenner, Gradient and Dipol-dipol arrays. Based on these considerations, the inversion model geometry is determined within the inversion software and inverted specific resistivities are calculated on this model grid. We have revised the ERT section and included the spacing, the layout length and maximum penetrations depth of each profile. We also added, how the topography was integrated.

Profile lengths of 240m (L1), 320m (C1), and 400m (C2 and C2) were achieved with an electrode spacing of 3m, 4m, and 5m, respectively. All profiles were measured with the multiple gradient array, which reached maximum penetration depths of 41m for L1, 60 m for C1 and 68 m for C2 and L2.

The surface topography was integrated based on dGNSS measurements of each electrode along the profiles and the topographic shift of the subsurface nodes of the inversion models were exponentially damped with depth (Loke, 2018).

The y-axis depth scale of the SRT depends on the p-wave velocities of the subsurface layers velocities and the maximum penetration depth of the seismic P-waves for all shot points. In the inversion model, it is inversely estimated from the traveltimes at each geophone location by the so-called ray-tracing method. The topography of the profile and each geophone was hereby included in the start model of the inversion and the traveltimes analysis.

L217 Perhaps change “while” to “then”. I am assuming that the injection of current and measurement of potential difference does not occur exactly at the same time. The injection is first, then the measurement.

Resistivity surveys are carried out by injecting current and simultaneously measuring the potential differences between the potential electrodes, as the voltage differences are a result of the current injections. Of course there is a very short time lag until the potential difference is build up, but we didn't measure the decay of the potential differences after the current injection stopped, which is done for induced polarization surveys. So, “while” was not changed to “then”.

L223-225 Please indicate the spacing between electrodes. This is indirectly mentioned in the seismic section, but it would be good to explicitly mention it here.

The spacing was added.

Profile lengths of 240m (L1), 320m (C1), and 400m (C2 and C2) were achieved with an electrode spacing of 3m, 4m, and 5m, respectively. All profiles were measured with the multiple gradient array, which reached maximum penetration depths of 41m for L1, 60 m for C1 and 68 m for C2 and L2.

L231 Please indicate the maximum depth range obtained after the inversion process (e.g. 20-30 m). Also, were the ERT data topographically corrected? If not please justify why this was not done in response to this comment. If yes, please specify how the GPS data were collected (type of GPS). This comment also applies to the seismic refraction section.

We have included the maximum depth range of the inversion process in the method section. See also reply to L223-225. Fig. 5 and 6 show clearly that the ERT and SRT were topographically corrected. The topography of each profile was measured with the D-GPS in the base and rover configuration, (same configuration as for the ground control points). The surface elevations of each electrode (and geophone) position were measured and used for the topographic modelling

of ERT and SRT. The vertical uncertainties of all elevations coordinates range between 0.005 and 0.027 m and were considered as negligible compared to resolution capacity and maximum penetration depth of the tomographies. The travel times of the p-waves were corrected for the surface topography of the profiles and the same surface topography was used for the inversion start model. Accordingly, the surface topography was included in the inversions for both ERT (see reply to L216) and SRT data.

L227 Change “have been” to “were”

In L227, “have been” has been changed to “were”.

L237/238 was marked

The sentence structure has been reworded.

Significantly different elastic properties between the frozen and the unfrozen state of the subsurface can be measured using its P-wave velocities.

L255 Consider changing “according to” to “in alignment with”

In L255, “according to” has been changed to “in alignment with”

L282 How is the rock fraction (f_r) determined? Please specify.

The rock fraction equals one minus the porosity. This definition is given in the first section of 3.3.3.

L285 was marked

The sentence has been rewritten

The equations 5–7 allow to calculate the fractions f_w , f_i , and f_a based on the input data ρ and v from ERT and SRT, respectively if the other material properties (ϕ , ρ_w , m , n , v_w , v_r , v_i , and v_a , cf. Table 4) are prescribed.

L338 Please be more explicit here and define what is meant by “paired positive and negative annual volumetric changes.” Are the pairs made up of a furrow and a ridge?

Yes the paired positive and negative annual volumetric changes should refer to the furrow and ridge structure. The sentence has been reworded to be more explicit. The following sentence takes up the explanation in the rewritten sentence.

The spatial pattern of interannual positive volumetric changes along the front of the transverse ridges and negative volumetric changes on the back of the transverse ridges indicate the advance of the surface of the rock glacier (Fig. 4). The highest amounts of these paired positive and negative volumetric changes [...]

L340 change “in” to “to”

In L340, “in” has been changed to “to”

L344-348 has been marked

The sentences were reworded.

Positive volume changes of the upper front slopes reflect the advancement and oversteepening above the shear layer, which is also visible on the aerial images (cf. Figs. 2a, 3, 4). Negative volumetric changes delineate superimposed linear erosion features at the upper frontal slopes. Positive volumetric changes below the shear layer show downslope transported and accumulated debris at the front slopes.

L354 How do you know that the changes in the water storage occurred in the active layer? I would assume that you could have changes below the active layer and this would still be expressed as a change in elevation at the surface. Consider modifying this sentence.

Please see reply to L355

L355 In this sentence are you saying that a change in the active layer depth, without a change in water storage, could result in a change in volume? That seems to be what is implied. Please clarify and explain why this would result in a change in volume.

Thanks for the two comments. The active layer has been removed from the sentence (L354) referring to the estimated water storage changes.

The sentence L355 has been moved to the last section in order to avoid interpretations and repetitions in the middle of the result chapter. Volume expansion of water during freezing and volume losses due to the melt of ice would result in a change of volume. This assumption was also added to the method section.

If the amounts of interannual storage changes are considered as mean depth variations of an ice-rich permafrost table, they would mean the growth or melting of ground ice at the top of frozen core by several centimetres per year. Observed wet active layer conditions above ice-rich permafrost during the summer thaw in our study and other studies (Arenson et al., 2010; Croce and Milana, 2002; Kenner et al., 2019) add to the interpretation that active layer and ice-rich permafrost tables are potential sinks and sources of interannual storage changes. Yet, the interannual growth and decay of ground ice in and around other parts of the frozen core could add to the interannual storage changes of the rock glacier.

L358 Suggest changing “regarding the” to “with a.” L365 Change “was” to “were”

Both suggestions have been changed

L369-374 Please modify these sentences to make the more concise and avoid repetition of information.

Thank you for the suggestion. The repetitions have been excluded to make the sentences more concise.

Thus, detected volumetric changes for 2017–18 can be regarded as more reliable due to their higher accuracy. The lower accuracy for the period 2016–17 might be related to bulging effects causing spatial errors (Mosbrucker et al., 2017) in the central part of the 2016 DEM due to technical difficulties during dGNSS measurements of central ground control points. However, the 95% and 99% confidence intervals yielded still comparable magnitudes of volumetric changes for both periods and give rather conservative estimates.

L376 was marked

The sentence starting in L376 has been changed

If the amounts of interannual storage changes are considered as mean depth variations of an ice-rich permafrost table, they would mean the growth or melting of ground ice at the top of the frozen core by several centimetres per year.

L382 I think this final sentence is more appropriate for the discussion section, than the results section.

The sentence has been moved to the discussion. The manuscript changes are given below at comment L498.

L394 Suggestion to change “to be invoked by variable active layer and permafrost conditions” to “as follows”

In L394, “to be invoked by variable active layer and permafrost conditions” has been changed to “as follows”.

L397 The sentence starting on this line is useful information to include, but disrupts the flow in this paragraph and is a very general statement related to the interpretation of resistivity values in permafrost. Consider moving this to the methodology section or removing it. Also, it would be good to simplify this sentence. For example, “Resistivity values are impacted by substrate characteristics (lithology: : :.”

The sentence has been removed

L399 Suggestion to make this sentence more concise. For example “Thus, we interpret the active layer to be mainly characterized by very dry : : :”

The sentence has been changed accordingly

L403 Consider modifying to “Horizontal and vertical contrasts and anomalies of resistivity permitted a clear delineation of the permafrost body within the rock glacier.”

The sentence has been changed accordingly.

L404 This sentence repeats a lot of information already mentioned in the sentence that starts on L399. Please combine it with the sentence on

First we give a general interpretation of the observed resistivity distribution and how the specific resistivities values could be related to material composition. Then we describe the spatial pattern of the observed resistivities distribution in relation to topography, which is an essential observation of the internal structure. The repetition of resistivity values has been removed from description of the spatial pattern. Instead we referred to figure 5 to make clear that the text relates to the interpreted structure given in figure 5.

Lower electrical resistivities below depressions and furrows could indicate higher water and/or lower ice content in the rock glacier due to percolating water and/or local permafrost degradation between interpreted ice-rich permafrost (Fig. 5).

L409 From the photographs it looks like there may be a fair amount of finer sediment (e.g. sand sized). If this is true do you think that air voids in the subsurface would be filled by these sediments? Perhaps your field observations could help the interpretation here.

That is right. The dominant fine sediments are sand sized. Of course large voids could be filled with fine sediment. This can be assumed for crevasses and thermal erosions features at the surface and in unfrozen sediments. In the frozen subsurface, it is very speculative and I would guess if voids can be filled by finer sediments, depends on the grains size, size of voids, pore connectivity, ice content, and compaction (stiffness) of the surrounding sediments. But I wouldn't expect much refill between voids of ice cemented sediments. If water percolates until it refreezes it could transport fines into voids, but then the mass transfer of water into the voids should be higher than sediment refill. Observations from drill cores have shown that various material composition of ice, water, air (voids) and different grain sizes of sediments can be present in vertical column of a rock glacier.

L419 After reading this paragraph it seems that there are three layers: 1) < 1500 (sandy material), 2) 1500-2000 (transition area from unfrozen to permafrost), and 3) > 2000 (permafrost). I think the paragraph would be easier to follow, would flow better, and would be more concise if rewritten as follows (or something similar) starting at L419

“The upper low velocity layer (<1500 m s⁻¹) was interpreted to represent unfrozen areas, followed by a transition area (1500-2000 m s⁻¹; corresponding isolines shown on Fig. 6), then the highest velocity area (> 2000 m s⁻¹) interpreted as permafrost. The transition layer between unfrozen debris and permafrost observed on previous seismic surveys of rock glaciers in the study area during summer (Croce and Milana, 2002; Schrott, 1994), could either indicate the presence of unfrozen water (vw = 1500 m s⁻¹) above permafrost and/or be related to the vertical resolution of the smoothly inverted p-wave velocities.” Could be interpreted as wet active layer above permafrost, low per

Since there is no sharp velocity contrast between active layer and permafrost, the boundary between the two layers cannot be clearly observed. Therefore we added the isolines that could indicate the transition area between unfrozen and frozen conditions. Due to the depth we assumed that the boundary is in the range of 1500 m/s during summer. Since the velocity of permafrost in rock glaciers can vary greatly and wet sands can have the same velocity, the transition range could also indicate other conditions between the 1500 and 2000 m/s isolines. A pure transition layer cannot be deduced from this ambiguous velocity range. The vertical smoothing of the inversion adds to the inconclusive velocity range. So, the paragraph and the interpretations have not been rewritten as proposed.

L420 Do velocities of 1500-2000 definitively indicate permafrost? If another interpretation is possible, consider changing “indicates” to “is interpreted as”

“Indicating” and “interpreted as” has been changed.

The upper low velocity layer (<1500 m s⁻¹) indicates unfrozen areas, while the intermediate to high velocity layer (1500–4500 m s⁻¹) is interpreted as permafrost.

L429 Please remove “and” directly before “volcanic rocks” as it is unnecessary.

The “and” has been removed.

L433 Upon comparing the ERT and SRT most of the anomalies (ice-rich areas) roughly correspond, except on L1 at 50 and 210 m where there are large areas that are highly resistive. These two areas are not apparent on the SRT figure. It would be good to address this difference in the text somewhere.

General differences in the interpreted structures of ERT and SRT have been added to the paragraph.

Due to the ambiguities of velocity patterns and resistivity distributions, the spatial delineations differ in some areas of the independently interpreted structures in the SRT and ERT profiles (cf. spatial variations of ice-rich permafrost and active layer in Figs. 5 and 6).

L434 Please remove “yet” as it is unnecessary.

In L434, “yet” has been removed

L445 add “porosity” after 70% e.g. “:50%, and 70% porosity, respectively.”

In L445, porosity was added to the sentence

L496 Suggest removing “however.” Including “however” implies that your results are not that useful and undervalues your work. I think the results are very useful and would therefore suggest removing “however.”

In L496, “however” has been removed.

L498 This sentence is redundant as much of the information is provided at the end of the next paragraph. It also makes it sound like your results are very uncertain which contradicts the strong statement in the second paragraph that balances derived from volumetric surface changes reliably estimate interannual storage changes. I would suggest removing the sentence starting on L498 or incorporating the info here into the final sentence in the last paragraph.

Thanks for spotting the redundancy. The sentence has been removed and the references (Kääb et al 1997, 1998) that are related to the uncertainty of the approach have been added to the final section of the paragraph. In addition, a sentence from the results has been moved here (as suggested in the comment L382)

We are therefore confident, that volumetric surface changes reliably estimate interannual water storage changes dominantly associated with ice gains and losses, though these might well incorporate minor contributions from three-dimensional creep deformations and/or changes in bulk densities of the rock glacier material (Kääb et al., 1998; Kääb et al., 1997). The derived net changes in ground ice of -36 mm yr^{-1} and 28 mm yr^{-1} of the 95% confidence interval for the two observed hydrological years resulted in rather conservative estimates if compared to observed mean annual active layer thickening of $>150 \text{ mm yr}^{-1}$ at the Morenas Coloradas rock glacier complex in the Central Andes of Mendoza between 1992 and 2007 (Trombotto and Borzotta, 2009).

L520 Change “reasonable” to “reasonably” L534 Please change “have lower confidences” to “are of lower confidence”

Both suggestions have been changed.

L536 Please add “the” so the sentence reads “..in the deepest model areas.”

In L536, “the” has been added

L538 rewrite sentence as “: : 7.4% with only 7.7% filtered:”

The sentence was rewritten accordingly.

L547 rewrite sentence as “: : in turn ice content might”. Also consider providing a very brief explanation for the underestimation in ice content.

The sentence was rewritten accordingly. The very short explanation is already included in the sentence and the previous one, since the underestimation of the ice content is related to the overestimation of the water content (sum of all parts must equal one in the 4PM).

L567 change “contents” to “content”

As mentioned above “contents” has been changed to “content” throughout the paper.

L653 Are the depths (e.g. 20-25 m) the distance from the surface to the shear horizon, or the thickness of the stiff basal layer? Please specify.

The depths refer to the distance from the surface. The sentence was changed.

From digital topography we further delineate the approximate depth of the shear horizon below the surface (Figs. 2, 9).

L692 Here, do you mean to say that the total discharge at the spring is equal to 14-30% of the Dos Lenguas liquid water content in late summer? Please modify the sentence to be more explicit.

Please see our response to L692 below.

L693 Does the “total liquid water content” refer to the liquid water content calculated for the Dos Lenguas rock glacier? I would assume so, but it would be good to specify this in the text.

The whole section, including the sentences of L692 and L693 have been rewritten and specified in order to extend the discussion about the water balance, correct a calculation error and include the uncertainty ranges of the mean water content, which was also requested by the other referee M. Hayashi.

About 11-42 % of the mean water content of the rock glacier could become discharge at the rock glacier spring, since the estimated mean water content ($mean f_w$ corresponds to $244-570 \times 10^6$ l) was greater than the potential discharge at the spring during the thaw period. The remaining share of water content (58–89%) could leave the internal hydrological system of the rock glacier along other water pathways and could be involved in refilling or exchanging groundwater storages in and below the rock glacier.

L716 suggestion to summarize your results in this section. The conclusions are a qualitative discussion at present, and I think the section would be much stronger if you summarized your main results quantitatively and main points from the discussion briefly.

We have added a few quantitative estimates to the conclusion.

Based on this data set we found that increased water content in depressions and furrows, and ice-rich permafrost below ridges indicate interactions of the distinct ridge and furrow topography and the heterogeneous material composition structures the internal hydrology of Dos Lenguas rock glacier. Water pathways and traps are hereby located above, between and below the frozen core of the rock glacier during the thaw period. Horizontal surface deformations up to 2 m yr⁻¹ prove the active status of the rock glacier. Gains and losses of ground ice derived from volumetric surface changes for 2016–17 and 2017–18 give first order estimates of interannual water storage changes. Our findings suggest that water storage capacities and interannual storage changes can be estimated despite the uncertainties arising from the spatial heterogeneities and indirect measurements. We conclude that the ground ice content of $1.71(\pm 42\%) - 2(\pm 44\%) \times 10^9$ kg and the interannual water storage changes of -36 mm yr⁻¹ (-8.92×10^6 kg) and 28 mm yr⁻¹ (6.64×10^6 kg) of the active rock glacier Dos Lenguas represent an important long-term water reservoir and seasonal water buffer in the Upper Agua Negra valley. 25-80% and 17-55% of annual precipitation may have been released and buffered by interannual water storage changes during the summer period 2016-17 and 2017-18, respectively. The water content of $0.36(\pm 32\%) - 0.43(\pm 32\%) \times 10^9$ kg of the rock glacier at the end of the thaw period corresponds to about one fifth of the ground ice content, 2-4% of the interannual water storage changes and 11-42% of the potential discharge at the spring. The major share of the water content may leave the internal hydrological system of the rock glacier via other groundwater paths. The estimated ice and water content and interannual water storage changes of the active rock glacier show exemplarily that rock glaciers and mountain permafrost can strongly influence the hydrology in sparsely glaciated and dry mountain catchments.

Fig. 4 The units for vertical change are in “m yr1”, but likely should be changed to “m yr-1”.

The superscript minus sign is present, but hardly visible.

Fig. 4 In general the figure is easy to understand and nicely displays the data. However, it is not clear if the bar graphs refer to data at one point location or a ridge and furrow set. I am assuming a ridge and furrow set as explained in the text, in which case it would be good to add a line or box on the glacier image to identify the data source (e.g. ridge and furrow pair).

Thank you again for pointing out that the reference of the bar graphs has to be specified. The single bars refer to the sum of positive and the sum of negative changes observed in the respective geomorphological unit. The caption has been revised to make the spatial reference of the bar graphs clearer.

Fig. 4: Vertical changes of Dos Lenguas from 03/2017 to 03/2018. The bar graphs show the total positive volumetric (bluish bars) and the total negative volumetric changes (reddish bars) for each

geomorphological area (Fig. 1b) as a function of the confidence intervals for the periods 2016-17 and 2017-18. Starting at the twelve o'clock position and following the clockwise direction, the five bar graphs contain the total volumetric changes of the root zone, the central area, the southern tongues, the front and side slopes, and the northern tongue. The corresponding total net changes of ice are given in table 6 as water equivalents.

Fig. 7 It would be helpful to briefly describe the legend at the top of the figure in the caption.

A brief description of the legend has been added to the caption. The description of the figures has been extended.

Fig. 1: Estimated mean vertical ice content ($f_{i\ vrt}$) and mean vertical water content ($f_{w\ vrt}$) along profiles C1, C2, L1 and L2 for all 4PM scenarios. The volumetric ice (upper panel) and volumetric water content (lower panel) of the 4PM model cells along the profiles were arithmetically averaged over the 4PM depth (vertical dimension) to compare the results of the various scenarios to each other. The porosity scenarios are color-coded and combined with different line types representing the pore water resistivities used. The mixed porosity (grey) and 70% porosity scenarios (blue) with pore water resistivities of 30 Ω m and 50 Ω m were evaluated as most reasonable for the active rock glacier, since the range of mean vertical ice content indicates ice-supersaturated conditions ($f_{i\ vrt} > 40\%$) and the mean vertical water content is mainly lesser than 10%. The estimated ranges of the mean f_i and mean f_w of the plausible scenarios with uncertainties are given in table 7 for each profile and for the extrapolated absolute ice and water content of the geomorphological units.

Table 1 Change "of" to "for" in the caption.

Of has been changed to for.

Table 2 Please modify the caption to describe what is contained in the table in more detail.

The caption has been modified accordingly. Table 2 has become Table 3, since we added another table.

Table 1: Details of the ERT surveys. The columns to the left of the acquisition date contain details of the layout geometry of each profile (see Fig. 1b for position of the profiles). The columns to the right of the acquisition date contain filtered data points and the quality of the inversion.

Table 4 The text at the very bottom of this table is very hard to read. Please increase the font size.

The font size has been increased.

Table 5 Remove "]" for 2016-2017 period header

"]" has been removed.

2 Referee #2: Masaki Hayashi

GENERAL COMMENTS

The manuscript presents an extensive investigation of an active rock glacier using innovative techniques in an attempt to delineate the internal structure and quantify the distribution and amount of ice and liquid water. This is an ambitious and impressive study. The high-quality data set produced in the study contributes significantly to advancing the scientific understanding of rock glaciers and their hydrological functions. The manuscript is well organized and written, and the quality of figures is superb. Photogrammetric survey data and geophysical data are analyzed with sufficient rigor, and the results are interesting and significant. However, considering that the main objective of this work is focussed on water storage, hydrological data interpretation could be strengthened by: (1) critically examining the assumptions used in calculations, (2) scrutinizing water balance calculations, and (3) including hydrologically relevant information such as the differences in air temperature and precipitation between 2016-2017 and 2017-2018. Please see below for specific suggestions.

First we would like to thank M. Hayashi for his constructive and specific comments to improve our manuscript. Our responses to the specific comments are inserted below.

SPECIFIC COMMENTS

Line 22. Please spell 'groundwater' in one word, following the standard practice in the contemporary literature.

The spelling of 'groundwater' has been revised throughout the manuscript.

Line 51. Please spell out RCP8.5 and briefly indicate what it represents.

RCP8.5 has been spelled out to indicate what it represents.

In the decades to come, the 0°C isotherm of the mean annual air temperature is predicted to rise more than 500 m under the representative concentration pathway based on an additional radiative forcing of 8.5 watts per square (RCP8.5), likely inducing widespread thermal disturbances and permafrost degradation in the Central Andes (Drewes et al., 2018).

Line 294. Estimates of ice and liquid water fraction must be also sensitive to other poorly constrained parameters such as the p-wave velocity of rock and the three Archie parameters. Please comment on the model sensitivity and uncertainty concerning these parameters, and briefly explain how the values were 'taken from literature'.

From the Archie parameters, "a" should be set to 1 anyway as it just multiplies (the unknown) pore water resistivities (ρ_w) with another unknown factor and there is no physical representation of this factor (e.g. Mollaret et al. 2020). We modified this in our revised version. The sensitivities of the other Archie parameter ρ_w , m and n were already discussed in Hauck et al. (2011) and it was found that ρ_w has by far the strongest influence (if not known through in-situ measurements). In our study, the in-situ measurements of ρ_w from the thermokarst pond and surface snow were used to cover potential ranges of this sensitive parameter and were therefore combined with the porosity scenarios. The uncertainty of an unknown P-wave velocity of the rock material has of course an influence, but this influence is less than the importance of porosity and it can also be easier constrained through literature (rock type and p-wave velocity tables are

generally available). We have now included a justification of our choice of the P-wave velocity of the rock material.

The equations 5–7 allow to calculate the fractions f_w , f_i , and f_a based on the input data ρ and v from ERT and SRT, respectively if the other material properties (ϕ , ρ_w , m , n , v_w , v_r , v_i , and v_a , cf. Table 4) are prescribed.

The p-wave velocities v_w , v_i and v_a are known material properties and were taken from previous studies in periglacial environments (Hauck and Kneisel, 2008). The p-wave velocity v_r of the frozen volcanic rocks was assumed to be 6000 m s^{-1} , since comparable frozen or unfrozen rock types range between 4000 m s^{-1} to 7000 m s^{-1} (Draebing, 2016; Schön, 2011) and the sensitivity of the 4PM is very low for v_r (Hauck et al., 2011). The free parameters a , m , and n in Archie's Law were adopted from studies that have been successfully conducted in different mountain permafrost environments (Pellet et al., 2016), including different rock glaciers (Hauck et al., 2011; Mewes et al., 2017; Schneider et al., 2013) or have been tested for unfrozen and frozen sands (King et al., 1988). These prescribed parameters of the 4PM were kept constant in the model scenarios. The most sensitive 4PM parameters from Table 4 are the porosity ϕ and the pore water resistivity ρ_w (Hauck et al., 2011). Hence, for this study model scenarios with different combinations of ϕ and ρ_w values were performed to estimate and evaluate modelled material compositions.

Line 296. I feel that 70% is a large number for a talus rock glacier. How were these values selected? Based on the literature? I am not sure how much information is in the literature, but Merz et al. (2016, Geophysics, 81, WA147-WA157) used 30% as a rough estimate, and pointed out the need for 'dependable estimates of porosity across the rock glacier' as a future challenge. As estimated ice and water volumes are high sensitive to porosity (Fig. 7), I think that the choice of these values need to be critically examined and justified in light of the existing body of literature.

The values were selected based on observations from other studies (e.g. Arenson et al., 2002, Haeberli et al., 1998, Krainer et al., 2017) and reasoning about the potential ice-saturations for active or inactive rock glaciers. Active, i.e. presently moving rock glacier, are ice-supersaturated in most parts, which would mean porosities $>40\%$ and up to 100% in case of larger ground ice occurrences (e.g. observed at Murtel-Corvatsch rock glacier). Without ice-rich, i.e.-super-saturated conditions the creep of frozen soils is restricted by interlocking particles (Arenson et al 2005, Arenson and Springman 2005).

Observations from drill cores have shown that heterogeneous material compositions and ice content (0-100%) exist in ice-free, ice-poor, and ice-rich layers, in rock glaciers at the point scale. Therefore 30-70% porosity represent the lower and upper bounds in the present modelling case, to assess potential min/max ranges of the ice content. The 30 and 50% porosity models allow just ice saturation ($<40\%$ absolute ice content) below or close to saturation, given that the voids in rock glaciers and the 4PM (the dominant grain size of Dos Lenguas are sands ($\sim 40\%$ porosity)) contain also water and air. Therefore those scenarios and porosity assumptions would be suitable for an inactive or intact rock glacier, which does presently not move. The porosity model with 70% allow for ice super-saturated conditions larger than 40% ice content, which are necessary to assess potential ice content using the 4PM for active rock glaciers. We expected from geomorphological proxies (e.g. oversteepened front slopes) that Dos Lenguas is an active rock glacier. Now that we have evidence that Dos Lenguas is moving at rates of up to 2 m/a , the 70% porosity is a plausible assumption for the start model to allow for potential icesaturation. And yet, the model can be still regarded as conservative for ice –rich permafrost as ice saturations $> 70\%$ and pure ground ice bodies were not permitted by our porosity assumption. Porosity

assumptions for geophysical models are further discussed in the new paper by Mollaret et al. (2020), where porosity is jointly inverted for and values of 30-70% are found there as well. A corresponding paragraph has been added to our revised manuscript.

We used three uniform porosity models with $\phi = 30\%$, 50% , and 70% , and one mixed porosity model by integrating different porosity ranges of 45–30%, 75–30% and 10–3% for active layer, permafrost and bedrock, respectively (Table 4), due to the high spatial variability of the porosity and volumetric ice content in rock glaciers. Observations from drill cores have shown that volumetric ground ice content can range from 0% to 90% in ice-free, ice-poor, and ice-rich layers in rock glaciers (Haeberli et al., 1998; Krainer et al., 2017; Monnier and Kinnard, 2013). The frozen core of active rock glaciers is mainly characterized by ice-supersaturated conditions ($> 40\%$ ice content) and can contain massive ground ice. Therefore the assumed uniform 70% porosity model and mixed porosity model represent the upper bound assumptions for the 4PM modelling approach of a talus rock glacier, like Dos Lenguas. Ice-supersaturated conditions could be expected for volumetric ice content greater than 40%, since the dominant grain sizes of Dos Lenguas are sands and pebbles (Schrott, 1994). The 30% and 50% porosity models allow volumetric ice content less than 30% and 50%, given that the voids in rock glaciers and the 4PM contain also water and air. Therefore the latter porosity models would be suitable for an inactive or intact rock glacier, which does presently not move, as the creep of frozen soils is restricted by interlocking particles without ice-supersaturated conditions (Arenson et al., 2002; Arenson and Springman, 2005). The spatial arrangement of mixed porosities was deduced from interpretations of the ERT and SRT data. Negative depth gradients ($0.01\text{--}0.03\text{ m}^{-1}$) were included to simulate substrate compaction with depth, while allowing higher volumetric ice content in the upper part of the frozen core of the rock glacier. Porosity assumptions for geophysical models are further discussed by Mollaret et al. (2020), who also found porosity values of 30-70% for active rock glaciers based on jointly inverted data sets.

Line 316. Mean fw and mean fi. Mean of what?

The mean volumetric fraction of ice and water of each profile were calculated from all 4PM model cells located below the rock glacier surface (i.e. model cells below side slopes and outside the rock glacier were excluded at profile C1 and C2). The standard deviation of the mean fraction of ice and water of each profile was used for the error estimation and error propagation. The manuscript has been changed accordingly.

The mean volumetric fraction of water (mean f_w) and ice (mean f_i) of all model cells located below the rock glacier surface of each profile (4PM model cells below side slopes and outside the rock glacier were excluded at profile C1 and C2) were converted to mass using densities of 997 kg m^{-3} and 900 kg m^{-3} for water and ice, respectively. The mean ice and water content along the profiles C1 (root zone), C2 (central area), L1 (northern tongue), and L2 (southern tongue) were extrapolated to the mean depth of ice-rich permafrost of each profile and to the respective surface area of the geomorphological units (Fig. 1b). The error estimation for the mean ice and water content in Dos Lenguas was calculated by linearly propagating the uncertainties of (i) the mean f_w and the mean f_i of all used model cells of each profile; (ii) mean depths of ice-rich permafrost; and (iii) two percent error attributed to the mapped surface areas derived from the high-resolution DEM.

Please explain. Line 340.

‘Paired positive and negative changes’ should mean that positive changes at the front of the transverse ridges and negative changes at the back of transvers ridges also show the advance of the ridge and furrow topography. The wording of the sentence was revised.

The spatial pattern of interannual positive volumetric changes along the front of the transverse ridges and negative volumetric changes on the back of the transverse ridges indicate the advance of the surface of the rock glacier (Fig. 4). The highest amounts of these paired positive and negative volumetric changes [...]

Please annotate ‘central area’ etc. in Fig. 4, so the reader can clearly understand which region is referred to here. Alternatively, this sentence can refer the reader to Fig. 1b. Table 5. This table is a bit

difficult to understand at a first glance. It will be helpful to add vertical lines across the two tables, so the reader can relate the top table to the bottom table.

The caption of Fig. 4 has been changed to include references to the geomorphological units in Fig. 1a and Table 5. Table 5 has been reformatted to better reflect the relationship between the upper and lower tables.

Fig. 4: Vertical changes of Dos Lenguas from 03/2017 to 03/2018. The bar graphs show the sum of the positive (reddish bars) and the sum of the negative volumetric changes (bluish bars) for each geomorphological area (Fig. 1b) as a function of the confidence intervals for the periods 2016-17 and 2017-18. Starting at the twelve o'clock position and following the clockwise direction, the five bar graphs contain the total volumetric changes of the root zone, the central area, the southern tongues, the front and side slopes, and the northern tongue. The corresponding total net changes of ice are given in Table 5 as water equivalents.

Line 357. How are these average values calculated? Simple average of all grid cells shown in Fig. 4? Please briefly explain it here.

The methods chapter (3.2.3) describing the calculation of volumetric changes has been extended to describe in more detail how the values are calculated. Therefore the sentence has been adapted to the terminology used in the Methods chapter. Furthermore, the information was added that the calculation of the annual net changes in ice content of the total rock glacier surface was calculated from the sum of total volumetric changes in each geomorphological units (except for the area of the side and front slopes).

The sum of the total volumetric changes in all geomorphological units (excluding the areas of the front and side slopes) gives an annual net change in ground ice of -36 mm yr^{-1} and $+27 \text{ mm yr}^{-1}$ in the years 2016-17 and 2017-18 respectively, with a confidence interval of 95% (Table 5).

Figure 5. 'Depth' is used for the vertical axis in this figure, but it is a bit odd because depth is always referenced to the ground surface of a particular location. Please use elevation instead of depth.

The vertical axes of figure 5 and figure 6 were changed to elevation.

Figure 6. The delineation of permafrost and ice-rich permafrost in SRT images are not consistent with that in ERT images (Fig. 5). Please comment on the differences in this paragraph, and discuss it again in the last paragraph of this section.

Restrictions of the resolution capacities of the two different tomographic data sets for the 4PM are discussed in the methodological discussion concerning the geophysical approach. However, we followed the reviewers' suggestion by including a short comment on the inconsistency between ERT and SRT in the specific paragraph of the result section.

However, a reliable discrimination between frozen unconsolidated rocks, and bedrock is difficult due to the large overlapping p-wave velocity ranges of permafrost (Draebing, 2016; Schrott and Hoffmann, 2008), volcanic rocks (Schön, 2011), and the limited resolution capacity in the lowest parts of the models. Due to the ambiguities of velocity patterns and resistivity distributions, the spatial delineations differ in some areas of the independently interpreted structures in the SRT and ERT profiles (cf. spatial variations of ice-rich permafrost and active layer in Figs. 5 and 6). However, the comparison of SRT and ERT profiles also shows similar spatial patterns in the interpreted structures.

Line 440.

Figure 7 shows the mean values of ice fraction and liquid water fraction over 'model depth', but I am not sure what the model depth refers to. Please explain how the model depth is defined.

The model area of the 4PM (see fig. 8, ice and water contents per porosity) is defined by the overlapping part of the two model grids of ERT and SRT for each profile and corresponds to the maximal depth penetration of the seismic waves due to their smaller investigation depth than ERT in our case. The model depth relates therefore to the vertical extent ('model depth' below surface) of the 4PM cells along the profile (x-axis/distance). This explanation is now added in the revised version as follows:

The model area and depth of the 4PM was spatially limited by the SRT data sets, due to the lower penetration depth of the p-waves compared to the resistivity measurements along the profiles.

In figure 7, the model depth relates to the vertical dimension ('model depth' below surface) of the 4PM cells along the profile. The definition of the mean fractions over model depth was added and the name of the parameter has been changed to mean vertical ice and mean vertical water content in the results sections and figure 7. The caption of figure 7 has been extended with the respective explanations.

Fig. 7: Estimated mean vertical ice content ($f_{i\text{ vrt}}$) and mean vertical water content ($f_{w\text{ vrt}}$) along profiles C1, C2, L1 and L2 for all 4PM scenarios. The volumetric ice (upper panel) and volumetric water content (lower panel) of the 4PM model cells along the profiles were arithmetically averaged over the 4PM depth (vertical dimension) to compare the results of the various scenarios to each other. The porosity scenarios are color-coded and combined with different line types representing the pore water resistivities used. The mixed porosity (grey) and 70% porosity scenarios (blue) with pore water resistivities of 30 Ωm and 50 Ωm were evaluated as most reasonable for the active rock glacier, since the range of mean vertical ice content indicates ice-supersaturated conditions ($f_{i\text{ vrt}} > 40\%$) and the mean vertical water content is mainly lesser than 10%. The estimated ranges of the mean f_i and mean f_w of the plausible scenarios with uncertainties are given in table 7 for each profile and for the extrapolated absolute ice and water content of the geomorphological units.

Line 445-446. High porosity values are used for the mixed porosity model. Please my comment on Line 296.

Please see response to comment of Line 296

Line 482-484. Liquid water saturation and ice saturation are used in Fig. 8, instead of water content and ice content. This way of presenting the spatial distribution of water and ice is a bit misleading, because the reader cannot actually see the amounts of water in 'aquifers'. For example, 'aquifers from adjacent talus slopes' are in the bedrock, not in talus sediments. In the bedrock, water saturation is high due to low porosity, but water content is small. For the discussion of water storage, it is more meaningful to show water and ice contents. Please revise the figures.

We agree that for the discussion of water storage the absolute quantities matter most. However, absolute values derived from the 4PM have still a quite high potential error due to the unknown porosity. Therefore, we used the different scenarios to model and evaluate reasonable ranges of saturations, which are much better constrained in the 4PM. The absolute values (given as mean vertical ice content ($f_{i\text{ vrt}}$) and the mean vertical water content ($f_{w\text{ vrt}}$) along all profile) based on all porosity scenarios and pore water resistivities are shown in Fig.7. The mean fractions of ice and water of the scenarios that were evaluated as most reasonable were used to estimate the ice storage capacities and the amount of water and calculate absolute values of water and ice storage (table 7), which was potentially present during the measurements towards the end of the thaw season.

In Fig. 8, we show content per porosity (and in all plots of the supplements) to better display the heterogeneous material compositions using the same colour bar (scaling) for all fractions and all 4PM plots. Fig. 8 is used here only to visually indicate potential hydrologic structures. To compare

the fraction of ice and water of the different scenarios the reader can use fig. 7 (or is referred to the supplements). Showing all profiles as both, absolute and saturation based images of the fractions would take up too much space. We modified the figure captions (see above the revised caption of figure 7) and adapted the text in our revised manuscript to explain better the difference between the two types of plots.

The porosity variations of ice-rich permafrost and bedrock structures that were found within the interpreted ERT and SRT profiles were built into mixed porosity model. The spatial distribution of the ice and water content per porosity, i.e. the ice saturation and the water saturation, was further used to estimate the internal hydrological structure of the rock glacier. In general, the 4PM results show the heterogeneous material composition in the rock glacier (Figs. 7, 8). The volumetric fractions of ice and water per porosity along the profiles are shown in the supplements for all porosity scenarios (Figs. S1-S16).

Along all profiles, the mean vertical ice content ($f_{i\ vrt}$) and the mean vertical water content ($f_{w\ vrt}$) of all scenarios show increasing volumetric ice content with higher porosity and increasing volumetric water content with higher pore water resistivity, respectively (Fig. 7). Modelled mean $f_{w\ vrt}$ show local maxima, where reduced ice content occurs along the profiles. Mean $f_{i\ vrt}$ range roughly from 5 to 15%, 20 to 30%, and 40 to 50% for the uniform porosity models with 30%, 50%, and 70% porosity, respectively. The mixed porosity model yielded intermediate volumetric ice content values that range between the uniform 50% and 70% porosity models. The comparison of the mean vertical ice content ($f_{i\ vrt}$) along the profiles indicates that the model scenarios with porosities lesser or equal than 50% do not yield ice-supersaturated conditions in the rock glacier.

Fig. 2: Spatial distribution of ice and water content per porosity, i. e. ice and water saturations, of the 4PM scenario with mixed porosity model and pore water resistivities of 50 Ω m for (a) cross-profile C1 in the root zone, (b) cross-profile C2 in the central rock glaciers area, (c) long-profile L1 in the northern tongue and (d) long-profile L2 in the Southern tongue. Porosities <10% represent potential bedrock occurrence based on SRT interpretations. Porosities >40% allow ice-rich permafrost conditions in the 4PM. Ice content per porosity ($f_i \Phi^{-1}$) shows heterogeneous distributions of ice-rich permafrost and indicates the active layer and unfrozen bedrock in ice free model. High water content per porosity ($f_w \Phi^{-1}$) indicates water pathways and traps in ice-free area, while increased water saturations between ice-rich permafrost could indicate aquitards and/or thawing permafrost in late summer. Note the different horizontal and vertical scales of the figures for the different profiles.

Line 490. The lines delineating aquifers and aquitards are similar, and not easily distinguishable. Please use more distinguishable line types. These diagrams show aquitards that look like vertical chimneys. It is hard to imagine how such vertical aquitards could form in rock glacier. A more plausible explanation for the presence of shallow perched aquifers (e.g. $x = 150$ m in C1) is the horizontal aquitard (i.e. permafrost) underneath the aquifer.

We have removed the lines of the vertical aquitards in Fig. 8.

Regarding the second part of this comment: You are of course right, that the interpretation of these vertical features in Fig. 8 is highly speculative, given also the inherent uncertainties of the underlying inversions and corresponding 4PM results. However, if we assume these features to be reliable, the formation of vertical water pathways could be related to the long-term evolution of the ridge and furrow structures and to the percolation of water in voids, channels, or crevasses/fractures between ice-rich permafrost. At first, different source areas of different talus slopes developing into single flow lobes might play a crucial role in the long-term evolution of the extensional ridge and furrow topography since ice-rich permafrost bodies of the developing lobes are separated by ice-free or ice poor outer edges before the different lobes flow together (if there is enough compression) or the lobes creep side by side. So, water could percolate into the ice-free or ice-poor voids between ice-rich permafrost. Second, if not separated from the beginning, the formation of surface crevasses and the separation of the two tongues shows that different creep

velocities could also produce vertical fractures (if tensile stress is sufficient to cause brittle failure) and split off ice-rich permafrost in transverse ridges. The voids or filled (ice-free) fractures between ice-rich permafrost could then also function as 'vertical' water pathways.

Yet, given the speculative nature of the above, we have revised the figure and consider the rock glacier permafrost generally as aquitard during the thawing season and just marked areas were increased water saturations indicate percolation or water pathways above, between or below ice-rich permafrost. In the specific location ($x = 150$ m in C1) we followed your suggestion to consider the water pathway as a perched aquifer, above permafrost.

Line 547-550. Please note that high water saturation does not necessarily indicate an aquifer. To qualify as an aquifer, the material needs to have high enough porosity and permeability. Please see my comment on Line 482-484 as well.

Thank you very much for the very valuable comments to L482-484, L490, and 547-550. We followed most of the suggestions and revised the text, terminology and figures to better explain the results and interpretations. In particular, it was made clear that the spatial distribution of ice and water saturations could be interpreted as potential water pathways and ice-rich permafrost. The reviewer is right that our use of the terminology has been somewhat misleading. In this context the term aquifer was avoided and removed from the text and figure 8. In order to prevent jumping to speculative conclusions we now use the alternative terminology of water pathways or potential supra-, intra-, and sub-permafrost flow (as suggested by Jones et al. 2019 for hydrological flowpaths in rock glaciers) in our revised manuscript

Line 503. Gruben rock glacier abruptly appears here. Please provide the context. The same applies to the Galena Creek rock glacier in Line 505.

A sentence indicating the context was added.

Previous studies investigating the geodetic mass balance of rock glaciers have been conducted at the Gruben rock glacier (Kääb et al., 1997) and the Galena creek rock glacier (Konrad et al., 1999).

Line 673. How is this number calculated from Table 6? Please explain the steps and assumptions. It seems that the range of uncertainty in this number is unrealistically small in light of all the uncertainties in model parameters, as well as the geophysical data inversion. Please provide an explanation as to why the number can be so well constrained.

We extended the explanation of the steps and assumption in the method section (see also our response to comment of Line 316). The uncertainties of the numbers were given in Table 7 and the result section. The idea was to use only the mean values without the uncertainty ranges to compare the different water and ice storage estimations and thereby avoid too many comparisons and numbers of different estimates in the discussion. Now, we have included the min and max values to show the larger ranges of the estimates throughout the revised discussion of the water storage capacities and interannual changes.

In the following we interrelate water and ice storage capacities and the interannual changes for the active rock glacier. The overall long-term ice storage of this rock glacier ranges between $1.71(\pm 42\%) - 2(\pm 44\%) \times 10^9$ kg based on the mean volumetric fractions of the most reasonable evaluated 4PM scenarios (Table 7). The mean volumetric fraction of water at the end of the thaw period was $0.36(\pm 32\%) - 0.43(\pm 32\%) \times 10^9$ kg (Table 7), which would potentially correspond to 9-57% of the ice content if the uncertainties ranges of the mean ice and mean water content of both scenarios are interrelated. If only the mean values of the two scenarios are compared, the water content is about one fifth of the ice content. The latter estimate must be seen as an upper bound, due to the uncertainties in quantifying thin water layers from ERT data mentioned above. Therefore, the ice to water content ratios suggest that the scenario with the

highest porosity and the lowest pore water resistivity provides the most plausible volumetric fractions of ice (mean f_i 24-64%) and water (mean f_w 2-15%) in the rock glacier during the end of the summer. The material composition and the potential ratios between ice and water content could mean that a relatively large amount of groundwater and meltwater is available for ice and water storage exchanges in the rock glacier at the end of the thaw period.

Line 681. I cannot follow the conversion between mm d-1 and kg. Also, I cannot understand why 36:28 is not equal to 19.8:14.7. Please explain how these numbers are calculated.

Thank you very much for spotting this error, which was due to a calculation error of the total surface area. We corrected the values. The steps and assumption of the calculated values has been extended in the respective method sections.

Thank you very much for spotting this error, which is due to a calculation error of the total surface area. The correct amounts of water in kg for the surface area of 247802 m² are: -36 mm yr⁻¹ (-8.92x10⁶ kg) for the first period 2016-17 and 27mm yr⁻¹ (6.64 x 10⁶ kg) for the second period 2017-18. Due to different volumetric changes between the first period 201617 and the second period 201718, the ratio of the two different observations periods should not and cannot be equal. The steps and assumption of the calculated values has been extended in the respective method sections. We updated the paragraph accordingly.

The production of multi-temporal DEMs allows for the calculation of volumetric surface changes between consecutive surveys. The vertical changes of the rock glacier surface area over the periods 2016–17 and 2017–18 were estimated by subtracting surface elevations of the 2016 DEM from the 2017 DEM and the 2017 DEM from the 2018 DEM, respectively. Then, the pixel wise volumetric change was derived by multiplying the vertical changes of each raster cell by cell size. The total positive and total negative volumetric changes (bar graphs in Fig. 4) for the different geomorphological units of Dos Lenguas (Fig. 1b) were summed up to derive negative and positive volumetric changes of the respective surface areas. The total volumetric net changes of the geomorphological units are the sum of positive and negative volumetric changes in the respective surface areas. The density of ice (900 kg m⁻³) was used to estimate the corresponding net change of ground ice, which is given as water equivalent (1 mm yr⁻¹ corresponds to 1 kg m⁻² yr⁻¹) for each geomorphological area except for the side and front slopes.

Interannual storage changes derived from volumetric changes revealed that only 2–4% of the water content (using the mean f_w as upper bound) would be required for the ice loss during the first observation period 2016-17 or the ice gain during the second observation period 2017-18 according to the 95% confidence interval with -36 mm yr⁻¹ (-8.92 × 10⁶ kg) and 28 mm yr⁻¹ (6.64 × 10⁶ kg), respectively. The small ratio of interannual ice storage changes with respect to the 4PM-derived water content again indicates that the water content may be overestimated, due the sensitivity of the 4PM and the wet ground conditions during the geophysical measurements at the end of the thaw period. However, this small ratio could also mean that the major amount of groundwater and meltwater passes along the water pathways through the rock glacier.

Line 688-690. The difference in meteorological conditions between the two seasons is casually discussed here, referring to a supplemental figure. I feel that this topic is central to the main objective of the paper and deserves more attention. For example, what was the difference in precipitation? What was the actual difference in mean air temperature during the two thawing seasons? Please expand the discussion and demonstrate a clear link between the meteorological condition and estimated storage change (negative in 2016-2017 and positive in 2017-2018).

Thank you for this of course very relevant comment! Unfortunately, there are no reliable precipitation data (rainfall and snow) at the meteo station available for the mentioned relevant parameters in the observation period 2016-2018. Therefore we have added a table with precipitation estimates derived from CHIRPS data archive (Funk et al., 2015).

Mean monthly air temperatures of the meteorological stations are available and were used for the mean annual temperatures given in the study site section (see table 1). However, as we recorded ground surface temperature directly at Dos Lenguas, we think the trend of the temperature regime is better displayed by the in-situ ground surface temperature than by interpolated air temperatures from meteorological stations located in different topo-climatic position (at the Paso de Agua Negra or in front of the Agua Negra glacier).

Based on the difference in precipitation (Table 2) and the temperature profile of the ground surface temperature during the observation periods, we extended the discussion and linked interannual storage changes to the meteorological conditions.

Table 2: Mean and maximum precipitation in the Agua Negra valley for the hydrological periods 2016-17 and 2017-18 from CHIRPS (Climate Hazards Group InfraRed Precipitation with Stations) data archive (Funk et al., 2015).

Hydrological period	Sum of monthly precipitation [mm]					
	Austral winter 01/04-30/09		Austral summer 01/10-31/03		Hydrological year 01/04-31/03	
	Mean	Max	Mean	Max	Mean	Max
2016-17	23	50	22	90	45	140
2017-18	13	55	38	113	51	168

Interannual storage changes derived from volumetric changes revealed that only 2–4% of the water content (using the mean f_w as upper bound) would be required for the ice loss during the first observation period 2016-17 or the ice gain during the second observation period 2017-18 according to the 95% confidence interval with -36 mm yr^{-1} ($-8.92 \times 10^6 \text{ kg}$) and 28 mm yr^{-1} ($6.64 \times 10^6 \text{ kg}$), respectively. The small ratio of interannual ice storage changes with respect to the 4PM-derived water content again indicates that the water content may be overestimated, due the sensitivity of the 4PM and the wet ground conditions during the geophysical measurements at the end of the thaw period. However, this small ratio could also mean that the major amount of groundwater and meltwater passes along the water pathways through the rock glacier. Nevertheless, the interannual water storage changes of -36 mm a^{-1} and $+28 \text{ mm yr}^{-1}$ of the 95% confidence interval suggest that significant amounts of mean to maximum annual precipitation of 45-140 mm and 51-168 mm (cf. Table 2, CHIRPS derived estimates (Funk et al., 2015)) could have been released and stored in the active rock glacier during the hydrological years 2016-17 and 2017-18. The mass loss of -36 mm yr^{-1} corresponds to 25-80% of the annual precipitation in the hydrological year 2016-17. The ice gain of 28 mm yr^{-1} corresponds to 17-55% of annual precipitation in the hydrological period 2017-18. Higher maximum precipitations during the latter hydrological year could have contributed to the positive interannual storage changes in 2017-18 compared to the hydrological year 2016-17. The mean annual precipitations with less than 51 mm yr^{-1} of the two hydrological years (Table 2) do not show significant differences that could explain the positive and negative volumetric net changes in ice storage, but would increase the significance of the interannual storage changes due to the dry meteorological conditions. Recorded ground surface temperatures of Dos Lenguas could indicate that the strongly fluctuating temperature regime (Fig. S17) could have additionally influenced the negative and positive interannual storage changes of Dos Lenguas in the years 2016-17 and 2017-18, respectively. During the thaw period 2016-17 the temperature profile of monthly median ground surface temperatures shows an earlier beginning and a higher summer maximum compared to summer 2017-18, which is characterized by a lower and later temperature maximum. The significantly lower amplitudes of the ground surface temperatures in winter 2016-17 compared to winter 2017-18, indicate that there was no damping of ground surface temperatures by snow in winter of 2017-18. Consequently, the generally higher ground surface temperature during austral summer 2016-17 could have led to the observed negative storage changes due to the deeper thaw penetration. In contrast, the ice gain during the hydrological year 2017-18 might have been fostered by higher precipitation, more effective penetration of cold winter temperatures and smaller active layer depths.

Line 691. Please show the location of the spring in Fig. 1b.

The location of the spring has been added to Fig. 1b.

Line 691-695. I feel that the discussion on the water balance needs a bit more care, again because this is central to the main objective of the paper. For example, if the area of the rock glacier is 0.36 km² (Line 127), then 104 x 10⁶ kg is equivalent to 290 mm of water averaged over the rock glacier area. This is a large magnitude compared to annual precipitation of 50-150 mm (Line 106). What is the source of this water? Does the spring flows only for five months (Line 692), or does it flow all year? What was the actual precipitation amounts in 2016-2017 and 2017-2018? How are 14-30% and 70-86% calculated?

Thank you very much for your careful reading of our manuscript and the very useful comments regarding the discussion on the water balance. We addressed the raised questions in the revised section of the water balance.

According to Schrott (1996) 104 x 10⁶ kg would be the upper bound if the spring flow is constant for 5 months with 8 l s⁻¹. You are right in saying that the corresponding 290 mm would be quite a large magnitude in this respect. Of course the data from Schrott (1996) relate to an observation period ~30 years ago and have therefore to be used with care when comparing it to present day conditions. The major additional water source (to precipitation) could be the contribution area of the rock glacier, which delivers water, snow and debris to the rock glacier. The calculated surface area feeding into the root zone of the rock glacier is 1.01 km². The contribution area of the surface area of the rock glaciers is ~ 2.7 km² (including the surface area of the rock glacier). A second source could be seasonal melt-water from the active layer and permafrost within the rock glacier and the contribution area. A third source could be sub-permafrost groundwater. If we consider the total contribution area and the area of the rock glacier as the catchment area of the spring the potential discharge would correspond to an upper bound of 38 mm (104 x 10⁶ kg / 2.7 km²). This is a reasonable magnitude compared to annual precipitation of 45-168 mm (Table 2).

During the field investigations in the 90ies the spring flow was observed from January until End of April with 58 l s⁻¹ (Schrott, 1996). There have been no observations during other times of the year. So it remains unknown if there could be discharge in the winter season. The ground surface temperature regime shows median temperatures >5°C for five months during summer and <-5°C during winter. The cold temperatures make it unlikely that there could be discharge in winter. Unfortunately, there are no observations as to when exactly the discharge starts with the beginning of the thawing season. The large amplitudes of the ground surface temperatures indicate no continuous and/or only a thin snow cover during the winter season (Fig. S17). Sublimation and partly infiltrating meltwater due to the melt of a thin snow cover (< 5cm) by strong solar radiation was observed a few times during the field work the day after precipitation events (snow and/or sleet) during summer. The drainage of meltwater from snow during winter due to strong solar radiation seems very unlikely given the ground surface temperature regime. It is rather likely that meltwater will refreeze during infiltration in winter.

14-30% gives the ratio of potential discharge at the spring to the amount of storage changes. Due to the calculation error of the storage change (see above), we have corrected the ratios. The discussion on the water budget related to the precipitation has been extended.

The measured discharge of 5–8 l s⁻¹ from the Dos Lenguas spring found by Schrott (1996) would translate to a total of 64.8–103.7 × 10⁶ l for a five month lasting thaw season. Due to the dry and cold meteorological conditions during winter, spring flow can be expected to be active only in summer. The discharge can be fueled by precipitation, snowmelt, melting ground ice and sub-permafrost groundwater flow in the catchment area of the spring (2.7 km²), which includes rock glacier (0.36 km²) and the contribution area of the root zone (1.01 km²). The potential range of discharge averaged over the catchment area of the spring corresponds to an output of 24-38 mm during thaw season. The potential

discharge would thus be in the range of the mean precipitation input of 22 mm and 38 mm in the austral summer periods 2016-17 and 2017-18, respectively (Table 2). However, the higher mean and maximum precipitation of 45-168 mm of the full hydrological years 2016-17 and 2017-18 indicate that additional precipitation input could be released along other groundwater pathways or is temporarily stored in the hydrological system of the rock glacier and its catchment. The negative interannual storage of -8.92×10^6 l in 2016-17 of the rock glacier would potentially correspond to 9-14% of the total discharge at the spring ($65-104 \times 10^6$ l). The positive interannual storage change of 6.64×10^6 l in 2017-18 could have decreased the potential discharge about 6-10%. The interannual storage changes due to freezing and thawing could therefore buffer the groundwater release and add or reduce groundwater flow during the course of the year.

Finally, about 11-42 % of the mean water content of the rock glacier could nourish discharge at the rock glacier spring, since the estimated mean water content (mean f_w corresponds to $244-570 \times 10^6$ l) was larger than the potential discharge at the spring during the thaw period. The remaining share of water content (58-89%) could leave the internal hydrological system of the rock glacier along other water pathways and/or is refilling or exchanging groundwater storages in and below the rock glacier. Although the several uncertainties in the estimation of the different components of the water balance have to be kept in mind, the estimated ice and water storage capacities and the interannual storage changes demonstrate that (a) an active rock glacier like Dos Lenguas could play a crucial role in buffering and regulating seasonal groundwater flow and recharge, while (b) it constitutes a long-term ice storage in the dry high mountain catchment, where currently only 2.8% of the surface area remain permanently covered with surface ice and snow.

Ice content and interannual water storage changes of an active rock glacier in the dry Andes of Argentina

Christian Halla¹, Jan Henrik Blöthe², Carla Tapia Baldis³, Dario Trombotto Liaudat³, Christin Hilbich⁴, Christian Hauck⁴, Lothar Schrott¹

¹Department of Geography, University of Bonn, 53115 Bonn, Germany

²Institute of Environmental Social Sciences and Geography, University of Freiburg, 79085 Freiburg, Germany

³Instituto Argentino de Nivología, Glaciología y Ciencias Ambientales, CCT CONICET, 5500 Mendoza, Argentina

⁴Department of Geosciences, University of Fribourg, 1700 Fribourg, Switzerland

Correspondence to: Christian Halla (chris.halla@uni-bonn.de)

Abstract

The quantification of volumetric ice and water contents in active rock glaciers is necessary to estimate their role as water stores and contributors to runoff in dry mountain catchments. In the semi-arid to arid Andes of Argentina, active rock glaciers potentially constitute important water reservoirs due to their widespread distribution. Here however, water storage capacities and their interannual changes have so far escaped quantification in detailed field studies. Volumetric ice and water contents were quantified using a petrophysical four-phase model (4PM) based on complementary electrical resistivities (ERT) and seismic refraction tomographies (SRT) in different positions of Dos Lenguas rock glacier in the Upper Agua Negra basin, Argentina. We derived vertical and horizontal surface changes of the Dos Lenguas rock glacier, for the periods 2016–17 and 2017–18 using drone-derived digital elevation models (DEM). Interannual water storage changes of -36 mm yr^{-1} and $+27 \text{ mm yr}^{-1}$ derived from volumetric surface changes for the periods 2016–17 and 2017–18, respectively, indicate that significant amounts of annual precipitation can be stored in and released from the active rock glacier.

Geophysical results show heterogeneous ice and water content with ice-rich permafrost and supra-, intra- and sub-permafrost aquifers water pathways at the end of the thaw period in the subsurface. Heterogeneous ice and water contents show ice-rich permafrost and supra-, intra- and sub-permafrost aquifers in the subsurface. Active layer and ice-rich permafrost control traps and pathways of shallow ground water groundwater, and thus regulate interannual storage changes and water releases from the active rock glacier in the dry mountain catchment. The ice content of $1.7\text{--}2.0 \times 10^9 \text{ kg}$ in the active Dos Lenguas rock glacier represents an important long-term ice reservoir, just like other ground ice deposits in the vicinity, if compared to surface ice that covers less than 3% of the high mountain catchment.

1 Introduction

Presently moving rock glaciers are classified as active rock glaciers (Barsch, 1996) that are defined as the “the visible expression of cumulative deformation by long-term creep of ice/debris mixtures under permafrost conditions” (Berthling, 2011, p. 105). Rock glaciers constitute predominant landforms in the extensive periglacial belts of arid high mountain regions, such as the Central Andes of Argentina and Chile (Corte, 1976; Trombotto et al., 1999). Here, rock glaciers show some of the highest spatial densities worldwide (Azocar and Brenning, 2010; Blöthe et al., 2019), covering more surface area than glaciers in some parts (IANIGLA, 2018).

~~Besides storing large amounts of sediment, r~~Rock glaciers have been identified and discussed as significant water reservoirs in the dry Andes due to their widespread distribution (Arenson and Jakob, 2010; Brenning, 2010; Corte, 1976, 1978). Recently, first order assessments of their water storage capacities suggest that significant amounts of ice are stored in rock glaciers (Jones et al., 2018a). However, field based studies that rigorously quantify rock glacier water storage capacities and their interannual changes are lacking in the region (Schaffer et al., 2019). In this study we investigate the water storage

capacities of a tongue-shaped rock glacier, whose material source ~~are is derived from~~ periglacial talus slopes, ~~located on the valley side~~. It is beyond the scope of this case study to discuss the multiple hypothesis regarding the genetic evolution of rock glaciers (Knight et al., 2019) and debate periglacial and glacial origins of rock glaciers (Berthling, 2011).

Under a changing climate, temperatures in the semi-arid to arid Andes are predicted to increase at a faster rate and higher compared to their lowlands (Bradley et al., 2006). ~~Coneomitant-Associated~~ changes in the mountain cryosphere, such as the degradation of glaciers (Braun et al., 2019; Dussailant et al., 2019), permafrost (Drewes et al., 2018; Rangecroft et al., 2016), and snowpack (Malmros et al., 2018; Saavedra et al., 2018), will strongly affect Andean watersheds currently dominated by runoff generated from snow and ice melt (Barnett et al., 2005; Bradley et al., 2006). Rising air temperatures shift the timing of seasonal snow cover and snow melt resulting in reduced discharges in summer and autumn when demands are highest (Barnett et al., 2005; Bradley et al., 2006). The sensitivity of the Central and Desert Andes of Argentina towards recent warming is reflected by more pronounced snow cover reduction and rising snowline elevations compared to the Western side of the Andes (Saavedra et al., 2018). In the semi-arid Andes of Argentina many active rock glaciers currently exist at or below the zero degree isotherm (Brenning, 2005; Trombotto et al., 1999).

For the next decades it is predicted that the 0°C isotherm of mean annual air temperature will increase by more than 500 m based on the representative concentration pathway of an additional radiative forcing of 8.5 watts per square meter (RCP8.5), which is likely to trigger widespread thermal disturbances and permafrost degradation in the Central Andes. In the decades to come, the 0°C isotherm of the mean annual air temperature is predicted to rise more than 500 m under RCP8.5, likely inducing widespread thermal disturbances and permafrost degradation in the Central Andes (Drewes et al., 2018). Yet, studies investigating changes in rock glacier volume over time are lacking so far.

Generally, ground ice in rock glaciers responds slower to climate change compared to surface snow and ice due to the presence of the seasonally frozen active layer which dampens thermal changes in the subsurface (Haeberli et al., 2006). Massive ground ice and ice-supersaturated, i.e. ice-rich permafrost in rock glaciers are less sensitive to climatic warming than permafrost with low ice content (Scherler et al., 2013) due to complex interactions of advective and convective heat fluxes and latent heat effects during freeze and thaw processes (Scherler et al., 2010). However, ice melt is also predicted for rock glaciers (Marmy et al., 2016) and already observed in the European Alps (Mollaret et al., 2019).

In addition, signs of permafrost warming have been reported for many active rock glaciers worldwide, often manifested ~~in~~ as rising permafrost temperatures that induce increased surface velocities (Kääb et al., 2007). Borehole data ~~showeds~~ that most of the rock glacier deformation occurs within shear horizons of creeping permafrost (Arenson et al., 2002; Haeberli et al., 1998). Velocity variations of rock glaciers are additionally affected by liquid water availability and ~~ground~~ water/groundwater fluxes (Ikeda et al., 2008) after rain fall and snowmelt ~~indicating-which increase~~ increased pore water pressure temporarily enhancing shearing (Cicoira et al., 2019; Kenner et al., 2017; Wirz et al., 2016). Thus, rock glacier movement is impacted by hydrology and ground temperatures ~~Thus, the kinematics of rock glaciers interacts with their hydrology and ground temperatures~~ (Kenner et al., 2019). Interannual vertical variations of the surface topography are mostly related to the mass balance of rock glaciers (Kääb et al., 1998; Konrad et al., 1999), although annual ice gains and losses (Kääb et al., 1997), just as annual water releases as discharge, are significantly lower from rock glaciers than from glaciers (Krainer and Mostler, 2002). Interannual vertical variations of the surface topography are mostly related to the mass balance of rock glaciers (Kääb et al., 1998; Konrad et al., 1999). Annual mass balance and discharge are significantly lower for rock glaciers compared to glaciers (Kääb et al., 1997; Krainer and Mostler, 2002).

The hydrologic system of rock glaciers receives water from precipitation, snowmelt, ice-melt and groundwater flow, while water is lost by discharge, groundwater flow, evaporation and sublimation (Burger et al., 1999; Krainer et al., 2007). Internal water flow, water storage capacities and changes are controlled by heterogeneous material compositions (debris, ice, water, and air) and their hydrothermal properties (e.g. porosity, solid or liquid phase state of water). On the temporal scale, ice-rich permafrost functions as long-term water storage ~~and aquitard~~ while the active layer functions as short term/seasonal reservoir

85 ~~and aquifer~~ (Jones et al., 2018b). Seasonal to annual ice gains and water releases have been mainly attributed to freezing and thawing of the active layer during winter and summer, respectively (Duguay et al., 2015). ~~Shallow ground-water~~ groundwater drainage in rock glaciers is regulated by unfrozen and frozen conditions with supra-, sub- and intra- permafrost flow (Jones et al., 2019). Rock glaciers can contribute to groundwater recharge and ~~add significant amounts of~~ basin streamflow during late summer, fall and winter (Harrington et al., 2018; Williams et al., 2006). ~~Active layer and permafrost regulate shallow ground-water~~ groundwater drainage and throughputs as aquifer, aquitard, and/or aquiclude in rock glaciers (Jones et al., 2019). ~~The water input and different hydraulic properties of hydrological flowpaths~~ flow paths of frozen and unfrozen ground delay and buffer the water release of rock glaciers (Harrington et al., 2018; Jones et al., 2019; Rogger et al., 2017) which impacts the runoff generation in mountain catchments. ~~The hydrological response of rock glaciers impacts runoff generation in mountains catchments by delaying and buffering water releases~~ (Geiger et al., 2014; Krainer and Mostler, 2002), ~~depending on the water input and different hydraulic properties of supra-, intra- and sub-permafrost aquifers (Harrington et al., 2018; Jones et al., 2019; Rogger et al., 2017).~~ Moreover, water releases of rock glaciers and permafrost degradation can impact surface freshwater in mountain catchments by changing their inorganic chemistry (Colombo et al., 2018a; Colombo et al., 2018b) and influencing the stream energy budget (Harrington et al., 2017). However, only few studies have investigated groundwater flow pathways in rock glaciers (Harrington et al., 2018) and other landforms of mountain watersheds sustaining stream runoff during dry periods (Langston et al., 2011; McClymont et al., 2012; McClymont et al., 2010).

The hydrologic importance of water storage capacities in rock glaciers compared to glaciers (Croce and Milana, 2002; Milana and Maturano, 1999) as well as river discharge (Schrott, 1996) and chemistry during summer months due to the melt of frozen ground (Lecomte et al., 2008) has been previously investigated in the Upper Agua Negra catchment in the dry Andes of Argentina. The present study of the talus rock glacier 'Dos Lenguas' builds upon this earlier research and presents results of high-resolution surface detections and extensive hydro-geophysical subsurface measurements in the data-scarce region of the dry Andes. ~~In situ electrical resistivity and seismic refraction measurements are combined in an petrophysical model, called four phase model (4PM) (Hauck et al., 2011), in order to quantify the ice and water contents~~ content at the end of the thaw season, while imaging the internal hydrologic structure with potential water pathways and ice rich parts in the rock glacier. ~~Volumetric surface changes are used to infer first order estimations of interannual water storage changes of the active rock glacier.~~

In spite of speculations on their hydrological significance (Azocar and Brenning, 2010; Corte, 1976; Jones et al., 2018a), almost no quantitative and measurement-based estimates about water storage capacities of Andean rock glaciers and their changes over different time-scales exist. With the present study, we try to fill this gap and aim to: (1) quantify long-term ~~water-ice~~ storage capacities and water content at the end of the thaw period by estimating the current material composition ~~(i.e. the volumetric ice content)~~, (2) analyse surface deformations and gain quantitative estimates of interannual storage changes and (3) infer the internal hydrologic structure ~~of different geomorphological units~~ areas of the active rock glacier from the spatial distribution of ice and water ~~contents~~ content in different geomorphological areas of the active rock glacier.

2 Study site

120 The Upper Agua Negra basin and Dos Lenguas rock glacier are located at approximately 30° S in the dry Andes of Argentina (Fig. 1a). The regional climate is characterised by semi-arid conditions ~~with a mean annual precipitation of roughly 50–150 mm yr⁻¹ (TRMM derived estimates (Bookhagen and Burbank, 2006))~~ and extremely high solar radiation intensities throughout the year (Schrott, 1998). Precipitation above 4000 m a.s.l. is mainly solid and falls as snow and sleet during winter. Due to the absent or thin snow cover during eight months of the year, the incoming solar radiation controls surface temperatures and upper ground thermal regime (Schrott, 1991). ~~Few a~~ A available annual records from ~~different~~

125 meteorological stations in recent years show mainly negative mean annual air temperature in the catchment (Table 1). The mean to maximum annual precipitation in the Aqua Negra catchment area was between 45 mm yr⁻¹ and 168 mm yr⁻¹ in the hydrological years 2016-17 and 2017-18 (Table 2, CHIRPS derived estimates (Funk et al., 2015)). Continuous permafrost has been estimated to cover roughly 16% or 9 km² of the watershed above 5200 m asl (Schrott, 1996). The lower limit of discontinuous permafrost ~~has been manifested to reach down~~ extends to ~~about~~ ~4000 m a.s.l. potentially covering large areas
130 in the basin, including active rock glaciers (0.88 km²) (Schrott, 1994; Tapia-Baldis and Trombotto-Liaudat, 2020). Surface ice and snow stored in mountain glaciers (1.4 km²) and perennial snowfields (0.18 km²) together account for 2.8% of the watershed (Fig. 1). The high mountain cryosphere of the Upper Agua Negra basin has been one of the areas where previous studies investigated the hydrologic significance of runoff from the high mountain cryosphere. Discharge measurements confirmed that meltwater from areas affected by permafrost conditions and seasonally frozen ground account
135 for an important share of ~20% discharge, which increases up to 30% after snow melt during the ablation season (Schrott, 1994; Schrott, 1996). Hydrochemical analysis of melt water indicates significant internal recycling by sublimation and evaporation and delayed meltwater throughputs from -Dos Lenguas and other rock glaciers in the Upper Aqua Negra basin (Lecomte et al., 2008). Geophysical investigations on the El Paso rock glacier suggest that the active layer traps and conducts water and interacts with the permafrost table during summer thaw, while ice-rich permafrost is an important water reservoir releasing water mainly during droughts (Croce and Milana, 2002).
140 Previous studies at Dos Lenguas have investigated hydrological-geomorphological aspects such as the active layer and the discharge of 5-8 l s⁻¹ during the thaw period (Schrott, 1994; Schrott, 1996) The Dos Lenguas rock glacier has been the subject of earlier studies (Lecomte et al., 2008; Schrott, 1994; Schrott, 1996). The tongue-shaped talus rock glacier is roughly 1200 m long, between 200 and 600 m wide in its upper and lower part, respectively, and extends from 4200 m at the foot to 4500
145 m in the root zone (Fig. 1b). Its surface covers an area of ~0.36 km² including side and front slopes and 0.25 km² excluding them. In its lower part the west-southwest flowing rock glacier separates into a northern and a southern tongue (Dos Lenguas Spanish for “two tongues”) both with distinct transverse ridges and furrows terminating in oversteepened frontal slopes (>35°). The surface morphology of the root zone is featured by longitudinal ridges and furrows. In the central part of Dos Lenguas longitudinal ridges transition into transverse structures downslope, where crevasses indicate the splitting of the
150 tongues (Fig. 2). Melt water ponds occur in transversal furrows in the central part and on the northern tongue of Dos Lenguas. The headwall talus system (1.01 km²) is located at a fault system and delivers mass input to the root zone by rock falls and groundwater from the contributing area above. The debris supply is composed of weathered volcanic rocks of the Permian-Triassic Choiyoi group consisting of rhyolites, dacites, andesites and basaltic lavas, tuffs, breccias and ignimbrites (Heredia et al., 2012; 2002). The rock glacier surface is predominantly characterized by a thin layer (<0.5 m) of coarse
155 pebbles to small boulders supported by a sandy matrix (Schrott, 1994), with isolated large boulders that occur more frequently closer to the headwalls.

3 Methods

3.1 Timing of field surveys

All field surveys were carried out between late February and mid-March in 2016, 2017 and 2018. During late summer, the
160 active layer depth and the melt water content could be close their maximum. Therefore, the time span is particularly suitable to detect internal hydrological structures and quantify ice and water ~~contents~~ content by means of geophysical methods. The ice content and the liquid water content during the end of the thaw period were only estimated once at each geophysical profile.

The horizontal and vertical surface changes were surveyed on a yearly basis with an unmanned aerial vehicle (UAV). Accordingly, interannual storage changes between 2016–17 and 2017–18 were derived from the volumetric changes of the surface towards the end of thaw season.

3.2 DEM generation and analysis

To investigate the kinematics, i.e. vertical and horizontal surface changes, of Dos Lenguas rock glacier, we relied on the production of DEMs from aerial photography collected with an UAV. Using Structure from Motion Multi-View Stereo (SfM-MVS) algorithms, we derived dense point clouds from overlapping aerial imagery with Agisoft Photoscan Professional (Version 1.4.4).

3.2.1 Data acquisition and DEM processing

During late summer in 2016, 2017 and 2018, we surveyed Dos Lenguas using a Phantom 3 Advanced Multicopter equipped with a standard camera (12.4 MP, FOV 94°), taking between 550 and 1800 overlapping images per survey. Survey flights were accomplished in a single day (13/03/2016), or spanning multiple days (24/02 – 02/03/2017 and 03/03 – 07/03/2018), depending on weather conditions. Across the survey area, which covered the rock glacier and its surrounding stable surfaces, we distributed 34 ground control points (Fig. 1b) that were repeatedly measured with a Trimble R8s/R2 differential global navigation satellite system (dGNSS) operating in a real-time kinematic base-rover configuration. The positions of ground control points were recorded with horizontal root-mean-squared errors (RMS) of 0.012 and 0.013 m for 2017 and 2018, respectively and vertical RMS of 0.022 and 0.027 m for 2017 and 2018, respectively. For all three years, the identical workflow was followed in PhotoScan, starting with image alignment, followed by the manual identification of ground control points and camera optimisation.

3.2.2 Measurement of horizontal rock glacier displacement

With the advancement of SfM-MVS software solutions and the availability of UAV at low cost, the production of high-resolution DEMs and orthoimages has offered new time-efficient possibilities for the assessment of rock glacier kinematics (Dall'Asta et al., 2017). Here we use two complementary approaches, a) the repeated measurement of 34 ground control points using a dGNSS device and b) an automated image matching approach, to quantify horizontal movement on the rock glacier.

For automated image co-registration in optical imagery we used the freely available stand-alone Environmental Motion Tracking (EMT) software (<https://tu-dresden.de/geo/emt>), originally developed for motion tracking in oblique pictures (Schwalbe and Maas, 2017), but likewise applicable to vertical images. As orthoimages collected in consecutive years show large spectral differences, caused by shadowing effects, snow cover, surface moisture, etc., we used DEMs and their derivatives as input for image matching applications (Dall'Asta et al., 2017). EMT software applies area-based matching to automatically find corresponding patches of pixel values in multi-temporal images using least squares matching or cross-correlation algorithms (Förstner, 1986; Schwalbe and Maas, 2017). Images are loaded into EMT software, where starting points (patch centres) are defined, patch size and search area are set and tracking method as well as master and slave images are selected. While the patch size defines the area of master image values to match, the search area defines the maximum offset of the patch in the slave image. We applied least squares matching with a patch size of 150 x 150 pixel and a search area of 50 x 50 pixel on hillshade images with 0.5 x 0.5 m resolution, resulting in a patch size of 75 x 75 m and a search area of 25 x 25 m.

3.2.3 Volumetric surface changes

Besides analysing the horizontal displacements of the rock glacier, short-term surface elevation changes between two times can be used to approximate the geodetic mass balance of a rock from photogrammetric investigations (Kääb et al., 1998; Kääb et al., 1997) or dGNSS measurements (Konrad et al., 1999).

The production of multi-temporal DEMs allows for the calculation of volumetric surface changes between consecutive surveys. ~~The vertical changes of the rock glacier surface area over the periods 2016–17 and 2017–18 were estimated by subtracting surface elevations of the 2016 DEM from the 2017 DEM and the 2017 DEM from the 2018 DEM, respectively. Then, the pixel wise volumetric change was derived by multiplying the vertical changes of each raster cell by cell size. The total positive and total negative volumetric changes (bar graphs in Fig. 4) for the different geomorphological units of Dos Lenguas (Fig. 1b) were summed up to derive negative and positive volumetric changes of the respective surface areas. The total volumetric net changes of the geomorphological units are the sum of positive and negative volumetric changes in the respective surface areas. The density of ice (900 kg m⁻³) was used to estimate the corresponding net change of ground ice, which is given as water equivalent (1 mm yr⁻¹ corresponds to 1 kg m⁻² yr⁻¹) for each geomorphological area except for the side and front slopes. Therefore, it was assumed that the net changes in ground ice are mainly caused by volume expansion due to freezing of water and volume reduction due to melting of ground ice or thawing of ice-supersaturated permafrost. The net change in ground ice content per year was interpreted as a first order estimate of the interannual water storage change. The volumetric changes over the periods 2016–17 and 2017–18 are estimated by subtracting surface elevations of the 2016 DEM from the 2017 DEM and the 2017 DEM from the 2018 DEM, respectively and multiplying by the cell sizes. First order estimates of interannual water storage changes are derived, assuming that the sum of positive and negative volumetric changes which does not equal zero (net balance over one year stated as water equivalent) is mainly caused by melting or gaining ground ice at the transition from the active layer to ice-rich permafrost in the rock glacier. This assumption implies that spatial variations of the flow regime, bulk density changes of debris, and edge effects of surface areas of the rock glacier are included in total volumetric net changes, but potentially of minor importance for the considered time scale.~~

Different sources of error might complicate the interpretation of volumetric surface changes, amongst these errors are dGNSS measurements, manual ground control points tagging, aerial image quality, interpolation algorithms and others (Wheaton et al., 2010). Therefore, a minimum level of detection (LoD) was calculated that incorporates propagated uncertainties from individual DEMs and determines a threshold to discriminate significant changes from non-significant noise. Following Brasington et al. (2003) we define the minimum LoD using Eq. (1):

$$LoD = t \sqrt{\sigma_{DEM_i}^2 + \sigma_{DEM_{i+1}}^2}, \quad (1)$$

where t is the critical value of a given confidence interval in a two-sided student's t-distribution and σ is the ~~standard deviation of the error associated with of the DEM, from two epochs calculated from the average reprojection error of 34 ground control points for epochs i and $i+1$. To yield rather conservative estimates of surface changes, we used the root mean square error (RMS) of the individual DEMs as a surrogate for standard deviation. Raster values less than the (Table 5) and masked out values $>LoD$ and $<-LoD$ were later excluded from the calculation of the total positive and total negative volumetric changes of the respective surface areas (Fig. 4, Table 5) for all volumetric calculations.~~

3.3 Geophysics

2-D Electrical resistivity tomography (ERT) and seismic refraction tomography (SRT) were conducted along identical long- and cross-profiles on the Dos Lenguas rock glacier (Fig. 1b) to image the internal structure (~~Hauck and Kneisel, 2008; Kneisel et al., 2008~~) and to quantify its material composition based on a petrophysical model, the so-called Four-Phase Model (4PM, see below) (Hauck et al., 2011). ~~Previous studies on the internal structure of rock glaciers have revealed large~~

~~spatial heterogeneities in material composition within single landforms (Emmert and Kneisel, 2017; Hausmann et al., 2012; Monnier and Kinnard, 2013; Springman et al., 2012).~~

The layout and survey geometry of the profiles were chosen according to the surface morphology of the rock glacier (Fig. 1b): (i) to gather subsurface properties in the four main structural units of the rock glacier i.e. the root zone (profile C1), the central part (profile C2) and both tongues (profiles L1, L2), (ii) to include longitudinal profiles and cross-profiles, which cover side slopes; (iii) to survey perpendicular to potential water pathways (Langston et al., 2011) and water traps indicated by depressions and local slope of surface topography.

3.3.1 Electrical resistivity tomography (ERT)

Subsurface resistivity is measured by injecting direct current into the ground through two electrodes while measuring the potential difference between two other electrodes coupled to the ground. Iterative tomographic inversions of apparent resistivities measured at different electrode locations and separations along a profile finally yield a two-dimensional model of the specific resistivity of the subsurface. The application of ERT has become a standard technique to image and monitor variations of electrical resistivity in the near subsurface of mountain permafrost due to its sensitivity to the state of water (liquid or solid) in unfrozen and frozen conditions (Hauck, 2013; Hilbich et al., 2008; Mollaret et al., 2019).

Four 2-D ERT profiles were measured with an Abem Terrameter LS system (four channels) with four cables and 81 electrodes. Sponges were placed around steel electrodes and wetted with salt water to reduce contact resistance of the dry and loose surface material (sands and pebbles to boulders) in order to improve galvanic coupling (Maurer and Hauck, 2007). Profile lengths of 240m (L1), 320m (C1), and 400m (C2 and C2) were achieved with an electrode spacing of 3m, 4m, and 5m, respectively (Table 3).

~~Multiple gradient arrays were measured along all survey lines~~ All profiles were measured with the multiple gradient array, which reached maximum penetration depths of 41m for L1, 60 m for C1 and 68 m for C2 and L2.- Before data inversion, data points exceeding the threshold of 1% of the coefficient of variation ~~have been~~ were removed.

Data inversion was done using the Res2Dinv Inversion software (www.geotomosoft.com). Default inversion settings were adapted to comply with high resistivity contrasts on the order of several magnitudes typical for permafrost environments. The robust inversion scheme (L1 norm) with no limits for the resistivity range was used as sharp boundaries and high resistivities for ice-rich permafrost were expected. The surface topography was integrated based on dGNSS measurements of each electrode along the profiles and the topographic shift of the subsurface nodes of the inversion models were exponentially damped with depth (Loke, 2018).

The mean absolute misfit error of the inversion model is given by the difference between calculated and measured apparent resistivity of the model blocks (~~Table 2~~) (Loke, 2018). Data outliers of measured apparent resistivities were filtered using a filter criterion of RMS error >100% after a first inversion run before the inversion was repeated with the filtered data set (Loke, 2018). In total, 92% of all gathered data points were used after filtering (Table 3).

3.3.2 Seismic refraction tomography (SRT)

Significantly different elastic properties between the frozen and the unfrozen state of the subsurface can be measured using its P-wave velocities. ~~Similar to the electrical properties, also the elastic properties of the subsurface, measured through its seismic p-wave velocity, are markedly different between frozen and unfrozen state.~~ P-waves are refracted at subsurface layers with velocity contrasts. Subsurface layers and structures can be delineated by analysing first-arrival times at each receiver if velocities increase with depth. Velocity changes in active layer and permafrost are mainly influenced by the porosity of sediments and their saturation with air (330 m s^{-1}), water (1500 m s^{-1}) or ice (3500 m s^{-1}) and are thus more distinct in unconsolidated coarse-grained sediments than consolidated rocks (Hilbich, 2010). P-wave velocities in rock

glaciers derived from different field studies increase generally from the active layer ($<1500 \text{ m s}^{-1}$) to permafrost (range $1500\text{--}5000 \text{ m s}^{-1}$) (Draebing, 2016; Hauck and Kneisel, 2008).

Difficulties for the interpretation of structures can arise from overlapping p-wave velocities, e.g. sand ($200\text{--}2000 \text{ m s}^{-1}$) or bedrock ($1300\text{--}6200 \text{ m s}^{-1}$, cf. table A.3 in Hauck and Kneisel (2008)) and permafrost in rock glaciers ($1500\text{--}5000 \text{ m s}^{-1}$, cf. Draebing (2016)). Low-velocity layers sandwiched between or located below high velocities layers cannot be detected from p-waves (Schrott and Hoffmann, 2008). Despite the challenges in mountain permafrost terrain, refraction seismic surveys have been successfully applied on periglacial landforms like rock glaciers (Croce and Milana, 2002; Hausmann et al., 2007; Ikeda, 2006; Musil et al., 2002; Schrott, 1996), moraines (Langston et al., 2011), talus slopes (Otto and Sass, 2006) and debris-covered slopes (Hilbich, 2010)

We used a 24-channel Geode (Geometrics) with 14 Hz Geophones to record seismic waves with a sample interval of 0.125 ms and five stackings per shot point. A sledge hammer (7.5 kg) and an aluminium plate were used to generate p-waves. Eight to ten in-line shots and three to six offset shots were measured for each layout before “rolling” on. The geophone spacing range between 3–5 m ~~in alignment with according to~~ the spacing of the ERT profiles, as electrode positions were used for geophones to ensure consistent sensor positions within the same geophysical profile (Table 4Table 3). The complete data processing workflow, including first arrival picking, travel time analysis and data inversion, was performed with the ReflexW software package that uses an inversion algorithm based on the simultaneous iterative reconstruction technique (Sandmeier, 2016). Profile topography and an initial velocity gradient of $300 \text{ m s}^{-1}\text{m}^{-1}$ were integrated in all start models. The reliability of the tomograms is given by the RMS and by the sum of the total absolute time differences between observed and calculated travel times (Table 4Table 3) (Sandmeier, 2016).

3.3.3 Four-phase-model (4PM)

In order to quantify the material composition of the rock glacier, the complementary ERT and SRT field data were combined in the 4PM to estimate the volumetric fractions of ice, water, air and rock based on petrophysical relationships. Using the ERT-derived inverted specific resistivity distribution ρ and the P-wave velocity distribution from SRT, the 4PM determines the volumetric fractions of liquid water (f_w), ice (f_i), and air (f_a) within the ~~available predefined porosity pore space (ϕ) of the rock fraction (f_r) (or porosity, $\phi=1-f_r$, where f_r is the rock fraction)~~ by assuming that the sum of all fractions equals 1 in each model cell of the 2-D model domain (Hauck et al., 2011):

$$f_w + f_i + f_a + f_r = 1 \text{ with } 0 \leq f_w, f_i, f_a, f_r \leq 1 \quad (2)$$

In its simplest version, the estimation of f_w in the 4PM is based on Archie’s law that relates the measured and inverted electrical resistivity ρ (in Ωm) of sediments to the resistivity of pore water ρ_w , the porosity ϕ and the saturation with water

S_w :

$$\rho = \alpha \rho_w \phi^{-m} S_w^{-n} \quad (3)$$

where α (~~dimensionless factor~~), m (cementation index) and n (saturation exponent) are empirically determined parameters of the host material (Archie, 1942). This petrophysical relation is assumed to be still valid in partly frozen material and permafrost close to 0°C , where unfrozen water can still be present (Hauck et al., 2011). Regarding the seismic velocities, the 4PM incorporates and extends the time-average equation of Timur (1968) to four phases:

$$\frac{1}{v} = \frac{f_w}{v_w} + \frac{f_r}{v_r} + \frac{f_i}{v_i} + \frac{f_a}{v_a} \quad (4)$$

where v is the obtained p-wave velocity of the bulk material and v_w , v_r , v_i and v_a are p-wave velocities of water, rock, ice and air, respectively (Hauck et al., 2011). Equations (2), (3), and (4) can be combined and solved for f_w , f_i , and f_a by replacing $\phi = 1 - f_r$ and $S_w = f_w / \phi$ in equation (3) to give:

$$f_w = \left(\frac{\alpha \rho_w (1-f_r)^n}{\rho (1-f_r)^m} \right)^{1/n} \quad (5)$$

$$f_i = \frac{v_i v_a}{v_a - v_i} \left[\frac{1}{v} - \frac{f_r}{v_r} - \frac{1 - f_r}{v_a} - \left(\frac{\alpha \rho_w (1 - f_r)^n}{\rho (1 - f_r)^m} \right)^{1/n} \left(\frac{1}{v_w} - \frac{1}{v_a} \right) \right] \quad (6)$$

$$f_a = \frac{v_i v_a}{v_i - v_a} \left[\frac{1}{v} - \frac{f_r}{v_r} - \frac{1 - f_r}{v_i} - \left(\frac{\alpha \rho_w (1 - f_r)^n}{\rho (1 - f_r)^m} \right)^{1/n} \left(\frac{1}{v_w} - \frac{1}{v_i} \right) \right]. \quad (7)$$

~~The Thus, equation Eqs. (5–7) allow to calculate the fractions-fractions f_w , f_i , and f_a based on the input data ρ and v from ERT and SRT, respectively if the other~~

~~material properties (ϕ , ρ_w , m , n , v_w , v_r , v_i , and v_a , cf. Table 5) are prescribed. The p-wave velocities v_w , v_r , v_i , v_a and the free parameters in Archie's Law α , m and n were taken from literature and kept constant in the model scenarios.~~

~~The p-wave velocities v_w , v_i and v_a are known material properties and were taken from previous studies in periglacial environments (Hauck and Kneisel, 2008). The p-wave velocity v_r of the frozen volcanic rocks components was assumed to be 6000 m s^{-1} , since comparable frozen or unfrozen rock types range between 4000 m s^{-1} to 7000 m s^{-1} (Draebing, 2016; Schön, 2011) and the sensitivity of the 4PM is very low for variations in v_r (Hauck et al., 2011). The free parameters m , and n in Archie's Law were adopted from studies that have been successfully conducted in different mountain permafrost environments (Pellet et al., 2016), including different rock glaciers (Hauck et al., 2011; Mewes et al., 2017; Schneider et al., 2013) or have been tested for unfrozen and frozen sands (King et al., 1988). These prescribed parameters of the 4PM were kept constant in the model scenarios. The most sensitive 4PM parameters from table 5 are the porosity ϕ and the pore water resistivity ρ_w (Hauck et al., 2011). Hence, for this study model scenarios with different combinations of ϕ and ρ_w values were performed to estimate and evaluate modelled material compositions.~~

~~We used three uniform porosity models with $\phi = 30\%$, 50% , and 70% , and one mixed porosity model by integrating different porosity ranges of $45\text{--}30\%$, $75\text{--}30\%$ and $10\text{--}3\%$ for active layer, permafrost and bedrock, respectively (Table 5). Observations from drill cores have shown that volumetric ground ice content can range from 0% to 90% in ice-free, ice-poor, and ice-rich layers in rock glaciers (Haeberli et al., 1998; Krainer et al., 2017; Monnier and Kinnard, 2013). The frozen core of active rock glaciers is mainly characterized by ice-supersaturated conditions ($> 40\%$ ice content) and can contain massive ground ice. Therefore the assumed uniform 70% porosity model and mixed porosity model represent the upper bound assumptions for the 4PM modelling approach of a talus rock glacier, like Dos Lenguas. Ice-supersaturated conditions could be expected for volumetric ice content greater than 40% , since the dominant grain sizes of Dos Lenguas are sands and pebbles (Schrott, 1994). The 30% and 50% porosity models allow volumetric ice content less than 30% and 50% , given that the voids in rock glaciers and the 4PM contain also water and air. Therefore the latter porosity models would be suitable for an inactive or intact rock glacier, which does presently not move, as the creep of frozen soils is restricted by interlocking particles without ice-supersaturated conditions (Arenson et al., 2002; Arenson and Springman, 2005). The spatial arrangement of mixed porosities was deduced from interpretations of the ERT and SRT data. Negative depth gradients ($0.01\text{--}0.03 \text{ m}^{-1}$) were included to simulate substrate compaction with depth, while allowing higher volumetric ice content in the upper permafrost part of the frozen core of the rock glacier. Porosity assumptions for geophysical models are further discussed by Mollaret et al. (2020), who also found porosity values of $30\text{--}70\%$ for active rock glaciers based on jointly inverted data sets. The 30% porosity model is restricted to saturated subsurface conditions, whereas the other models allow supersaturated conditions.~~

All porosity scenarios were modelled for different pore water resistivities of 30 , 50 , 100 , and $200 \text{ } \Omega\text{m}$. Modelled pore water resistivities were based on in-situ measurements of specific electrical resistivity of surface waters derived from the spring ($\sim 30 \text{ } \Omega\text{m}$), thermokarst ponds ($\sim 50 \text{ } \Omega\text{m}$), and melted snow from the surface ($\sim 200 \text{ } \Omega\text{m}$). A fourth value $100 \text{ } \Omega\text{m}$ was assumed to represent an intermediate model response to snow-derived groundwater increasing its conductivity during percolation.

The 4PM model results were evaluated based on two criteria. First, we used the ratio of the number of model cells with physically consistent solutions (i.e. which satisfied equation (2)), to the total number of model cells as proxy for the

suitability of the sensitive 4PM parameters Φ and ρ_w . Second, the model results were qualitatively compared to check plausible material compositions in permafrost and active layer during summer thaw, e.g. whether ice ~~contents~~content in permafrost ~~is~~are sufficient to allow creep deformations and whether model results indicate unreasonable ice contents near the surface, i.e. active layer depths. After the evaluation, plausible conservative and maximum scenarios were chosen in order to estimate ranges of the ~~potential long-term~~total ice content of Dos Lenguas and the liquid water content at the end of the thaw season. The mean volumetric fractions of water (mean f_w) and ~~f_i and f_w~~ ice (mean f_i) of all model cells located below the rock glacier surface of each profile (4PM model cells below side slopes and outside the rock glacier were excluded at profile C1 and C2) were converted to mass using densities of 997 kg m^{-3} and 900 kg m^{-3} for water and ice, respectively. The mean mass of ice and water content along the profiles C1 (root zone), C2 (central area), L1 (northern tongue), and L2 (southern tongue) were extrapolated to the mean depth of ice-rich permafrost of each profile and to the respective surface area of the geomorphological units (Fig. 1b). ~~The fractions f_i and f_w were converted to mass using densities of 997 kg m^{-3} and 900 kg m^{-3} for water and ice, respectively.~~ The error estimation for the mean ice and water content in Dos Lenguas was calculated by linearly propagating the uncertainties of (i) the mean f_w and the mean f_i of all used model cells of each profile; (ii) mean ~~model~~-depths of ice-rich permafrost-profile; and (iii) two percent error attributed to the mapped surface areas derived from the high-resolution DEM.

Besides the quantification of the material composition, the 4PM was used to infer the internal hydrologic structure of the rock glacier from the spatial distribution of ice and water content per porosity, i.e. ice and water saturations, along the profiles. The resolution capacity of water and ice content along 4PM profiles was previously tested by Mewes et al. (2017) using synthetic models and field data to assess detectable hydrological structures in rock glaciers.

4 Results

4.1 Horizontal surface displacements

The Dos Lenguas rock glacier shows a heterogeneous pattern of horizontal surface displacements that are consistent in both direction and magnitude for the two epochs (Fig. 3). Generally, surface velocities fall between a few decimetres and two metres per year and decrease downslope and laterally from the central flowlines towards the side slopes. Highest surface speeds of $1.5\text{--}2 \text{ m yr}^{-1}$ are attained along the central flowline of the root zone, where surface morphology is dominated by longitudinal ridges and furrows indicating extensional flow in mainly western direction. Surface movements remain between $1.5\text{--}2 \text{ m yr}^{-1}$ in the upper central part, while the flow direction slightly turns to west-southwest. Grading into the southern tongue of the rock glacier, surface displacement decreases only moderately to between $1\text{--}1.25 \text{ m yr}^{-1}$ and bends towards southwest. In contrast to this, the boundary between the central part and the northern tongue is much sharper. Here, the flow continues in west-southwest direction and immediately drops down to below 0.75 m yr^{-1} . Approaching the front of the northern tongue, surface displacement accelerates again, reaching velocities of up to 1.25 m yr^{-1} . Opposed to this, the southern tongue further bends towards south-west keeping relatively high surface displacement rates between $1\text{--}1.5 \text{ m yr}^{-1}$ before slowing down to $0.75\text{--}0.5 \text{ m yr}^{-1}$ on top of the frontal slope. Consistently on both frontal slopes, however, displacement rates rapidly decrease downwards from approximately 1 m yr^{-1} to below the LoD.

The horizontal surface displacement rates confirm the active state of Dos Lenguas, while the displacements of ground control points with rates smaller than LoD and random bearings (Fig. 3) underline the inactive state of the rock glacier part north of dos Lenguas classified from surface morphology (Schrott, 1996).

4.2 Volumetric changes

For two epochs, 2016–17 and 2017–18, we calculated vertical surface changes and corresponding volumetric changes for the five morphological units of the Dos Lenguas rock glacier. The spatial pattern of interannual positive volumetric changes

405 ~~along the front of the transverse ridges and negative volumetric changes on the back of the transverse ridges indicate the advance of the surface of the rock glacier. The spatial pattern of paired positive and negative annual volumetric changes of the surface mirrors the downslope deformations of the rock glacier~~ (Fig. 4). The highest amounts of ~~these~~ paired positive and negative ~~volumetric~~ changes correlate spatially ~~in-to~~ the lower central area and along the southern tongue where strongly developed transverse ridges and furrows match with high horizontal displacements (cf. Figs. 3, 4). Although the highest displacement rates occurred in the root zone, volumetric changes are less pronounced here, as surface topography is characterized by longitudinal ridges and furrows. Conversely, weaker volumetric changes occurred also on the northern tongue, where slower movements of the transverse ridges predominate. ~~At the upper frontal slopes, negative volumetric changes delineate linear erosion at upper frontal slopes. Superimposed is a positive volumetric changes of the upper front slopes on the upper front slopes, which reflects the advancement and over-steepening of the active rock glacier above the shear layer, which is also visible on the aerial images at the front slope~~ (cf. Figs. 2a, 3, 4). ~~while positive changes show debris transport and accumulation further downslope at the lower parts of the frontal slopes of the Northern tongue. Negative volumetric changes delineate superimposed linear erosion features at the upper frontal slopes. Positive volumetric changes below the shear layer show downslope transported and accumulated debris at the front slopes.~~

If the volumetric changes of the surface topography were produced solely by the interannual forward movement, the sum of ~~total~~ positive and negative volumetric changes, ~~i.e. the geodetic net balance~~, should be close to zero within the given uncertainties. However, the ~~absolute total~~ positive and negative volumetric changes yielded different magnitudes for the ~~total~~ rock glacier surface (excluding front and side slopes) and the different ~~geomorphologic~~ units during the observation periods (cf. ~~bar plots-graphs~~ in Fig. 4). Thus, annual ~~net changes of the ground ice content~~ ~~net balances of positive and negative volumetric changes~~, i.e. volumetric gains and losses of ice, were estimated as a first order estimate of the interannual water storage changes ~~of the active layer~~ given in water equivalents (~~Table 6~~Table 5). ~~These interannual storage changes could be also interpreted as mean active layer depth variations above ice rich permafrost for the respective surface area and observation period. The sum of the total volumetric changes in all geomorphological units (excluding the areas of the front and side slopes) gives an annual net change in ground ice of -36 mm yr⁻¹ and +27 mm yr⁻¹ in the years 2016-17 and 2017-18 respectively, with a confidence interval of 95% (Table 6~~Table 5). ~~The volumetric changes of the rock glacier surface (excluding side and front slopes) signal an annual net balance of -36 mm yr⁻¹ and +27 mm yr⁻¹ in 2016-17 and 2017-18, respectively, regarding with a 95% confidence interval (Table 5).~~

430 The spatial differences in the first observation period 2016–17 indicate major ice losses of -61 mm yr⁻¹ in the central area and moderate losses between -23 and -30 mm yr⁻¹ in the other ~~geomorphological units~~units. During the second period 2017–18, the central part, northern tongue, and southern tongue, gained 14 mm yr⁻¹, 45 mm yr⁻¹, and 30 mm yr⁻¹, respectively, while gains of 4 mm yr⁻¹ indicate almost equilibrium conditions in the root zone. Thus, based on the 95% confidence interval, the total net ~~change of the ground ice balance~~ between March 2016 and March 2018 indicates ice losses of -23 mm yr⁻¹ and -47 mm yr⁻¹ in the root zone and central part, respectively, ice gains of 22 mm yr⁻¹ on the northern tongue, and equilibrium conditions with 0 mm yr⁻¹ for the southern tongue.

The robustness of volumetric estimates was ~~asere~~ assessed by calculating LoDs based on different confidence intervals as input to Eq. (1), using ~~t-values~~ ~~student~~student ~~t's~~ ~~t-distribution~~ (~~Table 6~~Table 6Table 5, Fig. 4). Most of the revealed vertical changes from 2016–17 had high limits of detection from 0.232 to 0.576 m for the 70 to 99% confidence intervals, respectively. In contrast, vertical changes from 2017 to 2018 had very narrow limits of detection between 0.073 and 0.183 m for the 70 to 99% confidence intervals, respectively. ~~Thus, even minor surface changes below 0.18 m were detected with high confidences giving high spatial resolutions for the period 2017-18. Thus, detected volumetric changes between for 2017-and 20-18 can be regarded as more reliable due to their higher accuracy. The lower accuracy of LoD for the period 2016-17 2016-17 might be related to bulging effects causing spatial errors (Mosbrucker et al., 2017) in the central part of the 2016 DEM due to technical difficulties during dGNSS measurements of central ground control points. However,~~

the 95% and 99% confidence intervals yielded still comparable magnitudes of volumetric changes for both periods and give rather conservative estimates of volumetric changes for both periods. The derived amounts of interannual storage changes considered as mean depth variations of the active layer indicates potential changes in the range of a few centimetres per year above ice-rich permafrost, even though the detected changes are predominantly related to the ridge and furrow topography. If the amounts of interannual storage changes are considered as mean depth variations of an ice-rich permafrost table, they would mean the growth or melting of ground ice at the top of frozen core by several centimetres per year. Observed wet active layer conditions above ice-rich permafrost during the summer thaw in our study and other studies (Arenson et al., 2010; Croce and Milana, 2002; Kenner et al., 2019) add to the interpretation that active layer and ice-rich permafrost tables are potential sinks and sources of interannual storage changes. Yet, the interannual growth and decay of ground ice in and around other parts of the rock glacier could add to the interannual water storage changes. The estimated magnitudes of interannual changes seem reasonable given the high variability of mountain weather conditions, micro-topographic effects, and strong influence of incoming solar radiation potentially controlling local active layer variations on rock glaciers in the Upper Agua Negra catchment (Schrott, 1998).

4.3 Internal structure, ice and water ~~contents~~content

4.3.1 ERT results and interpretations

The inversion results of all ERT data show a heterogeneous distribution of high, intermediate and low specific resistivities in the rock glacier (Fig. 5). High resistivity zones ($> 10^4 \Omega \text{ m}$) are mainly located underneath ridges of the rock glacier reaching depths of 10–30 m below the surface. Low resistivities ($< 10^3 \Omega \text{ m}$) predominantly occur in and near topographic depressions close to the surface in all profiles or below high resistivities at depths of approximately 40 m in both cross-profiles (C1 and C2) and below depths of 35 m in the longitudinal profile L2 (Fig. 5)

According to the heterogeneous pattern of resistivity ranges as well as field observations of the surface debris along the profiles, the resistivity ranges were interpreted ~~as follows; to be invoked by variable active layer and permafrost conditions:~~

(i) Low electrical resistivities ($< 10^3 \Omega \text{ m}$) correspond to unfrozen and wet subsurface conditions; (ii) High electrical resistivities ($> 10^4 \Omega \text{ m}$) close to the surface show dry unconfined sands and/or coarser debris with large voids, while high electrical resistivities ($> 10^4 \Omega \text{ m}$) in the subsurface indicate rather ice-rich permafrost in the rock glacier. ~~Thus, it has to be noted that the delineated structures of active layer and permafrost might be invoked by various substrate characteristics (lithology, grain sizes, porosities), different fillings of voids by ice, water and air and the subsurface temperature regime. Yet, thus, we interpret the ed structures indicate that~~ active layer ~~to be is~~ mainly characterised by very dry debris of ridges

and locally wet conditions located in longitudinal and compressional furrows or in topographic depression between side slopes and talus slopes of the rock glacier (Fig. 5). Direct proof of wet active layer conditions is given at L1 where melt water ponds are present in furrows next to the profile (Fig. 2d) on the northern tongue. ~~However, h~~Horizontal and vertical contrasts and anomalies of resistivity ~~did~~ permitted a clear delimitation of the permafrost body in the rock glacier. ~~Resistivities from 10^3 and $10^4 \Omega \text{ m}$~~ Lower electrical resistivities below depressions and furrows could indicate higher water and/or lower ice content in the rock glacier due to percolating water and/or local permafrost degradation between interpreted ice-rich permafrost ($> 10^4 \Omega \text{ m}$) (Fig. 5). Ice-rich permafrost shows large vertical variations and increasing thicknesses of 10–20 m, 15–25 m, and 15–30 m in the root zone, central area and both tongues, respectively. As the electrical conductivity (=1/resistivity) is mostly sensitive to liquid water content, it remains inconclusive if higher resistivities ~~may be~~ are caused by air or ice filled voids. Additionally, inversion model sensitivity decreases with depth and towards lateral borders of the ERT, and high resistivity contrasts can cause inversion artefacts in the model (Hilbich et al., 2009; Maescot et al., 2003).

Nevertheless, the mean thickness of ice-rich permafrost was roughly approximated from the vertical dimensions of high resistivities zones $15 \pm 5 \text{ m}$, $20 \pm 5 \text{ m}$ and $22 \pm 7 \text{ m}$ in the root zone, central area and both tongues, respectively (cf. interpreted structures in Fig 5).

4.3.2 SRT results and interpretations

490 All SRT profiles reveal a horizontal two layer structure of smoothly increasing p-wave velocities with depth (Fig. 6). P-wave velocities $<600 \text{ m s}^{-1}$ of the active layer reflect dry unconfined sands and pebble to boulder sized material close to the surface ($<3 \text{ m}$ depth). Increasing velocities up to 1500 m s^{-1} at depths of 3–8 m indicate a more compacted and/or moister sandy material above the permafrost table. Inverted p-wave velocities of the lower layer have a wide range from 1500–5000 m s^{-1} thereby showing spatially heterogeneous velocity distributions. The upper low velocity layer ($<1500 \text{ m s}^{-1}$)
495 ~~indicates was interpreted to represent~~ unfrozen areas, while the intermediate to high velocity layer (1500–4500 m s^{-1}) ~~indicates is interpreted as~~ permafrost. The gradually increasing p-wave velocities are partly vertically incised between higher p-wave velocities (cf. 2000 m s^{-1} isoline in Fig. 6) indicating ~~thea~~ transition from unfrozen debris to ~~thawing~~ permafrost between 1500–2000 m s^{-1} during summer ~~thaw~~ which has been observed on previous seismic surveys of rock glaciers in the study area (Croce and Milana, 2002; Schrott, 1994). The p-wave velocities of the transition area ~~around the~~
500 ~~permafrost table~~ could either indicate ~~the presence of higher~~ water ($v_w = 1500 \text{ m s}^{-1}$) and lower ice content and/or be related to the vertical resolution of the smoothly inverted p-wave velocities.

Higher velocities ~~indicate were interpreted as~~ ice-rich permafrost (2500–4500 m s^{-1}) and bedrock occurrences ($> 4500 \text{ m s}^{-1}$), where Dos Lenguas starts to split up (cf. Figs. 6b, 6c) and below the talus slope next to the root area (cf. Fig. 6a). However, a reliable discrimination between frozen unconsolidated rocks, and bedrock is difficult due to the large
505 overlapping p-wave velocity ranges of permafrost (Draebing, 2016; Schrott and Hoffmann, 2008), ~~and~~ volcanic rocks (Schön, 2011), and the limited resolution capacity in the lowest parts of the models.

~~Due to the ambiguities of velocity patterns and resistivity distributions, the spatial delineations differ in some areas of the independently interpreted structures in the SRT and ERT profiles (cf. spatial variations of ice-rich permafrost and active layer in Figs. 5 and 6). However, the comparison of SRT and ERT profiles also shows similar spatial patterns in the interpreted structures. Especially vertical structures and anomalies are displayed along all profiles (cf. Fig 5, 6). Both methods locally indicate the influence~~ presence of water in unfrozen areas potentially affecting permafrost composition underneath. For example, vertical structures are indicated along cross-profile C2 between 150 and 200 m (cf. Fig. 5b, 6b), where open crevasses on the surface show the rupturing of the rock glacier core and expose fine material (Fig. 2b) and where meltwater and groundwater could percolate.

510 ~~Comparing the velocity patterns to resistivity distributions show similar vertical structures and anomalies, e.g. along cross-profile C2 between 150 and 200 m (cf. Fig. 5b, 6b) where open crevasses expose fine material due to the rupturing of Dos Lenguas (Fig. 2b). However, large variations of active layer depth could be interpreted due to heterogeneous patterns observed in ERT and SRT. Yet, both methods locally indicate the influence of water in unfrozen areas potentially affecting permafrost composition underneath.~~ Interpreted bedrock structures from SRT were transferred to the mixed porosity model
515 of the 4PM. The combined interpretation of ERT and SRT data is given in the following section.

4.3.3 4PM results and interpretations

The 4PM was applied to quantify the ice and water content of Dos Lenguas based on complementary ERT and SRT measurements. ~~The model area and depth of the 4PM was spatially limited by the SRT data sets, due to the lower penetration depth of the p-waves compared to the resistivity measurements along the profiles.~~ The porosity variations of ice-rich
525 permafrost and bedrock structures that were found within the interpreted ERT and SRT profiles were built into the ~~this “best guess”~~ mixed porosity model. The spatial distribution of the ice and water ~~contents~~ content per porosity, i.e. the ice saturation and the water saturation, ~~can was then be further~~ used to estimate the internal hydrological structure of the rock glacier. In general, the 4PM results show the heterogeneous material composition in the rock glacier (Fig. 7) ~~Figs. 7, 8). The volumetric fractions of ice and water per porosity, i.e. the ice saturation and the water saturation, along the profiles are shown in the~~
530 ~~supplements for all porosity scenarios (Figs. S1-S16).~~

Along all profiles, ~~modelled the mean vertical fractions of ice content~~ ($f_{i,vrt}$) and ~~the mean vertical fraction of water content~~ ($f_{w,vrt}$) of all scenarios show increasing volumetric ice content with higher porosity and increasing volumetric water content with higher pore water resistivity, respectively (Fig. 7). Modelled mean $f_{i,vrt}$ ~~over the full model depth~~ show local maxima, where reduced ice ~~contents~~ ~~occur~~ along the profiles. Mean $f_{i,vrt}$ range roughly from 5 to 15%, 20 to 30%, and 40 to 50% for the uniform porosity models with 30%, 50%, and 70% porosity, respectively. The mixed porosity model yielded intermediate volumetric ice content values that range between the uniform 50% and 70% porosity models. The comparison of the mean vertical ice content ($f_{i,vrt}$) along the profiles indicates that the model scenarios with porosities lesser or equal than 50% do not yield ice-supersaturated conditions in the rock glacier.

The 4PM scenarios using the highest porosities and lowest pore water resistivities yielded the highest quantities of physically consistent numerical solutions, whereas scenarios with lower porosities and higher pore water resistivities yielded the lowest quantities of physically consistent numerical solutions (Table 7Table 6). Thus along all profiles, the scenario using $\phi_{uniform} = 70\%$ and $\rho_w = 30 \Omega m$ yielded the highest amount of physical consistent model solutions giving the highest volumetric ice ~~contents~~ and lowest mean fraction of water. However, despite resulting in maximal physically consistent model solutions for all profiles, the respective model results showed substantial ice contents within the active layer close to the surface, which is clearly unrealistic. Hence, the model scenario using variable porosities for active layer, permafrost and bedrock were interpreted as most plausible. This mixed porosity model provided conservative estimates for f_i , since these scenarios prevent overestimations caused by uniform porosity assumptions. Likewise, pore water resistivities of 30 Ωm and 50 Ωm were interpreted as most plausible, as the scenarios using higher pore water resistivities reduced the ice content, while the modelled water content in active layer and permafrost were unreasonable high for the dry mountain environment. Thus, lower solved model cell ratios, relative low mean ice ~~contents~~ (<40%), and unreasonable high water ~~contents~~ of the 4PM scenarios with $\phi \leq 50\%$ and $\rho_w \geq 100 \Omega m$ were interpreted as not suitable and less plausible for an active rock glacier with displacement rates up to 2 m yr⁻¹. Consequently, the scenario with $\phi_{uniform} = 70\%$ and $\rho_w = 30 \Omega m$ was interpreted as maximum model for the ice content estimation, while the scenario with ϕ_{mixed} and $\rho_w = 50 \Omega m$ represents conservative ice content estimates along the profiles. Based on these scenarios, the calculated mass of ice and water in the rock glacier ranges from 1.71×10^9 kg ($\pm 42\%$) to 2.00×10^9 kg ($\pm 44\%$) and from 0.36×10^9 kg ($\pm 32\%$) to 0.43×10^9 kg ($\pm 32\%$), respectively (Table 7Table 6).

The ~~modelled volumetric~~ fractions of ice and water ~~content~~ per porosity, i.e. the ice saturation and the water saturation, were used to infer the internal hydrological structure of Dos Lenguas towards the end of the thaw season (Fig. 8), as they indicate the spatial distribution of active layer, ice-rich permafrost, and areas influenced by shallow groundwater pathways and storages for the scenario with ϕ_{mixed} and $\rho_w = 50 \Omega m$ (~~figures of all modelled scenarios are shown in the supplements (S1)~~). Ice-free model cells indicate the active layer depth above model cells containing ice. Ice saturation ~~per porosity~~ varies spatially strongly from ~30% to 90%. Modelled ice-rich permafrost ($f_i > 40\%$) is dissected by permafrost conditions with lower volumetric ice saturations ($f_i < 40\%$). Water saturations ~~larger than >102510%~~ show locations with moist to saturated conditions that occur preferentially beneath and close to depressions of longitudinal and transvers furrows. Water saturations ~~<less than~~ 10% indicate either relatively dry conditions of the active layer close to the surface or minor amounts of liquid water in permafrost. ~~A high water saturation (> 25%) indicates were interpreted to function as potential seasonal groundwater pathways and water traps in the rock glacier during summer thaw in potentially unfrozen areas ($f_i = 0$). no ice content~~ Model areas with low volumetric ice content ($f_i < 40\%$) and increased water saturation (> 10%) could indicate that the frozen core of the rock glacier thaws locally during summer and therefore functions as an aquitard.

The spatial occurrence of increased ~~ground water~~ groundwater ~~contents~~ and ~~the visible~~ thermokarst ponds indicate a strong influence of the ridge and furrow topography on the water pathways and traps within the rock glacier (cf. Figs. 8, 9). Areas with high water saturations ~~The water content distribution of profile C1 in profile CI could in the root zone~~ indicates the presence of a perched aquifers above permafrost (e.g. at ~1560 m in profile C1, Fig.8a) ~~water pathways~~ below

575 longitudinal furrows and ~~groundwater pathways aquifers~~ from adjacent talus slopes (Fig. 9) ~~adding water to the root zone from the catchment above.~~ Profile C2 indicates water pathways in the active layer and below the northern side slope, and sub-permafrost or intra-permafrost ~~aquifers-flowpaths~~ where bedrock porosities have been implemented (Fig. 8b). Vertical structures with increased water and reduced ice saturations could indicate water pathways along crevasses in the central part of the profile, where Dos Lenguas starts to split up (Fig. 1b). The longitudinal profile L1 on the northern tongue shows water pathways and traps below compressional furrows and indicates ~~water-saturated~~ bedrock ~~aquifer~~ below ice-rich permafrost. 580 Melt water ponds next to L1 (Fig. 2) are consistent with modelled shallow ~~ground-water~~~~groundwater~~ content in the depressions. Profile L2 on the southern tongue indicates ~~aquifers-water pathways~~ between compressional ridges in the active layer and ~~an-aquitard-increased water saturations~~ between ice-rich permafrost. More details on the internal hydrological structure are discussed below in combination with interannual surface changes of the rock glacier.

5 Discussion

5.1 Methodological discussion

5.1.1 Volumetric changes

The sum of positive and negative volumetric changes of the rock glacier surface gives a first order estimate of interannual water storage changes due to seasonal freeze and thaw processes in the subsurface. ~~However,~~ ~~o~~ Our results do not show a clear signal of positive and negative interannual changes in different morphological units of Dos Lenguas over the two-year observation period (Fig. 10b). ~~Although the interannual net changes are dominated by ice gains and losses in the subsurface (Kääb et al., 1998), vertical surface changes are additionally caused by three dimensional creep deformations, accumulation and excavations, and compression and consolidation of the sediments (Kääb et al., 1997).~~

Our volumetric estimates exclude values that lie within the LoDs of respective confidence intervals, translating to cut-off limits of ± 0.368 m and ± 0.117 m for the 90% confidence interval for 2016–17 and 2017–18, respectively (Table 6). ~~Previous studies investigating the geodetic mass balance of rock glaciers have been conducted at the Gruben rock glacier (Kääb et al., 1997) and the Galena creek rock glacier (Konrad et al., 1999).~~ Assuming incompressibility of the Gruben rock glacier, vertical changes associated with the spatial variations of the flow regime have been estimated to attain magnitudes on the order of cm yr^{-1} (Kääb et al., 1997). Similarly, Konrad et al. (1999) estimated that vertical changes from differential ice gains and losses of the Galena Greek rock glacier are one order of magnitude greater than vertical changes induced by the flux of ice, assuming isotropic creep behaviour, ice thickness and no basal sliding of the rock glacier. Thus, our calculated interannual vertical changes based on LoDs are at least one magnitude greater than vertical changes expected from spatial variations of the flow regime. We are therefore confident, that ~~net balances derived from~~ volumetric surface changes reliably estimate interannual ~~water~~ storages changes dominantly associated with ice gains and losses, though these might well incorporate minor contributions from three-dimensional creep deformations and/or changes in bulk densities of the rock glacier material. ~~Although the interannual net changes are dominated by ice gains and losses in the subsurface (Kääb et al., 1998; Kääb et al., 1997), vertical surface changes are additionally caused by three dimensional creep deformations, accumulation and excavations, and compression and consolidation of the sediments (Kääb et al., 1997). The derived net changes in ground ice of -36 mm yr^{-1} and 28 mm yr^{-1} of the 95% confidence interval for the two short term observation hydrological years period resulted in rather conservative estimates if compared to observed mean annual active layer thickening of $>150 \text{ mm yr}^{-1}$ at the Morenas Coloradas rock glacier complex in the Central Andes of Mendoza between 1992 and 2007 (Trombotto and Borzotta, 2009).~~

5.1.2 Geophysical approach

The 4PM approach was applied for a first quantitative approximation of the water and ice content of the active talus rock glacier Dos Lenguas in the semi-arid Andes of Argentina. In the absence of a-priori information or calibration data from boreholes for the 4PM (Pellet et al., 2016), the most sensitive model parameters Φ and ρ_w were used to build scenarios to cover a plausible range of model estimations and to account for uncertainties arising from the heterogeneous material composition observed in drill cores of rock glaciers (Arenson et al., 2002). In combination with the large spatial coverage of the conducted 2-D geophysical surveys, this approach is considered to yield plausible ranges of ice and water contents for the whole rock glacier. Previous studies applying and testing the 4PM on rock glaciers showed that estimated ice and water contents can be reasonably well delineated and are in good agreement with nearby boreholes and complementary data sets (Hauck et al., 2011; Mewes et al., 2017; Schneider et al., 2013).

However, several limitations accompanied the geophysical approach, which are mainly caused by the inherent ambiguity of ERT and SRT inversion and the uncertainties associated with the petrophysical relationships, and their free parameters, used in the 4PM (Duvillard et al., 2018; Hauck et al., 2011; Mewes et al., 2017). In addition, the spatial resolution of the geophysical approach depends on the sensor spacing in the field in relation to the dimension of the observed layers and anomalies causing a trade-off between the spatial coverage of the landform (profile length and investigation depth) and the resolution capacity for small scale structures in the model domain. Mewes et al. (2017) showed that the resolution capacity of the 4PM is suitable to detect hydrological structures and permafrost degradation in rock glaciers with sensor spacings comparable to the spacings used in this study (Tables 3, 4). However they emphasize that the resolution capacity of vertical structures is generally good in the 4PM, whereas horizontal saturated layers may be overestimated due to inversion artefacts (Mewes et al., 2017).

With respect to the SRT input data, the accuracy or data misfit between our modelled and observed travel times of roughly 2 ms (Table 4) is in good accordance with SRT results from other permafrost investigations (Hilbich, 2010; Krautblatter and Draebing, 2014). However, modelled p-wave velocities towards the base of the tomograms are of lower confidences (Hilbich, 2010) due to generally decreasing ray densities with increasing depth that limit the interpretations of overlapping velocity ranges (Draebing, 2016; Schrott and Hoffmann, 2008) in the deepest model areas.

The overall quality of ERT data is very good considering the extreme rock glacier conditions, with mean absolute misfit errors of the inversion models between 5.1 and 7.4% and with only 7.7% filtered data points during processing (Table 3). We used the multiple gradient measurement as input for the 4PM as this configuration yields a higher spatial resolution of horizontal and vertical resistivity heterogeneities in the inversion models (Aizebeokhai and Oyeyemi, 2014) compared to the Wenner array (Dahlin and Zhou, 2004). Nevertheless, higher uncertainties remain in and below high resistive ice-rich permafrost (Hilbich et al., 2009) and towards lateral and lower boundaries of ERT profiles due to the low sensitivities in these model areas.

Vertical dimensions of water saturated horizontal layers/aquifers above the permafrost body can be overestimated in the 4PM due to inversion artefacts of ERT as demonstrated in Mewes et al. (2017). As a consequence, the thickness of the 4PM-derived water pathways or perched aquifers (Fig. 8) above aquitards and the respective calculated water contents close to the surface could be overestimated where large resistivity contrasts (Fig. 5) occur while in turn ice contents might be underestimated in these model parts. However, almost water saturated aquifer-ground conditions ($\sim 70\% f_w \Phi^{-1}$) close to the surface were only modelled at profile L2, where a thermokarst pond in the furrow next to the profile confirms saturated active layer conditions (cf. Figs. 2, 9). Besides that, only potential bedrock occurrences with low porosities indicate water saturated conditions. Although these water saturated aquifers-ground conditions could be overestimated in their vertical dimension (Fig. 8), all other interpreted aquifers-water pathways and aquitards indicate unsaturated conditions with lower fractions of water saturations below contents per porosity of $<50\%$ or $<20\%$, respectively. Concomitant-Associated with these moist conditions at the transition from active layer to permafrost, observed p-wave velocity patterns indicate relatively

655 low permafrost velocities of 1500–2000 m s⁻¹ (Fig. 6). This range of p-wave velocities correlates well with decreasing p-wave velocities of permafrost from austral summer to autumn ranging between 1500 and 2400 m s⁻¹ compared to 3400 m s⁻¹ during winter found at the neighbouring El Paso rock glacier (Croce and Milana, 2002). Thus, relatively low inverted velocities <2000 m s⁻¹ may potentially indicate the seasonal influences of permafrost thaw and increased melt water contents at the permafrost table.

660 5.2 Spatial pattern and interrelations of internal hydrologic structures and surface kinematics

In order to interrelate spatial heterogeneities of internal hydrological structures of the rock glacier during summer thaw we now focus on the individual geomorphologic units and the concurrent observed vertical and horizontal surface velocities.

5.2.1 Root zone

665 Cross-profile C1 reveals the influence of shallow ~~ground-water~~groundwater on the ice content and the internal hydrologic structure of the root zone of the rock glacier (Fig. 8a). The 4PM results suggest that the central longitudinal depression at the surface of the rock glacier (horizontal distance 150 m) acts as a trap and pathway for ground and melt water from the contributing area above. Here, the relatively high water contents in the active layer ~~isare~~ in accordance with observed wet surface debris a few hours before the field measurements due to previous precipitation and snow melt. While the rock glacier composition below this depression is characterized by reduced ice and elevated water ~~eontents~~content, areas below longitudinal ridges show ice-rich permafrost. This suggested interplay of reduced ice contents and increased water content 670 could be related to different processes: First, the highest surface velocities of 1.5–2 m yr⁻¹ occur along the central flow line characterizing an extensional flow regime with longitudinal furrows (Fig. 10). The extensional deformation potentially creates drainage pathways for melt and shallow groundwater from the active layer that infiltrates into the ground ice of the rock glacier (Ikeda et al., 2008), increasing the hydraulic conductivity of ice-rich permafrost and shifting the rock glacier 675 body from an aquiclude towards an aquitard (Fig. 8, 10). Second, increased water ~~eontents~~content could be related to local permafrost degradation, seasonal thawing or talik evolution due to localised effects of either conduction, radiation or advection effects of water or air (Haeberli et al., 2006; Luethi et al., 2017; Scherler et al., 2013). Negative and positive vertical changes in the root zone show a spatially heterogeneous pattern with ice gains and losses in 2016–17 and in 2017–18, respectively (Fig.10). Therefore, homogeneous thaw settlement can be excluded from our data over the observation 680 period 2016–2018 (Fig.4) and it is more likely that locally increased water ~~eontents~~content points to water pathways below longitudinal furrows and/or seasonal thaw effects induced by the micro-topography (Fig. 10). Besides internally developed water pathways in active layer and permafrost, subsurface compositions of adjacent side slopes illustrate the influence of ~~ground-water~~groundwater draining towards a sub-permafrost ~~aquifer~~flowpaths from the side and talus slopes below the root zone of Dos Lenguas (horizontal distances < 50 m and > 250 m in Fig. 8a). The Northern left part of the profile shows little 685 ice remnants and shallow ~~ground-water~~groundwater influences of the talus slope from the inactive rock glacier next to Dos Lenguas, while the lower parts of the southern talus slope depicts water saturated conditions for assumed bedrock porosities in the 4PM.

The generally high horizontal velocities > 1 m yr⁻¹ in the root zone compared to the other geomorphological units could be related to ice-rich permafrost above bedrock, steepest mean slopes of the surface, and might be enhanced by increased water 690 supply from the surface and catchment, which reduces resisting forces in shear layers due to positive pore water pressures (Kenner et al., 2017).

5.2.2 Central part

The influence of groundwater draining underneath the active rock glacier from the northern depression at the side slope is also suggested in the cross-profile C2 (Fig. 8b). High seismic velocities at 20 to 30 m depth below the surface indicate

695 bedrock occurrences in the lower central part of the rock glacier that were incorporated in the mixed porosity model of the
4PM, which indicates sub-permafrost water pathways in an-unfrozen and water saturated bedrock aquifer. The permafrost
body above bedrock shows vertical structures with increased water and reduced ice contents illustrating water
pathways along filled fissures and crevasses in the subsurface due to the splitting of the central rock glacier part into the
northern and southern tongues (see also vertical structures of ERT and SRT in Fig. 5b and Fig. 6b, respectively). Locally,
700 relatively high water contents could indicate channelized unsaturated aquifers-flowpaths in the southern part of the profile.
The spatial pattern of horizontal surface velocities generally shows a decelerating trend approaching the tongues (Fig. 3),
portraying the transition from extensional to compressional flow that is also expressed in a transition from longitudinal
structures to transverse ridge and furrow topography. Further downslope, the moving rock glacier mass decelerates towards
the less inclined northern tongue, while the surface velocities remain high in direction of the southern tongue. As a
705 consequence, lateral velocity contrasts of $\sim 0.5 \text{ m yr}^{-1}$ cause shear-induced tearing apart of the tongues in the lower central
part of Dos Lenguas, which is also documented by longitudinal rupturing of transverse ridges with open crevasses at the
surface (Fig. 2). These surface findings are corroborated by higher mean air contents at C2 compared to C1 (cf. Table
67 and supplements-Figs. S1-S9) indicating a thickening of the active layer and a lateral spread of the cross-section from the
root zone towards the lower central part.
710 The volumetric changes of 2017–18 are increased in the central part (14 mm yr^{-1}) compared to the root zone (1 mm yr^{-1}).
The spatial pattern of gains and losses illustrates higher volumetric changes along distinct transverse ridges and furrows in
the lower part of the central area. Besides mimicking the advance of ridges and furrows (Kääb et al., 2003; Kääb and Weber,
2004), the small scale topography might enhance differential ice gain and losses (Kääb et al., 1998) due to shading effects in
furrows preventing direct sublimation of snow and vaporisation of water. Thus, meltwater infiltration could be more efficient
715 in furrows due to micro-topographic effects. In addition, shallow groundwater drainage along furrows (4PM) could be
transferred to lower rock glacier areas and locally be trapped in the deepest parts of transverse furrows. This process is
indicated by potential aquifers-and drainage pathways along furrows in C1 and C2 and a thermokarst pond with a delta in the
central part (Fig. 2), as well as water traps in transverse furrows of both tongues (cf. Figs. 8, 9, 10).

5.2.3 Tongues

720 Below the Northern tongue our results indicate an extended bedrock occurrence from the central part further downslope. Ice-
rich permafrost is dissected by areas with high water contents, indicating aquifers-and water drainage-pathways along
furrows (cf. Figs. 8, 9). Here, 4PM results are in accordance with direct observations of thermokarst ponds occurring 20–30
m south of the profile, where meltwater is trapped and exposed at the surface in the deepest part of the furrows. This is
similar to L2 on the southern tongue, where high water contents indicates unsaturated-aquifers water pathways and
725 water traps located in depressions in front of and behind of compressional ridges. Moreover, gully like structures on the
surface perpendicular to transvers ridges and furrows indicate thermal erosion along meltwater pathways in the subsurface in
some parts of the southern tongues (cf. Figs. 2, 8, 9).

The flatter northern tongue, hosting numerous thermokarst ponds, shows the largest positive interannual storage change
2017–18 and is the only morphological unit of Dos Lenguas, which gained ice over both observation years. The steeper
730 southern tongue appeared to be in equilibrium between 2016 and 2018 with equal negative and positive interannual storage
changes of 30 mm yr^{-1} in 2016–17 and 2017–18, respectively (Fig. 10). The increasing interannual storage changes from the
root zone over the central parts to both tongues in 2017–18 could reflect the role of drainage pathways and water traps in and
along furrows. Longitudinal furrows could build more effective drainage pathways transferring meltwater inputs downslope
from steeper areas of the rock glacier. Decreasing mean surface slopes and a strong transverse ridge and furrow topography
735 might better trap and collect inputs from drainage pathways and percolating water from the surface (precipitation, snow
melt). On both tongues, shallow-aquifers water pathways and meltwater-water traps along transverse furrows (Figs. 9, 10)

overlap with the spatial pattern of locally increased volume gains and losses. Especially along transverse ridges and furrows with increased water ~~content~~, meltwater and ground ice could interact at the permafrost table, potentially causing significant amounts of volumetric changes and respective vertical changes due to the seasonal thaw of an ice-rich permafrost table and/or refreezing of a wet active layer bottom.

The clear contrast in horizontal velocities between both tongues coincides with the overall slope gradient. While the steeply descending southern tongue experiences high horizontal velocities of 0.75–1.5 m yr⁻¹, potentially enhanced by the influence of melt water, the generally flatter northern tongue, shows decelerated horizontal surface velocities (0.25–1.0 m yr⁻¹), potentially also related to bedrock obstacles at the rock glacier bed. Whereas the southern tongue decelerates towards its front, the surface velocities of the Northern tongue accelerate towards the steep frontal slope mimicking the creep behaviour of over-steepened cliffs (Cuffey and Paterson, 2010).

5.2.4 Front and side slopes

Surface velocities generally decrease towards the side and frontal slopes given the increase in friction, which indicates lower or no ice content within material accumulated at the outer margins. Lower to no ice ~~content~~ within the side slopes is also indicated in the 4PM derived material composition of the cross-profiles C1 and C2.

The advancement of the rock glacier is reflected by volumetric changes and horizontal displacement at the front slopes. Here, two superimposed processes act: First, the upper front is over-steepened (>35°) by permafrost creep, and second, gravitational processes transfer debris to lower front slope positions. The over-steepened advance of the upper slope shows increasing horizontal displacement rates towards the surface, indicating cumulative deformations of creeping permafrost.

From digital topography we further delineate the approximate depth of the shear horizon ~~and the stiff basal layer~~ below the surface (Figs. 2, 9). Derived depths of 20–25 m and 15–20 m below the surface at the northern and southern tongue, respectively, match roughly to observed depth ranges of ice-rich permafrost in ERT and 4PM profiles. Whether the stiff basal layer below the shear horizon and deeper parts of the rock glacier are frozen or unfrozen, potentially functioning as sub-permafrost aquifer (Haeberli et al., 1998), or intra-permafrost aquifers in case of talik evolution (Kenner et al., 2017; Luethi et al., 2017), remains unclear judging from our data. However, our detected depths of ice-rich permafrost and calculated ice and water ~~content~~ in Dos Lenguas are in line with borehole data from active rock glaciers in the Alps which revealed that ice-rich permafrost and internal deformations occur mainly in and above shear zones in depths of less than ~30 m (Arenson et al., 2002; Buchli et al., 2018; Haeberli et al., 1998; Kenner et al., 2017; Krainer et al., 2017). As a consequence, estimations of ice ~~content~~ in active rock glaciers should exclude side and front slopes and the depth of ice-rich permafrost should be either limited (threshold <30 m depth) or based on observations. Taking this into account could in particular improve potential estimates of regional water storage capacities of rock glaciers that were based on area thickness relationships (Azocar and Brenning, 2010; Jones et al., 2018a; Rangescroft et al., 2015) in order to avoid overestimations of ice-rich permafrost thicknesses in large rock glaciers.

Frontal advances by accumulated sediment at the frontal slopes revealed that Dos Lenguas efficiently transports sediments, deposits and overruns them. Long-term sediment transfer and slope instabilities at the front of the northern tongue (Kummert et al., 2018) could further push the Agua Negra river towards the opposite valley side, putting the pass route at risk and/or building a rock glacier dam that endangers downstream infrastructures and modulates sediment and water transfer (Blöthe et al., 2019).

5.3 Water storage capacities and interannual changes

~~In the following we interrelate water and ice storage capacities and the interannual changes for the active rock glacier. The overall long-term ice storage of this rock glacier ranges between $1.71(\pm 42\%) \times 10^9$ kg and $-2(\pm 44\%) \times 10^9$ kg based on the mean volumetric fractions of the most reasonable evaluated 4PM scenarios (Table 7). The mean volumetric fraction of water~~

at the end of the thaw period was $0.36(\pm 32\%) - 0.43(\pm 32\%) \times 10^9$ kg (Table 7). If only the mean values of the two scenarios are compared, the water content is about one fifth of the ice content. The latter estimate must be seen as an upper bound, due to the uncertainties in quantifying thin water layers from ERT data mentioned above. Therefore, the ice to water content ratios suggest that the scenario with the highest porosity and the lowest pore water resistivity provides the most plausible volumetric fractions of ice (mean f_i 24-64%) and water (mean f_w 2-15%) in the rock glacier during the end of the summer. The material composition and the potential ratios between ice and water content could mean that a relatively large amount of groundwater and meltwater is available for ice and water storage exchanges in the rock glacier at the end of the thaw period. Interannual storage changes derived from volumetric changes revealed that only 2-4% of the water content (using the mean f_w as upper bound) would be required for the ice loss during the first observation period 2016-17 or the ice gain during the second observation period 2017-18 according to the 95% confidence interval with -36 mm yr^{-1} (-8.92×10^6 kg) and 28 mm yr^{-1} (6.64×10^6 kg), respectively. The small ratio of interannual ice storage changes with respect to the 4PM-derived water content again indicates that the water content may be overestimated, due the sensitivity of the 4PM and the wet ground conditions during the geophysical measurements at the end of the thaw period. However, this small ratio could also mean that the major amount of groundwater and meltwater passes along the water pathways through the rock glacier. Nevertheless, the interannual water storage changes of -36 mm a^{-1} and $+28 \text{ mm yr}^{-1}$ of the 95% confidence interval suggest that significant amounts of mean to maximum annual precipitation of 45-140 mm and 51-168 mm (cf. Table 2, CHIRPS derived estimates (Funk et al., 2015)) could have been released and stored in the active rock glacier during the hydrological years 2016-17 and 2017-18. The mass loss of -36 mm yr^{-1} corresponds to 25-80% of the annual precipitation in the hydrological year 2016-17. The ice gain of 28 mm yr^{-1} corresponds to 17-55% of annual precipitation in the hydrological period 2017-18. Higher maximum precipitations during the latter hydrological year could have contributed to the positive interannual storage changes in 2017-18 compared to the hydrological year 2016-17. The mean annual precipitations with less than 51 mm yr^{-1} of the two hydrological years (Table 2) do not show significant differences that could explain the positive and negative volumetric net changes in ice storage, but would increase the significance of the interannual storage changes due to the dry meteorological conditions. Recorded ground surface temperatures of Dos Lenguas could indicate that the strongly fluctuating temperature regime (Fig. S17) could have additionally influenced the negative and positive interannual storage changes of Dos Lenguas in the years 2016-17 and 2017-18, respectively. During the thaw period 2016-17 the temperature profile of monthly median ground surface temperatures shows an earlier beginning and a higher summer maximum compared to summer 2017-18, which is characterized by a lower and later temperature maximum. The significantly lower amplitudes of the ground surface temperatures in winter 2016-17 compared to winter 2017-18, indicate that there was no damping of ground surface temperatures by snow in winter of 2017-18. Consequently, the generally higher ground surface temperature during austral summer 2016-17 could have led to the observed negative storage changes due to the deeper thaw penetration. In contrast, the ice gain during the hydrological year 2017-18 might have been fostered by higher precipitation, more effective penetration of cold winter temperatures and smaller active layer depths.

The ~~constant-measured~~ discharge of $5-8 \text{ l s}^{-1}$ from the Dos Lenguas spring found by Schrott (1996) would translate to a total of $64.8-103.7 \times 10^6 \text{ l}$ for a five month lasting thaw season. Due to the dry and cold meteorological conditions during winter, spring flow can be expected to be active only in summer. The discharge can be fueled by precipitation, snowmelt, melting ground ice and sub-permafrost groundwater flow in the catchment area of the spring (2.7 km^2), which includes the surface area of the rock glacier (0.36 km^2) and the contribution area of the root zone (1.01 km^2). The potential range of discharge at the spring-averaged over the catchment area of the spring corresponds to an output of 24-38 mm during thaw season. The potential discharge would thus be in the range of the mean precipitation input of 22 mm and 38 mm in the austral summer periods 2016-17 and 2017-18, respectively (Table 2). However, the higher mean and maximum precipitation of 45-168 mm of the full hydrological years 2016-17 and 2017-18 (Table 2) indicate that additional precipitation input could be released along other groundwater pathways or is temporarily stored in the hydrological system of the rock glacier and its

catchment ~~Dos Lenguas~~. The negative interannual storage of -8.92×10^6 l in 2016-17 of the rock glacier would potentially correspond to 9-14% of the total discharge at the spring ($65-104 \times 10^6$ l). The positive interannual storage change of 6.64×10^6 l in 2017-18 could have decreased the potential discharge about 6-10%. The interannual storage changes due to freezing and thawing could therefore buffer the groundwater release and add or reduce groundwater flow during the course of the year.

Finally, about 11-42 % of the mean water content of the rock glacier could nourish discharge at the rock glacier spring, since the estimated mean water content (mean f_w , corresponds to $244-570 \times 10^6$ l) was larger than the potential discharge at the spring during the thaw period. The remaining share of water content (58-89%) could leave the internal hydrological system of the rock glacier along other water pathways and/or is refilling or exchanging groundwater storages in and below the rock glacier. Comparing the potential total discharge at the spring with the total liquid water content in late summers indicates that only 14–30% of the seasonal groundwater could be transferred to the Agua Negra river, while 70–86% of groundwater could be involved in refilling and exchanging ground water storages and aquifers in and below the rock glacier. Although the several uncertainties in the estimation of the different components of the water balance have to be kept in mind, the estimated ice and water storage capacities and the interannual storage changes demonstrate that (a) an active rock glacier like Dos Lenguas could play a crucial role in buffering and regulating seasonal groundwater flow and recharge, while (b) it constitutes a long-term ice storage in the dry high mountain catchment, where currently only 2.8% of the surface area remain permanently covered with surface ice and snow.

Given the widespread distribution (IANIGLA, 2018) and the slower response of active rock glaciers (Haeberli et al., 2006) to the predicted temperature increases in the dry Andes (Barnett et al., 2005) compared to down-wasting Andean glaciers (Braun et al., 2019), our results suggests that long-term water storages and seasonal buffers in ice-rich permafrost and active layer, respectively could become more important for Andean watersheds in the future.

6 Conclusions

Water storage capacities and interannual changes were quantified for an active rock glacier in the semi-arid Andes of Argentina. For this, we interrelated surface changes and the material composition in different morphological units of the Dos Lenguas rock glacier. Based on digital elevation models and their derivatives from Structure from Motion Multi-View Stereo algorithms, horizontal and volumetric surface changes were calculated using motion tracking and Digital Elevation Models of Differences, respectively. Electrical resistivity and seismic refraction tomography data sets from field measurements were used as input data for a petrophysical model called 4-phase model (4PM). Ice and water contents were quantified based on different scenarios of the most sensitive parameters used in the 4PM. Additionally, spatial heterogeneities of ice and water contents revealed the internal hydrological structure of Dos Lenguas towards the end of the thaw season.

Based on this data set we found that increased water content in depressions and furrows, and ice-rich permafrost below ridges indicate interactions of the distinct ridge and furrow topography and the heterogeneous material composition and structures the internal hydrology in the subsurface of Dos Lenguas rock glacier. The spatial distribution of the ground ice content, especially ice rich permafrost, structures the internal hydrology of the block glacier. Water pathways and traps are hereby located above, between and below the frozen core of the rock glacier during the thaw period.

Horizontal surface deformations up to 2 m yr^{-1} prove the active status of the rock glacier. The geophysics derived aquifers in seasonal unfrozen ground, taliks and potential aquitards through thawing ice rich permafrost function as water traps and pathways during the thaw period, while the observed ground ice occurrences are structuring the internal hydrology of the rock glacier. Net

~~Gains and losses of ground ice balances~~ derived from volumetric surface changes for 2016–17 and 2017–18 give first order estimates of interannual water storage changes ~~of the active rock glacier Dos Lenguas.~~

Our findings suggest that water storage capacities and interannual storage changes can be estimated ~~using interrelations from surface and subsurface properties,~~ despite the uncertainties arising from the spatial heterogeneities and indirect measurements. We conclude that the ground ice content of $1.71(\pm 42\%) - 2(\pm 44\%) \times 10^9$ kg and the interannual water storage changes of -36 mm yr^{-1} (-8.92×10^6 kg) and 28 mm yr^{-1} (6.64×10^6 kg) of the active rock glacier Dos Lenguas represent an important long-term water reservoir and seasonal water buffer in the Upper Agua Negra valley, ~~in addition to other rock glaciers and ice rich permafrost occurrences in the Upper Negra catchment, as less than 3% of the dry mountain catchment is covered with surface ice.~~ 25-80% and 17-55% of annual precipitation may have been released and buffered buffered by inter-annual water storage changes and released during the summer period 2016-17 and 2017-18, respectively. The water content of $0.36(\pm 32\%) - 0.43(\pm 32\%) \times 10^9$ kg of the rock glacier at the end of the thaw period corresponds to 2-4% of the interannual water storage changes and 11-42% of the potential discharge at the spring. The major share of seasonal groundwater water content ~~Most of the water content could~~ may leave the internal hydrological system of the rock glacier via other water pathways. The estimated ice and water content and interannual water storage changes of the active rock glacier show exemplarily that rock glaciers and mountain permafrost can strongly influence the hydrology in sparsely glaciated and dry mountain catchments. ~~The interannual storage changes suggest that a significant portion of annual precipitation can be buffered and/or released by seasonal ground freeze and thaw processes in active rock glaciers of dry mountain catchments.~~

The detection of basal layers at rock glacier fronts may help to better constrain depths and volumes of ice-rich permafrost for different rock glacier types and sizes and could further help to calibrate area thickness relationships. Front and side slopes should be excluded from rock glacier areas to avoid overestimations of local, and especially, regional water storage estimations. This study closes an important knowledge gap with respect to the quantification of ice ~~contents~~content and water storages changes of rock glaciers in the dry Andes and can serve as a benchmark for regional ice/water estimations using rock glacier inventories.

For further understandings of rock glacier hydrology, such field-based studies and monitoring approaches are necessary to elucidate quantities and functions of long- and short-term storage changes, as well as their interactions with catchment hydrology. Especially in dry mountain catchments further insights into hydrological contributions, functions, and changes in active rock glaciers might become more important under climate change forcing rapid adaptations in the cryosphere.

Data availability. The data sets can be obtained on request to the authors.

Supplement. The supplement related to this article is available online.

Author contributions. CH designed the study, conducted field work, collected and processed geophysical and SfM data, wrote manuscript and conceptualized figures; JB collected and processed SfM data, helped with data processing, conducted field work; CTB and DT contributed to field logistics and data acquisition; CHi and CHa helped with geophysical data processing and analysis; LS conducted field work, contributed to study design, data acquisition, obtained funding; all authors contributed to the revision of the text.

Acknowledgements

This research was funded by the German Research Foundation (SCHR 648/3-1). We further thank Lorenz Banzer, Henning Clemens, Nico Griesang, Friedrich Fröhlich, Gerrit Heinmüller, Thorsten Höser, Julius Isigkeit, Martin Mendoza, Floreana Miesen, David Morche, Agostina Ortiz, and Simon Terweh for their help during field work.

References

- 905 Aizebeokhai, A. P. and Oyeyemi, K. D.: The use of the multiple-gradient array for geoelectrical resistivity and induced polarization imaging, *J Appl Geophys*, 111, 364-376, <https://doi.org/10.1016/j.jappgeo.2014.10.023>, 2014.
- Archie, G. E.: The Electrical Resistivity Log as an Aid in Determining Some Reservoir Characteristics, *SPE-942054-G*, 146, 54-62, 10.2118/942054-G, 1942.
- Arenson, L., Hoelzle, M., and Springman, S.: Borehole deformation measurements and internal structure of some rock glaciers in Switzerland, *Permafrost and Periglacial Processes*, 13, 117-135, Doi 10.1002/Ppp.414, 2002.
- 910 Arenson, L. and Springman, S.: Triaxial constant stress and constant strain rate tests on ice-rich permafrost samples, *Can Geotech J*, 42, 412-430, Doi 10.1139/T04-111, 2005.
- Arenson, L. U. and Jakob, M.: The Significance of Rock Glaciers in the Dry Andes - A Discussion of Azocar and Brenning (2010) and Brenning and Azocar (2010), *Permafrost and Periglacial Processes*, 21, 282-285, Doi 10.1002/Ppp.693, 2010.
- 915 Arenson, L. U., Pastore, S., Trombotto, D., Bolling, S., Quiroz, M. A., and Ochoa, X. L.: Characteristics of two rock glaciers in the dry Argentinean Andes based on initial surface investigations, 2010.
- Azocar, G. F. and Brenning, A.: Hydrological and Geomorphological Significance of Rock Glaciers in the Dry Andes, Chile (27 degrees-33 degrees S), *Permafrost and Periglacial Processes*, 21, 42-53, Doi 10.1002/Ppp.669, 2010.
- Barnett, T. P., Adam, J. C., and Lettenmaier, D. P.: Potential impacts of a warming climate on water availability in snow-dominated regions, *Nature*, 438, 303-309, 2005.
- 920 Barsch, D.: *Rockglaciers: indicators for the present and former geocology in high mountain environments*, Springer, 1996.
- Berthling, I.: Beyond confusion: Rock glaciers as cryo-conditioned landforms, *Geomorphology*, 131, 98-106, <http://dx.doi.org/10.1016/j.geomorph.2011.05.002>, 2011.
- Blöthe, J. H., Rosenwinkel, S., Höser, T., and Korup, O.: Rock-glacier dams in High Asia, *Earth Surf Proc Land*, 44, 808-824, 10.1002/esp.4532, 2019.
- 925 Bookhagen, B. and Burbank, D. W.: Topography, relief, and TRMM-derived rainfall variations along the Himalaya, *Geophys Res Lett*, 33, 10.1029/2006GL026037, 2006.
- Bradley, R. S., Vuille, M., Diaz, H. F., and Vergara, W.: Threats to water supplies in the tropical Andes, *Science*, 312, 1755-1756, 2006.
- Brasington, J., Langham, J., and Rumsby, B.: Methodological sensitivity of morphometric estimates of coarse fluvial sediment transport, *Geomorphology*, 53, 299-316, [https://doi.org/10.1016/S0169-555X\(02\)00320-3](https://doi.org/10.1016/S0169-555X(02)00320-3), 2003.
- 930 Braun, M. H., Malz, P., Sommer, C., Farías-Barahona, D., Sauter, T., Casassa, G., Soruco, A., Skvarca, P., and Seehaus, T. C.: Constraining glacier elevation and mass changes in South America, *Nat Clim Change*, 9, 130-136, 10.1038/s41558-018-0375-7, 2019.
- Brenning, A.: Geomorphological, hydrological and climatic significance of rock glaciers in the Andes of Central Chile (33-35 degrees S), *Permafrost and Periglacial Processes*, 16, 231-240, Doi 10.1002/Ppp.528, 2005.
- 935 Brenning, A.: The significance of rock glaciers in the dry Andes – reply to L. Arenson and M. Jakob, *Permafrost and Periglacial Processes*, 21, 286-288, 10.1002/ppp.702, 2010.
- Buchli, T., Kos, A., Limpach, P., Merz, K., Zhou, X., and Springman, S. M.: Kinematic investigations on the Furggwanhorn Rock Glacier, Switzerland, *Permafrost and Periglacial Processes*, 29, 3-20, 10.1002/ppp.1968, 2018.
- Burger, K. C., Degenhardt Jr, J. J., and Giardino, J. R.: Engineering geomorphology of rock glaciers, *Geomorphology*, 31, 93-132, [http://dx.doi.org/10.1016/S0169-555X\(99\)00074-4](http://dx.doi.org/10.1016/S0169-555X(99)00074-4), 1999.
- 940 CEAZA: Datos provistos por CEAZA, obtenidos desde www.ceazamet.cl, 2019. 2019.
- Cicoira, A., Beutel, J., Faillettaz, J., and Vieli, A.: Water controls the seasonal rhythm of rock glacier flow, *Earth Planet Sc Lett*, 528, 115844, <https://doi.org/10.1016/j.epsl.2019.115844>, 2019.
- Colombo, N., Salerno, F., Gruber, S., Freppaz, M., Williams, M., Fratianni, S., and Giardino, M.: Review: Impacts of permafrost degradation on inorganic chemistry of surface fresh water, *Global Planet Change*, 162, 69-83, 2018a.
- 945 Colombo, N., Sambuelli, L., Comina, C., Colombero, C., Giardino, M., Gruber, S., Viviano, G., Antisari, L. V., and Salerno, F.: Mechanisms linking active rock glaciers and impounded surface water formation in high-mountain areas, *Earth Surf Proc Land*, 43, 417-431, 10.1002/esp.4257, 2018b.

- Corte, A.: The Hydrological Significance of Rock Glaciers, *J Glaciol*, 17, 157-158, 10.3189/S0022143000030859, 1976.
- 950 Corte, A.: Rock glaciers as permafrost bodies with a debris cover as an active layer. A hydrological approach, *Andes of Mendoza, Argentina*, 1978, 262-269.
- Croce, F. A. and Milana, J. P.: Internal structure and behaviour of a rock glacier in the Arid Andes of Argentina, *Permafrost and Periglacial Processes*, 13, 289-299, 10.1002/ppp.431, 2002.
- Cuffey, K. M. and Paterson, W. S. B.: *The physics of glaciers*, Academic Press, 2010.
- 955 Dahlin, T. and Zhou, B.: A numerical comparison of 2D resistivity imaging with 10 electrode arrays, *Geophys Prospect*, 52, 379-398, 10.1111/j.1365-2478.2004.00423.x, 2004.
- Dall'Asta, E., Forlani, G., Roncella, R., Santise, M., Diotri, F., and Morra di Cella, U.: Unmanned Aerial Systems and DSM matching for rock glacier monitoring, *Isprs J Photogramm*, 127, 102-114, <https://doi.org/10.1016/j.isprsjprs.2016.10.003>, 2017.
- Draebing, D.: Application of refraction seismics in alpine permafrost studies: A review, *Earth-Sci Rev*, 155, 136-152, 10.1016/j.earscirev.2016.02.006, 2016.
- 960 Drewes, J., Moreiras, S., and Korup, O.: Permafrost activity and atmospheric warming in the Argentinian Andes, *Geomorphology*, 323, 13-24, <https://doi.org/10.1016/j.geomorph.2018.09.005>, 2018.
- Duguay, M. A., Edmunds, A., Arenson, L. U., and Wainstein, P. A.: Quantifying the significance of the hydrological contribution of a rock glacier—A review. In: *GEOQuébec 2015: Challenges From North to South*, Québec, Canada, 2015.
- 965 Dussaillant, I., Berthier, E., Brun, F., Masiokas, M., Hugonnet, R., Favier, V., Rabatel, A., Pitte, P., and Ruiz, L.: Two decades of glacier mass loss along the Andes, *Nat Geosci*, 12, 802-808, 10.1038/s41561-019-0432-5, 2019.
- Duvillard, P. A., Revil, A., Qi, Y., Soueid Ahmed, A., Coperey, A., and Ravanel, L.: Three-Dimensional Electrical Conductivity and Induced Polarization Tomography of a Rock Glacier, *Journal of Geophysical Research: Solid Earth*, 123, 9528-9554, 10.1029/2018JB015965, 2018.
- 970 Emmert, A. and Kneisel, C.: Internal structure of two alpine rock glaciers investigated by quasi-3-D electrical resistivity imaging, *The Cryosphere*, 11, 841-855, 10.5194/tc-11-841-2017, 2017.
- Förstner, W.: A feature based correspondence algorithm for image matching, *International Archives of Photogrammetry and Remote Sensing*, 26, 150-166, 1986.
- 975 Funk, C., Peterson, P., Landsfeld, M., Pedreros, D., Verdin, J., Shukla, S., Husak, G., Rowland, J., Harrison, L., Hoell, A., and Michaelsen, J.: The climate hazards infrared precipitation with stations—a new environmental record for monitoring extremes, *Sci Data*, 2, 150066, 10.1038/sdata.2015.66, 2015.
- Geiger, S. T., Daniels, J. M., Miller, S. N., and Nicholas, J. W.: Influence of rock glaciers on stream hydrology in the La Sal Mountains, Utah, *Arct Antarct Alp Res*, 46, 645-658, Doi 10.1657/1938-4246-46.3.645, 2014.
- 980 Haeberli, W., Hallet, B., Arenson, L., Elconin, R., Humlun, O., Kaab, A., Kaufmann, V., Ladanyi, B., Matsuoka, N., Springman, S., and Vonder Muehl, D.: Permafrost creep and rock glacier dynamics, *Permafrost and Periglacial Processes*, 17, 189-214, 10.1002/ppp.561, 2006.
- Haeberli, W., Hoelzle, M., Käab, A., Keller, F., Vonder Muehl, D., and Wagner, S.: Ten years after drilling through the permafrost of the active rock glacier Murtèl, Eastern Swiss Alps: answered questions and new perspectives, 1998, 403-410.
- Harrington, J. S., Hayashi, M., and Kurylyk, B. L.: Influence of a rock glacier spring on the stream energy budget and cold-water refuge in an alpine stream, *Hydrol Process*, 31, 4719-4733, 10.1002/hyp.11391, 2017.
- 985 Harrington, J. S., Mozil, A., Hayashi, M., and Bentley, L. R.: Groundwater flow and storage processes in an inactive rock glacier, *Hydrol Process*, 32, 3070-3088, 2018.
- Hauck, C.: New Concepts in Geophysical Surveying and Data Interpretation for Permafrost Terrain, *Permafrost and Periglacial Processes*, 24, 131-137, 10.1002/ppp.1774, 2013.
- 990 Hauck, C., Botcher, M., and Maurer, H.: A new model for estimating subsurface ice content based on combined electrical and seismic data sets, *Cryosphere*, 5, 453-468, DOI 10.5194/tc-5-453-2011, 2011.
- Hauck, C. and Kneisel, C.: *Applied Geophysics in Periglacial Environments*, Cambridge University Press, 2008.
- Hausmann, H., Krainer, K., Bruckl, E., and Mostler, W.: Internal structure and ice content of reichenkar rock glacier (Stubai alps, Austria) assessed by geophysical investigations, *Permafrost and Periglacial Processes*, 18, 351-367, Doi 10.1002/Ppp.601, 2007.

- 995 Hausmann, H., Krainer, K., Bruckl, E., and Ullrich, C.: Internal Structure, Ice Content and Dynamics of Olgrube and Kaiserberg Rock Glaciers (Otzal Alps, Austria) Determined from Geophysical Surveys, *Austrian J Earth Sci*, 105, 12-31, 2012.
- Heredia, N., Farias, P., García-Sanseguendo, J., and Giambiagi, L.: The basement of the Andean Frontal Cordillera in the Cordón del Plata (Mendoza, Argentina): Geodynamic evolution, *Andean Geol*, 39, 242-257, <http://dx.doi.org/10.5027/andgeoV39n2-a03>, 2012.
- 1000 Heredia, N., Rodríguez Fernández, L. R., Gallastegui, G., Busquets, P., and Colombo, F.: Geological setting of the Argentine Frontal Cordillera in the flat-slab segment (30°00'–31°30'S latitude), *J S Am Earth Sci*, 15, 79-99, [https://doi.org/10.1016/S0895-9811\(02\)00007-X](https://doi.org/10.1016/S0895-9811(02)00007-X), 2002.
- Hilbich, C.: Time-lapse refraction seismic tomography for the detection of ground ice degradation, *The Cryosphere*, 4, 243-259, 10.5194/tc-4-243-2010, 2010.
- 1005 Hilbich, C., Hauck, C., Hoelzle, M., Scherler, M., Schudel, L., Voelksch, I., Muehll, D. V., and Maeusbacher, R.: Monitoring mountain permafrost evolution using electrical resistivity tomography: A 7-year study of seasonal, annual, and long-term variations at Schilthorn, Swiss Alps, *J Geophys Res-Earth*, 113, Artn F01s90
Doi 10.1029/2007jf000799, 2008.
- Hilbich, C., Marescot, L., Hauck, C., Loke, M. H., and Mäusbacher, R.: Applicability of electrical resistivity tomography monitoring to coarse blocky and ice-rich permafrost landforms, *Permafrost and Periglacial Processes*, 20, 269-284, 10.1002/ppp.652, 2009.
- 1010 IANIGLA: Data provided by Instituto Argentino de Nivología, Glaciología y Ciencias Ambientales (IANIGLA), "Agua Negra" and "Diaguita" meteorological stations, <http://bdhi.hidricosargentina.gob.ar>. 2019.
- IANIGLA: Inventario Nacional de Glaciares. Informe de la subcuenca río Blanco Superior. Cuenca del río Jáchal. IANIGLA-CONICET, Ministerio de Ambiente y Desarrollo Sustentable de la Nación., 65 pp., 2018.
- Ikeda, A.: Combination of conventional geophysical methods for sounding the composition of rock glaciers in the Swiss Alps, *Permafrost and Periglacial Processes*, 17, 35-48, Doi 10.1002/Ppp.550, 2006.
- 1015 Ikeda, A., Matsuoka, N., and Kaab, A.: Fast deformation of perennially frozen debris in a warm rock glacier in the Swiss Alps: An effect of liquid water, *J Geophys Res-Earth*, 113, Artn F01021
10.1029/2007jf000859, 2008.
- Jones, D. B., Harrison, S., Anderson, K., and Betts, R. A.: Mountain rock glaciers contain globally significant water stores, *Sci Rep-Uk*, 8, 2018a.
- 1020 Jones, D. B., Harrison, S., Anderson, K., Selley, H. L., Wood, J. L., and Betts, R. A.: The distribution and hydrological significance of rock glaciers in the Nepalese Himalaya, *Global Planet Change*, 160, 123-142, 10.1016/j.gloplacha.2017.11.005, 2018b.
- Jones, D. B., Harrison, S., Anderson, K., and Whalley, W. B.: Rock glaciers and mountain hydrology: A review, *Earth-Sci Rev*, doi: <https://doi.org/10.1016/j.earscirev.2019.04.001>, 2019. <https://doi.org/10.1016/j.earscirev.2019.04.001>, 2019.
- 1025 Kääh, A., Frauenfelder, R., and Roer, I.: On the response of rockglacier creep to surface temperature increase, *Global Planet Change*, 56, 172-187, <https://doi.org/10.1016/j.gloplacha.2006.07.005>, 2007.
- Kääh, A., Gudmundsson, G. H., and Hoelzle, M.: Surface deformation of creeping mountain permafrost. Photogrammetric investigations on rock glacier Murtèl, Swiss Alps, 1998, 531-537.
- Kääh, A., Haerberli, W., and Gudmundsson, G. H.: Analysing the creep of mountain permafrost using high precision aerial photogrammetry: 25 years of monitoring Gruben Rock Glacier, Swiss Alps, *Permafrost and Periglacial Processes*, 8, 409-426, 1997.
- 1030 Kääh, A., Kaufmann, V., Ladstädter, R., and Eiken, T.: Rock glacier dynamics: Implications from high-resolution measurements of surface velocity fields, 8th International Conference on Permafrost, Zürich, 501-506, 2003.
- Kääh, A. and Weber, M.: Development of transverse ridges on rock glaciers: Field measurements and laboratory experiments, *Permafrost and Periglacial Processes*, 15, 379-391, 2004.
- 1035 Kenner, R., Phillips, M., Beutel, J., Hiller, M., Limpach, P., Pointner, E., and Volken, M.: Factors Controlling Velocity Variations at Short-Term, Seasonal and Multiyear Time Scales, Ritigraben Rock Glacier, Western Swiss Alps, *Permafrost and Periglacial Processes*, 28, 675-684, 10.1002/ppp.1953, 2017.
- Kenner, R., Pruessner, L., Beutel, J., Limpach, P., and Phillips, M.: How rock glacier hydrology, deformation velocities and ground temperatures interact: Examples from the Swiss Alps, *Permafrost and Periglacial Processes*, 0, 10.1002/ppp.2023, 2019.
- 1040 King, M. S., Zimmerman, R. W., and Corwin, R. F.: Seismic and Electrical Properties of Unconsolidated Permafrost, *Geophys Prospect*, 36, 349-364, 10.1111/j.1365-2478.1988.tb02168.x, 1988.

- Kneisel, C., Hauck, C., Fortier, R., and Moorman, B.: Advances in geophysical methods for permafrost investigations, *Permafrost and Periglacial Processes*, 19, 157-178, Doi 10.1002/Ppp.616, 2008.
- Knight, J., Harrison, S., and Jones, D. B.: Rock glaciers and the geomorphological evolution of deglaciating mountains, *Geomorphology*, 324, 14-24, <https://doi.org/10.1016/j.geomorph.2018.09.020>, 2019.
- 1045 Konrad, S. K., Humphrey, N. F., Steig, E. J., Clark, D. H., Potter, N., Jr, and Pfeffer, W. T.: Rock glacier dynamics and paleoclimatic implications, *Geology*, 27, 1131-1134, 10.1130/0091-7613(1999)027<1131:rgdapi>2.3.co;2, 1999.
- Krainer, K., Bressan, D., Dietre, B., Haas, J. N., Hajdas, I., Lang, K., Mair, V., Nickus, U., Reidl, D., Thies, H., and Tonidandel, D.: A 10,300-year-old permafrost core from the active rock glacier Lazaun, southern Ötztal Alps (South Tyrol, northern Italy), *Quaternary Res*, 83, 324-335, 10.1016/j.yqres.2014.12.005, 2017.
- 1050 Krainer, K. and Mostler, W.: Hydrology of active rock glaciers: Examples from the Austrian Alps, *Arct Antarct Alp Res*, 34, 142-149, Doi 10.2307/1552465, 2002.
- Krainer, K., Mostler, W., and Spötl, C.: Discharge from active rock glaciers, Austrian Alps: a stable isotope approach, *Austrian J Earth Sci*, 100, 102-112, 2007.
- Krautblatter, M. and Draebing, D.: Pseudo 3-D P wave refraction seismic monitoring of permafrost in steep unstable bedrock, *Journal of Geophysical Research: Earth Surface*, 119, 287-299, 10.1002/2012jf002638, 2014.
- 1055 Kummert, M., Delaloye, R., and Braillard, L.: Erosion and sediment transfer processes at the front of rapidly moving rock glaciers: Systematic observations with automatic cameras in the western Swiss Alps, *Permafrost and Periglacial Processes*, 29, 21-33, 2018.
- Langston, G., Bentley, L. R., Hayashi, M., McClymont, A., and Pidlisecky, A.: Internal structure and hydrological functions of an alpine proglacial moraine, *Hydrol Process*, 25, 2967-2982, 10.1002/hyp.8144, 2011.
- 1060 Lecomte, K. L., Milana, J. P., Formica, S. M., and Depetris, P. J.: Hydrochemical appraisal of ice- and rock-glacier meltwater in the hyperarid Agua Negra drainage basin, Andes of Argentina, *Hydrol Process*, 22, 2180-2195, Doi 10.1002/Hyp.6816, 2008.
- Loke, M. H.: Tutorial : 2-D and 3-D electrical imaging surveys, 2018. 2018.
- Luethi, R., Phillips, M., and Lehning, M.: Estimating Non-Conductive Heat Flow Leading to Intra-Permafrost Talik Formation at the Ritigraben Rock Glacier (Western Swiss Alps), *Permafrost and Periglacial Processes*, 28, 183-194, 10.1002/ppp.1911, 2017.
- 1065 Malmros, J. K., Mernild, S. H., Wilson, R., Tagesson, T., and Fensholt, R.: Snow cover and snow albedo changes in the central Andes of Chile and Argentina from daily MODIS observations (2000–2016), *Remote Sens Environ*, 209, 240-252, <https://doi.org/10.1016/j.rse.2018.02.072>, 2018.
- Marescot, L., Loke, M., Chapellier, D., Delaloye, R., Lambiel, C., and Reynard, E.: Assessing reliability of 2D resistivity imaging in mountain permafrost studies using the depth of investigation index method, *Near Surf Geophys*, 1, 57-67, 2003.
- 1070 Marmy, A., Rajczak, J., Delaloye, R., Hilbich, C., Hoelzle, M., Kotlarski, S., Lambiel, C., Noetzli, J., Phillips, M., Salzmann, N., Staub, B., and Hauck, C.: Semi-automated calibration method for modelling of mountain permafrost evolution in Switzerland, *The Cryosphere*, 10, 2693-2719, 10.5194/tc-10-2693-2016, 2016.
- Maurer, H. and Hauck, C.: Instruments and methods - Geophysical imaging of alpine rock glaciers, *J Glaciol*, 53, 110-120, Doi 10.3189/172756507781833893, 2007.
- 1075 McClymont, A. F., Hayashi, M., Bentley, L. R., and Liard, J.: Locating and characterising groundwater storage areas within an alpine watershed using time-lapse gravity, GPR and seismic refraction methods, *Hydrol Process*, 26, 1792-1804, Doi 10.1002/Hyp.9316, 2012.
- McClymont, A. F., Hayashi, M., Bentley, L. R., Muir, D., and Ernst, E.: Groundwater flow and storage within an alpine meadow-talus complex, *Hydrol Earth Syst Sc*, 14, 859-872, 2010.
- 1080 Mewes, B., Hilbich, C., Delaloye, R., and Hauck, C.: Resolution capacity of geophysical monitoring regarding permafrost degradation induced by hydrological processes, *Cryosphere*, 11, 2957-2974, 2017.
- Milana, J. P. and Maturano, A.: Application of Radio Echo Sounding at the arid Andes of Argentina: the Agua Negra Glacier, *Global Planet Change*, 22, 179-191, Doi 10.1016/S0921-8181(99)00035-1, 1999.
- Mollaret, C., Hilbich, C., Pellet, C., Flores-Orozco, A., Delaloye, R., and Hauck, C.: Mountain permafrost degradation documented through a network of permanent electrical resistivity tomography sites, *The Cryosphere*, 13, 2557-2578, 10.5194/tc-13-2557-2019, 2019.
- 1085 Mollaret, C., Wagner, F. M., Hilbich, C., Scapozza, C., and Hauck, C.: Petrophysical Joint Inversion Applied to Alpine Permafrost Field Sites to Image Subsurface Ice, Water, Air, and Rock Contents, *Frontiers in Earth Science*, 8, 10.3389/feart.2020.00085, 2020.

- Monnier, S. and Kinnard, C.: Internal structure and composition of a rock glacier in the Andes (upper Choapa valley, Chile) using borehole information and ground-penetrating radar, *Ann. Glaciol.*, 54, 61-72, Doi 10.3189/2013aog64a107, 2013.
- 1090 Mosbrucker, A. R., Major, J. J., Spicer, K. R., and Pitlick, J.: Camera system considerations for geomorphic applications of SfM photogrammetry, *Earth Surf Proc Land*, 42, 969-986, 2017.
- Musil, M., Maurer, H., Green, A. G., Horstmeyer, H., Nitsche, F. O., Vonder Muhll, D., and Springman, S.: Shallow seismic surveying of an Alpine rock glacier, *Geophysics*, 67, 1701-1710, Doi 10.1190/1.1527071, 2002.
- Otto, J. C. and Sass, O.: Comparing geophysical methods for talus slope investigations in the Turtmann valley (Swiss Alps), *Geomorphology*, 76, 257-272, 2006.
- 1095 Pellet, C., Hilbich, C., Marmy, A., and Hauck, C.: Soil Moisture Data for the Validation of Permafrost Models Using Direct and Indirect Measurement Approaches at Three Alpine Sites, *Frontiers in Earth Science*, 3, 10.3389/feart.2015.00091, 2016.
- Rangecroft, S., Harrison, S., and Anderson, K.: Rock Glaciers as Water Stores in the Bolivian Andes: An Assessment of Their Hydrological Importance, *Arctic, Antarctic, and Alpine Research*, 47, 89-98, 10.1657/AAAR0014-029, 2015.
- 1100 Rangecroft, S., Suggitt, A. J., Anderson, K., and Harrison, S.: Future climate warming and changes to mountain permafrost in the Bolivian Andes, *Climatic Change*, 137, 231-243, 10.1007/s10584-016-1655-8, 2016.
- Rogger, M., Chirico, G. B., Hausmann, H., Krainer, K., Brückl, E., Stadler, P., and Blöschl, G.: Impact of mountain permafrost on flow path and runoff response in a high alpine catchment, *Water Resour Res*, 53, 1288-1308, 10.1002/2016WR019341, 2017.
- Saavedra, F. A., Kampf, S. K., Fassnacht, S. R., and Sibold, J. S.: Changes in Andes snow cover from MODIS data, 2000–2016, *The Cryosphere*, 12, 1027-1046, 10.5194/tc-12-1027-2018, 2018.
- 1105 Sandmeier, K. J.: ReflexW version 8.0. Program for the Processing of Seismic, Acoustic or Electromagnetic Reflection, Refraction and Transmission Data, User's Manual, 2016. 578, 2016.
- Schaffer, N., MacDonell, S., Réveillet, M., Yáñez, E., and Valois, R.: Rock glaciers as a water resource in a changing climate in the semiarid Chilean Andes, *Reg Environ Change*, doi: 10.1007/s10113-018-01459-3, 2019. 10.1007/s10113-018-01459-3, 2019.
- 1110 Scherler, M., Hauck, C., Hoelzle, M., and Salzmann, N.: Modeled sensitivity of two alpine permafrost sites to RCM-based climate scenarios, *J Geophys Res-Earth*, 118, 780-794, Doi 10.1002/Jgrf.20069, 2013.
- Scherler, M., Hauck, C., Hoelzle, M., Stahli, M., and Volksch, I.: Meltwater Infiltration into the Frozen Active Layer at an Alpine Permafrost Site, *Permafrost and Periglacial Processes*, 21, 325-334, Doi 10.1002/Ppp.694, 2010.
- 1115 Schneider, S., Daengeli, S., Hauck, C., and Hoelzle, M.: A spatial and temporal analysis of different periglacial materials by using geoelectrical, seismic and borehole temperature data at Murtèl–Corvatsch, Upper Engadin, Swiss Alps, *Geogr. Helv.*, 68, 265-280, 10.5194/gh-68-265-2013, 2013.
- Schön, J.: Physical properties of rocks: A workbook, Elsevier, 2011.
- Schrott, L.: Die Solarstrahlung als steuernder Faktor im Geosystem der subtropischen semiariden Hochanden (Agua Negra, San Juan, Argentinien), 1994. Dissertation, Geographisches Inst. der Univ. Heidelberg, Heidelberg, 1994.
- 1120 Schrott, L.: Global solar radiation, soil temperature and permafrost in the Central Andes, Argentina: A progress report, *Permafrost and Periglacial Processes*, 2, 59-66, 10.1002/ppp.3430020110, 1991.
- Schrott, L.: The hydrological significance of high mountain permafrost and its relation to solar radiation, A case study in the high Andes of San Juan, Argentina. *Bamberger Geographische Schriften*, Bd, 15, 71-84, 1998.
- Schrott, L.: Some geomorphological-hydrological aspects of rock glaciers in the Andes (San Juan, Argentina), *Z. Geomorph. N.F., Suppl.-Bd.* 104, 1996.
- 1125 Schrott, L. and Hoffmann, T.: Refraction seismics. In: *Applied Geophysics in Periglacial Environments*, Hauck, C. and Kneisel, C. (Eds.), Cambridge University Press, Cambridge, 2008.
- Schwalbe, E. and Maas, H. G.: The determination of high-resolution spatio-temporal glacier motion fields from time-lapse sequences, *Earth Surf. Dynam.*, 5, 861-879, 10.5194/esurf-5-861-2017, 2017.
- 1130 Springman, S. M., Arenson, L. U., Yamamoto, Y., Maurer, H., Kos, A., Buchli, T., and Derungs, G.: Multidisciplinary Investigations on Three Rock Glaciers in the Swiss Alps: Legacies and Future Perspectives, *Geogr Ann A*, 94A, 215-243, DOI 10.1111/j.1468-0459.2012.00464.x, 2012.

Tapia-Baldis, C. and Trombotto-Liaudat, D.: Permafrost model in coarse-blocky deposits for the Dry Andes, Argentina (28°-33° S), Cuadernos de Investigación Geográfica 46, doi: <http://dx.doi.org/10.18172/cig.3802>, 2020. <http://dx.doi.org/10.18172/cig.3802>, 2020.

1135 Timur, A.: Velocity of Compressional Waves in Porous Media at Permafrost Temperatures, Geophysics, 33, 584-&, Doi 10.1190/1.1439954, 1968.

Trombotto, D. and Borzotta, E.: Indicators of present global warming through changes in active layer-thickness, estimation of thermal diffusivity and geomorphological observations in the Morenas Coloradas rockglacier, Central Andes of Mendoza, Argentina, Cold Reg Sci Technol, 55, 321-330, DOI 10.1016/j.coldregions.2008.08.009, 2009.

1140 Trombotto, D., Buk, E., and Hernández, J.: Rock glaciers in the Southern Central Andes (approx. 33–34S), Cordillera Frontal, Mendoza, Argentina, Bamberger Geographische Schriften, 19, 145-173, 1999.

Wheaton, J. M., Brasington, J., Darby, S. E., and Sear, D. A.: Accounting for uncertainty in DEMs from repeat topographic surveys: improved sediment budgets, Earth Surf Proc Land, 35, 136-156, 10.1002/esp.1886, 2010.

Williams, M. W., Knauf, M., Caine, N., Liu, F., and Verplanck, P. L.: Geochemistry and source waters of rock glacier outflow, Colorado Front Range, Permafrost and Periglacial Processes, 17, 13-33, Doi 10.1002/Ppp.535, 2006.

1145 Wirz, V., Gruber, S., Purves, R. S., Beutel, J., Gartner-Roer, I., Gubler, S., and Vieli, A.: Short-term velocity variations at three rock glaciers and their relationship with meteorological conditions, Earth Surf Dynam, 4, 103-123, 10.5194/esurf-4-103-2016, 2016.

Tables

1150 **Table 1: Potential mean annual air temperatures (MAAT) of recent years derived from different local meteorological stations of for the Upper Agua Negra basin. The altitudes of 4300 and 4500 m a.s.l. correspond to the elevation range of the Dos Lenguas rock glacier, respectively.**

Station (altitude)	Year	MAAT [°C]		Reference
		4300 m asl*	4500 m asl*	
El Paso rock glacier (4720 m a.s.l.)	1990–91	1.8	–0.1	Schrott (1996)
Paso Agua Negra (4774 m a.s.l.)	2015	–0.4	–2.3	CEAZA (2019)
Agua Negra (4460 m a.s.l.)	2016	–2.5	–4.5	IANIGLA (2019)
Diaguaita (3880 m a.s.l.)	2017	–1.1	–3.1	IANIGLA (2019)
Diaguaita (3880 m a.s.l.)	2018	–0.5	–2.5	IANIGLA (2019)

*A dry adiabatic lapse rate of 0.98°C km⁻¹ was used to derive potential MAAT in different elevations from each station.

1155 **Table 2: Mean and maximum precipitation in the Agua Negra valley for the hydrological periods 2016-2017 and 2017-2018 from CHIRPS (Climate Hazards Group InfraRed Precipitation with Stations) data archive (Funk et al., 2015).**

Hydrological period	Sum of monthly precipitation [mm]					
	Austral winter		Austral summer		Hydrological year	
	01/04-30/09		01/10-31/03		01/04-31/03	
	Mean	Max	Mean	Max	Mean	Max
2016-17	23	50	22	90	45	140
2017-18	13	55	38	113	51	168

1160 **Table 3:-Details of the ERT surveys. The columns to the left of the acquisition date contain details of the layout geometry of each profile (see Fig. 1b for position of the profiles). The columns to the right of the acquisition date contain filtered data points and the quality of the inversion. (cf. Fig. 1b for position of the profiles).**

ERT profiles	Length	Electrode	Acquisition	Number of data points		Abs. error after
				Collected	Used	
Dos Lenguas	Orientation	[m]	spacing [m]	date		

C1 (cross-profile) Root zone	NNW→SSE	320	4	23 rd Feb 2017	1160	992 (86%)	6,2
C2 (cross-profile) Central part	N→S	400	5	27 th Feb 2017	1168	1075 (92%)	5,1
L1 (long. profile) Northern tongue	ENE→WSW	240	3	2 nd Mar 2017	1168	1117 (96%)	6,7
L2 (long. profile) Southern tongue	NE→SW	400	5	2 nd Mar 2018	951	919 (97%)	7,4

Table 4: Details of the SRT surveys. Sensor spacing and orientation of all SRT profiles is identical to the corresponding ERT profiles (cf. Table 32).

SRT profiles	Geophone positions on	Acquisition	Shot		RMS	Total absolute
Dos Lunguas	ERT profile [m]	date	points	Iterations	deviation [ms]	time difference [ms]
C1 (cross-profile) Root zone	20–304	24 th Feb 2017	25	9	2.7	2.0
C2 (cross-profile) Central part	20-360	28 th Feb 2017	25	14	4.7	3.8
L1 (long. profile) Northern tongue	6-213	3 rd Mar 2017	25	13	3.2	2.4
L2 (long. profile) Southern tongue	0-400	3 rd Mar 2018	43	11	2.6	2.0

1165

Table 5: Model parameters for 4PM calculation.

Prescribed 4PM parameters	
a	1
m	2
n	2
v_w (m s ⁻¹)	1500
v_r (m s ⁻¹)	6000
v_i (m s ⁻¹)	3500
v_a (m s ⁻¹)	330
Values for model scenarios	
ρ_w (Ω m)	30; 50; 100; 200
$\Phi_{uniform}$	0.3, 0.5, 0.7
* Φ_{mixed}	0.75-0.03
** $\Phi_{active\ layer}$	0.45-0.3
** $\Phi_{permafrost}$	0.75-0.3
** $\Phi_{bedrock}$	0.1-0.03

*Mixed model includes different porosities of active layer, permafrost and bedrock
**Porosity ranges include depth gradient

1170

Table 6: (top) Level of detection (LoD) is given for different confidence intervals and t-values for detected vertical changes. (bottom) Associated net balance estimates derived from the sum of positive and negative interannual volumetric changes for the observation periods. The net changes of ice are given in water equivalent per year for the whole surface area and each geomorphological unit of the rock glacier. The net balance approximations correspond to interannual water storage change under the assumption that the volumetric changes were mainly caused by gains and losses of ice.

Confidence interval	70%	80%	90%	95%	99%
---------------------	-----	-----	-----	-----	-----

<u>t-value</u>	<u>1.036</u>	<u>1.282</u>	<u>1.645</u>	<u>1.96</u>	<u>2.576</u>					
<u>LoD 2016 – 2017 [m]</u>	<u>0.232</u>	<u>0.287</u>	<u>0.368</u>	<u>0.438</u>	<u>0.576</u>					
<u>LoD 2017 – 2018 [m]</u>	<u>0.073</u>	<u>0.091</u>	<u>0.117</u>	<u>0.139</u>	<u>0.183</u>					
<u>Net change of positive and negative volumetric changes for the observation periods [mm yr⁻¹]</u>										
<u>Period</u>	<u>2016-17</u>	<u>2017-18</u>	<u>2016-17</u>	<u>2017-18</u>	<u>2016-17</u>	<u>2017-18</u>	<u>2016-17</u>	<u>2017-18</u>	<u>2016-17</u>	<u>2017-18</u>
<u>Rock glacier surface</u>	<u>-109</u>	<u>+29</u>	<u>-86</u>	<u>+28</u>	<u>-55</u>	<u>+28</u>	<u>-36</u>	<u>+27</u>	<u>-15</u>	<u>+25</u>
<u>Root area</u>	<u>-116</u>	<u>+8</u>	<u>-89</u>	<u>+7</u>	<u>-49</u>	<u>+5</u>	<u>-27</u>	<u>+4</u>	<u>-9</u>	<u>+1</u>
<u>Central part</u>	<u>-141</u>	<u>+15</u>	<u>-117</u>	<u>+15</u>	<u>-84</u>	<u>+14</u>	<u>-61</u>	<u>+14</u>	<u>-33</u>	<u>+14</u>
<u>Northern tongue</u>	<u>-90</u>	<u>+50</u>	<u>-68</u>	<u>+49</u>	<u>-38</u>	<u>+46</u>	<u>-23</u>	<u>+45</u>	<u>-7</u>	<u>+42</u>
<u>Southern tongue</u>	<u>-95</u>	<u>+30</u>	<u>-74</u>	<u>+30</u>	<u>-47</u>	<u>+30</u>	<u>-30</u>	<u>+30</u>	<u>-13</u>	<u>+30</u>

1175

Table 7: Mean fractions of ice, water and air content for different scenarios containing the minimum and maximum model for ice and water content, and the scenario with mixed porosities for the anticipated internal structure and pore water resistivities from field measurements. The mean fractions are solely based on model cells below the rock glacier surface area (model area outside the rock glacier were excluded). The ratio of numerically solved model cells to the total model domain gives the amount of physical consistent solutions of the different 4PM scenarios. Absolute ice and water content is estimated based on mean f_i and f_w along the profiles that were extrapolated to surface area and mean depth of permafrost.

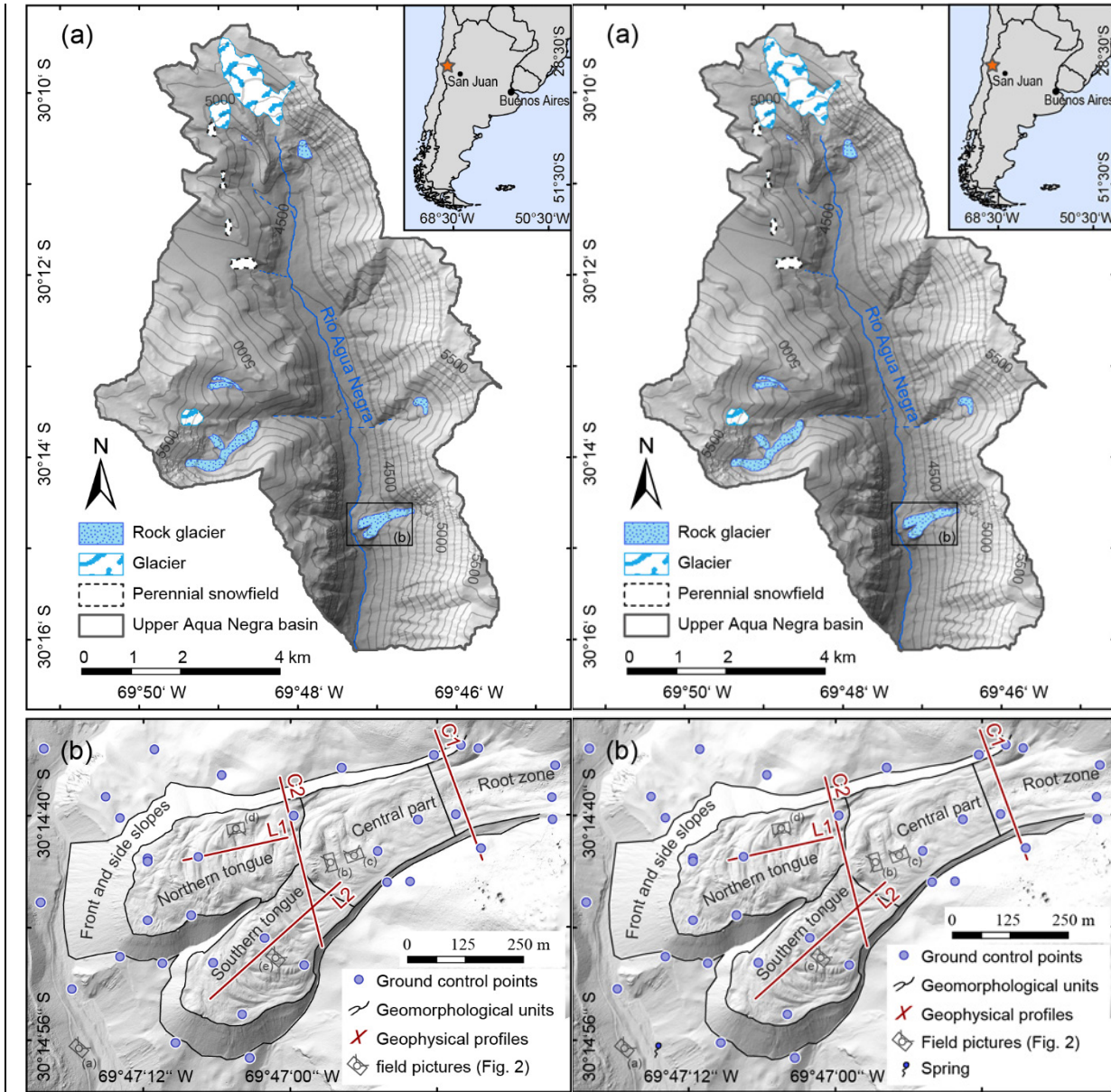
1180

Model scenarios		Mean f_i [%]¹	Mean f_w [%]¹	Mean f_a [%]¹	Solved model cell ratio [%]	Absolute ice content [10⁹ kg]²	Absolute water content [10⁹ kg]²
Cross-profile C1	$\Phi = 30\%$, $\rho_w = 200 \Omega \text{ m}$	12 ±6	13 ±5	5 ±4	43		
Root zone	$\Phi = 70\%$, $\rho_w = 30 \Omega \text{ m}$	48 ±16	8 ±5	14 ±14	88	0.364 (±43%)	0.071 (±32%)
(35,500 m²)	Φ_{mixed} , $\rho_w = 50 \Omega \text{ m}$	41 ±16	10 ±5	11 ±11	84	0.262 (±43%)	0.057 (±32%)
Cross-profile C2	$\Phi = 30\%$, $\rho_w = 200 \Omega \text{ m}$	9 ±5	14 ±5	7 ±5	41		
Central part	$\Phi = 70\%$, $\rho_w = 30 \Omega \text{ m}$	44 ±17	7 ±4	19 ±16	86	0.729 (±44%)	0.120 (±31%)
(66,600 m²)	Φ_{mixed} , $\rho_w = 50 \Omega \text{ m}$	38 ±16	8 ±4	14 ±11	65	0.513 (±43%)	0.105 (±31%)
Long. profile L1	$\Phi = 30\%$, $\rho_w = 200 \Omega \text{ m}$	9 ±5	12 ±7	9 ±7	41		
Northern tongue	$\Phi = 70\%$, $\rho_w = 30 \Omega \text{ m}$	45 ±16	7 ±5	19 ±16	86	0.694 (±43%)	0.138 (±32%)
(77,100 m²)	Φ_{mixed} , $\rho_w = 50 \Omega \text{ m}$	36 ±14	9 ±6	13 ±12	76	0.500 (±41%)	0.108 (±33%)
Long. profile L2	$\Phi = 30\%$, $\rho_w = 200 \Omega \text{ m}$	9 ±5	13 ±5	8 ±6	43		
Southern Tongue	$\Phi = 70\%$, $\rho_w = 30 \Omega \text{ m}$	42 ±18	7 ±4	21 ±17	88	0.625 (±45%)	0.109 (±31%)
(68,100 m²)	Φ_{mixed} , $\rho_w = 50 \Omega \text{ m}$	38 ±13	8 ±4	15 ±11	84	0.466 (±40%)	0.095 (±31%)
Rock glacier						2.00 (±44%)	0.432 (±32%)
(247,300 m²)						1.71 (±42%)	0.359 (±32%)

1 errors as standard deviation

2 errors as propagated uncertainties of f_w and f_i , permafrost thickness and surface area

Figures



1185 **Fig. 1: (a) Spatial distribution of active rock glaciers, glaciers, and perennial snowfields in the Upper Agua Negra catchment (hillshade based on TanDEM-X data © DLR 2017) mapped by the Glacier Inventory of Argentina (IANIGLA, 2018). The inset shows the location of the Upper Aqua Negra catchment. (b) Based on the drone-derived DEM 2016, the shaded relief map of Dos Lenguas rock glacier shows the geomorphological units subdivided into root zone, central part, northern and southern tongue, the locations of geophysical profiles, field pictures (Fig. 2), and ground control points, which were used for displacement**
 1190 **measurements.**

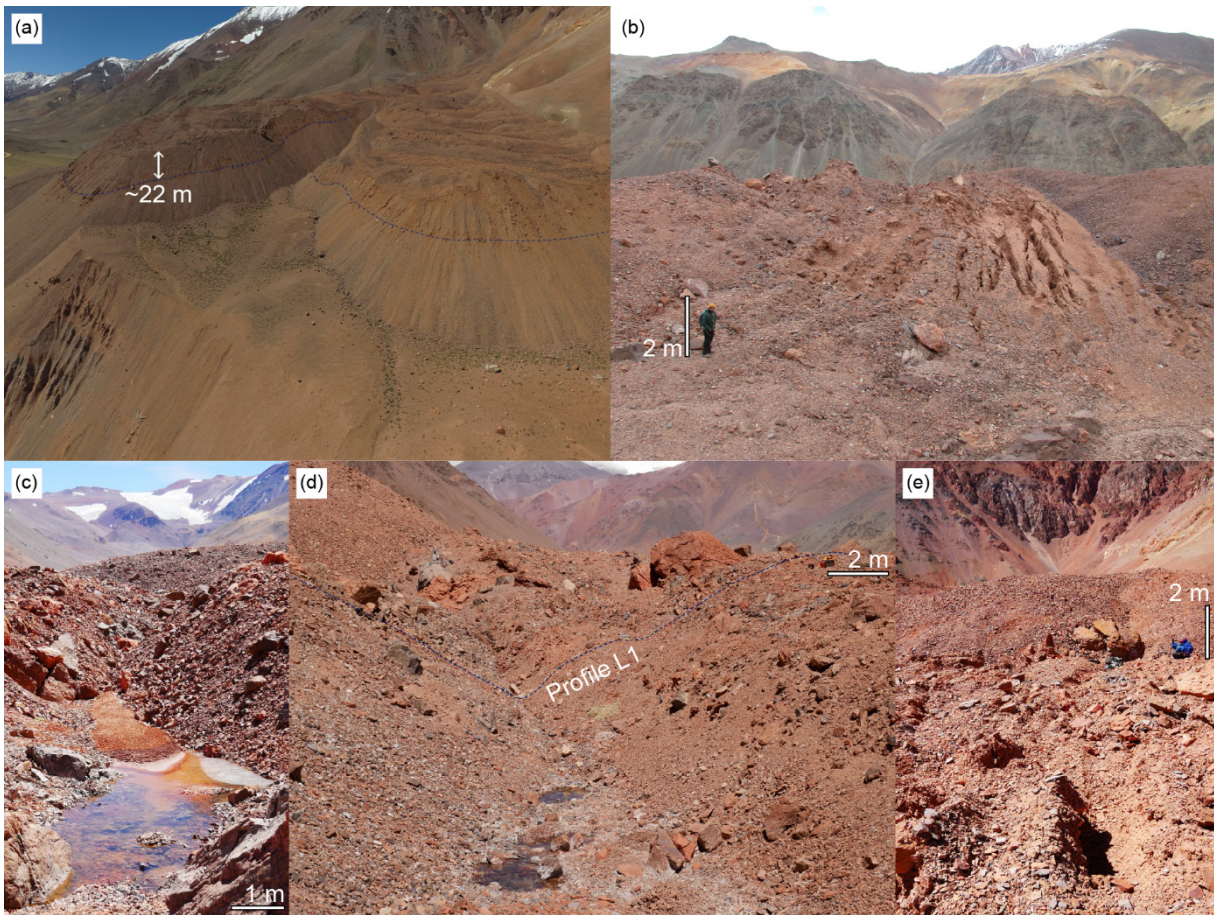


Fig. 2: Field images of Dos Lenguas: (a) View towards the Northern (left) and Southern (right) tongues of the rock glacier. Note gully-like structures in the upper over-steepened frontal slopes indicate the depths of the basal layer at both tongues (dotted lines); (b) Crevasses in the central rock glacier part indicate rupturing of transversal ridge thereby exposing fine debris; (c) Partly frozen thermokarst pond with delta indicating fine sediment transport and accumulation along water pathways in furrows; (d) Thermokarst ponds next to profile L1 on the northern tongue; (e) Gully like structures at the surface perpendicular to ridge and furrows indicate meltwater pathways in the active layer next to profile L2 on the southern tongue (larger gullies on the southern tongue are also visible in Figure 1b next to the field image location).

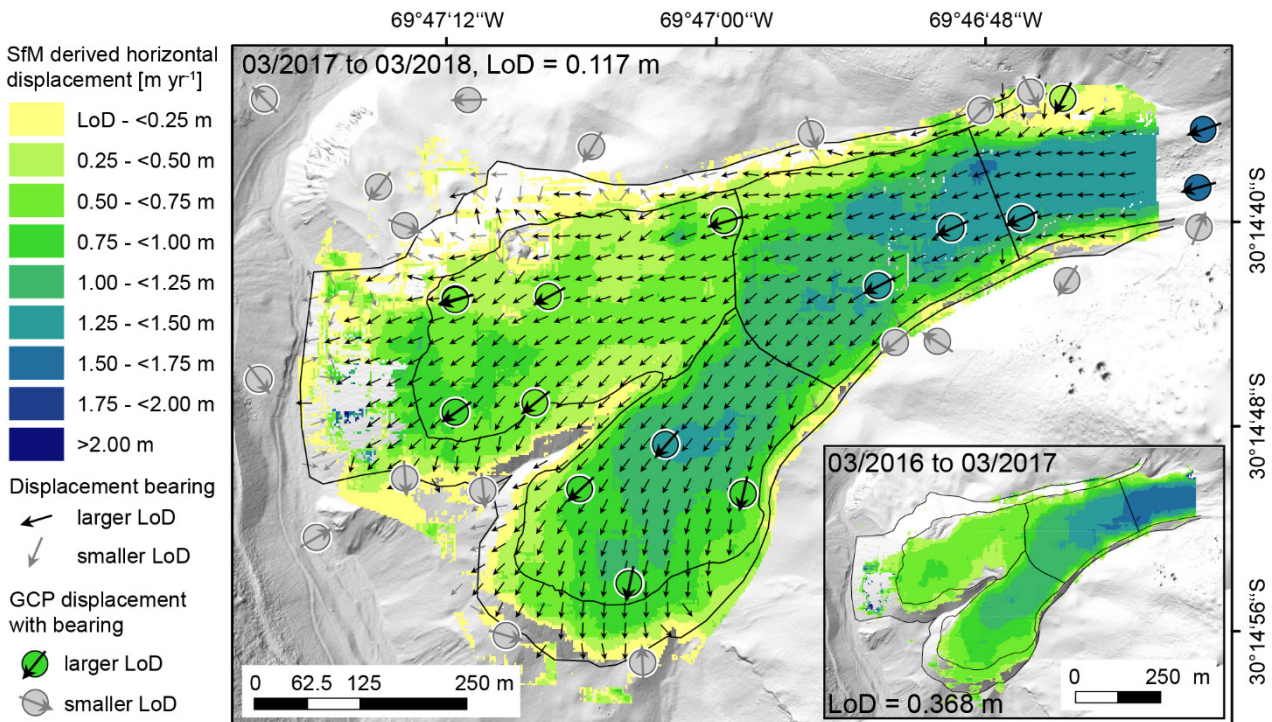


Fig. 3: Horizontal surface displacement on the Dos Lenguas rock glacier.

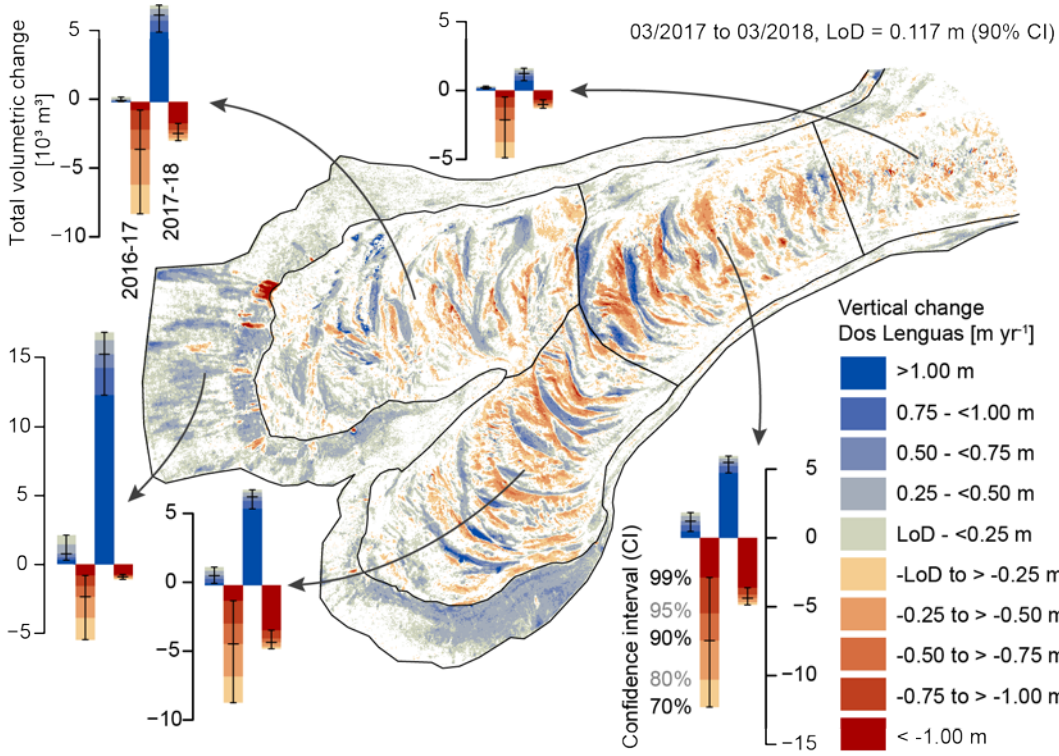
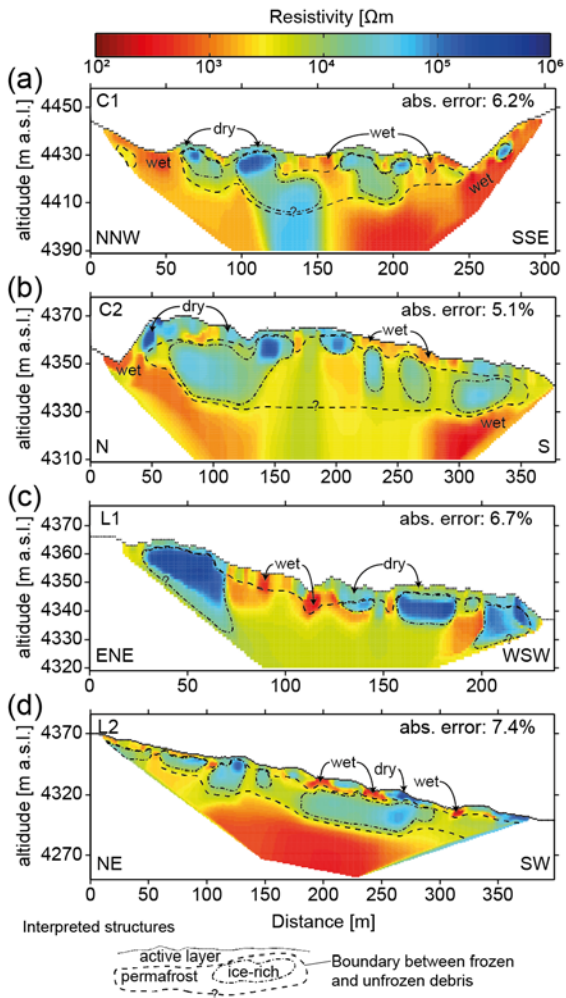


Fig. 4: Vertical changes of Dos Lenguas from 03/2017 to 03/2018. The bar graphs show the sum of the total positive volumetric (bluish bars) and the total negative volumetric changes (reddish bars) for each geomorphological area (Fig. 1b) as a function of the confidence intervals for the periods 2016-17 and 2017-18. Starting at the twelve o'clock position and following the clockwise direction, the five bar graphs contain the total volumetric changes of the root zone, the central area, the southern tongues, the front and side slopes, and the northern tongue. The corresponding total net changes of ice are given in table 6 as water equivalents.

1205



1210

Fig. 5: ERT of Dos Lenguas: a) Cross-profile C1 of the root area, b) Cross-profile C2 of the central rock glacier, c) Long-profile L1 of the Northern tongue, and d) Long-profile L2 of the southern tongue. Note the different horizontal and vertical scales for the different profiles.

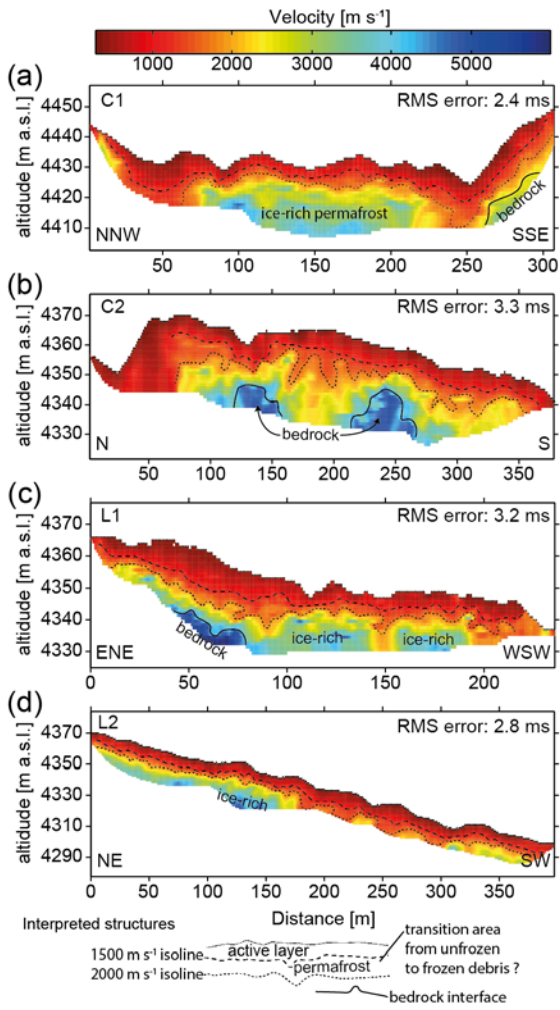


Fig. 6: SRT of Dos Lenguas: a) Cross-profile C1 of the root area, b) Cross-profile C2 of the central rock glacier, c) Long-profile L1 of the Northern tongue, and d) Long-profile L2 of the southern tongue. Note the different horizontal and vertical scales for the different profiles.

1215

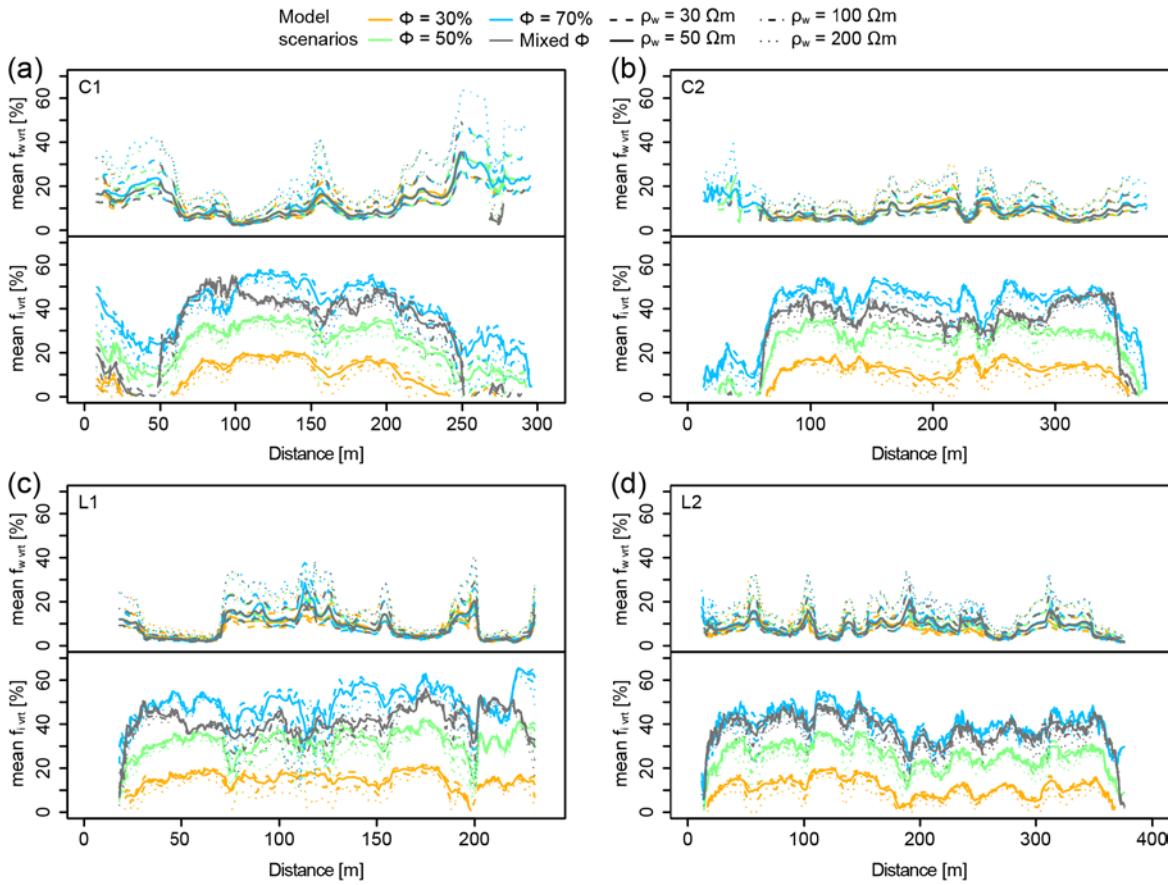
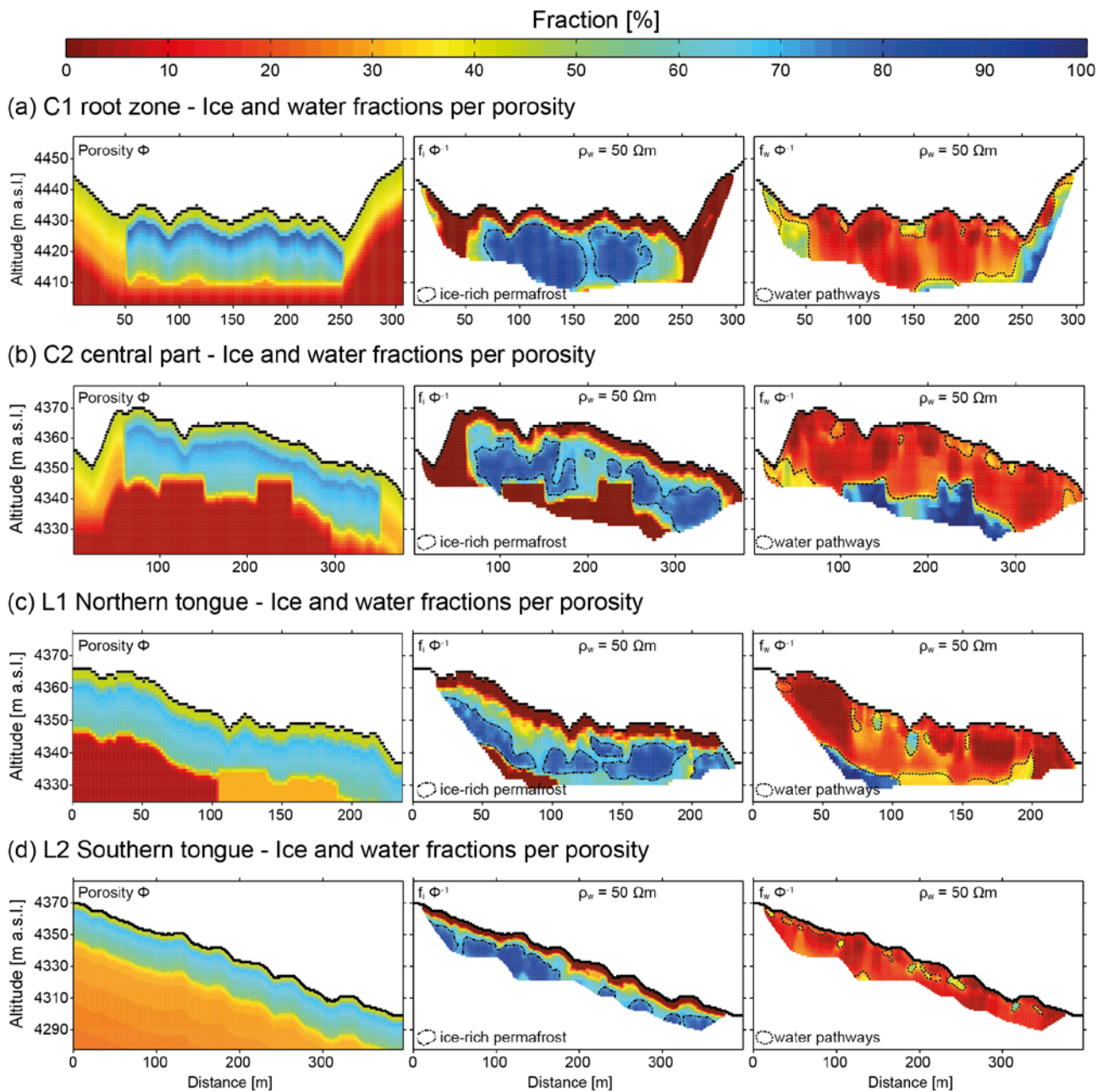
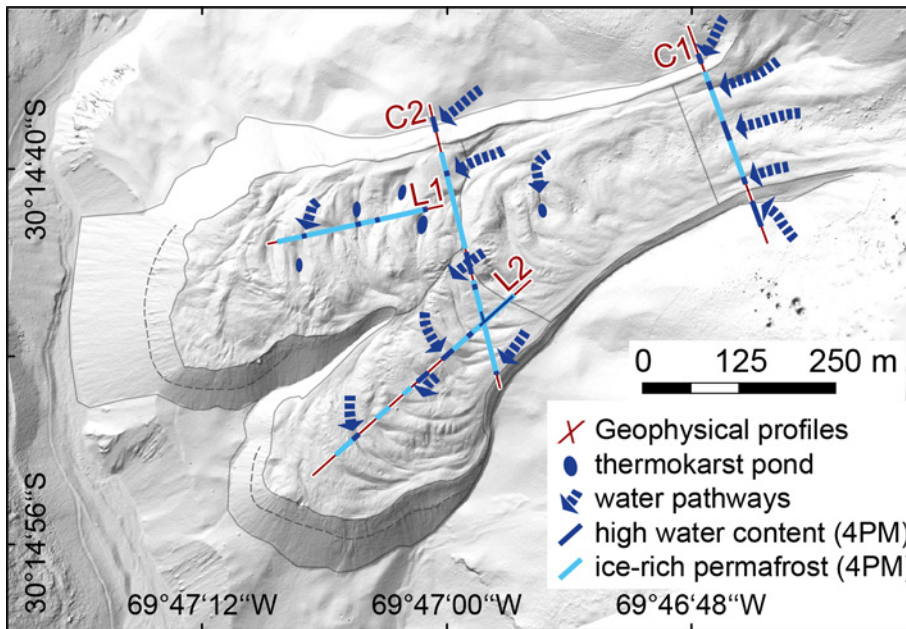


Fig. 7: Estimated mean vertical ice content ($f_{i\ vrt}$) and mean vertical water content ($f_{w\ vrt}$) along profiles C1, C2, L1 and L2 for all 4PM scenarios. The volumetric ice (upper panel) and volumetric water content (lower panel) of the 4PM model cells along the profiles were arithmetically averaged over the 4PM depth (vertical dimension) to compare the results of the various scenarios to each other. The porosity scenarios are color-coded and combined with different line types representing the pore water resistivities used. Estimated mean ice (f_i) and water (f_w) contents content over model depth along the profiles C1, C2, L1 and L2 for all 4PM scenarios. The mixed porosity (grey) and 70% porosity scenarios (blue) with pore water resistivities of 30 Ω m and 50 Ω m were evaluated as most reasonable for the active rock glacier, since the range of mean vertical ice content indicates ice-supersaturated conditions ($f_{i\ vrt} > 40\%$) and the mean vertical water content is mainly lesser than 10%. The estimated ranges of the mean f_i and mean f_w of the plausible scenarios with uncertainties are given in table 67 for each profile and for the extrapolated absolute ice and water content of the geomorphological units.



1230 | Fig. 8: Spatial distribution of ice and water ~~contents~~ per porosity, i. e. ice and water saturations, of the 4PM scenario with mixed porosity model and pore water resistivities of $50 \Omega \text{ m}$ for (a) cross-profile C1 in the root zone, (b) cross-profile C2 in the central rock glaciers area, (c) long-profile L1 in the northern tongue and (d) long-profile L2 in the Southern tongue. Porosities $<10\%$ represent potential bedrock occurrence based on SRT interpretations. Porosities $>40\%$ allow ice-rich permafrost conditions in the 4PM. Ice content per porosity ($f_i \Phi^{-1}$) shows heterogeneous distributions of ice-rich permafrost and indicates the active layer ~~in and unfrozen bedrock in~~ ice free model-cells. High water content per porosity ($f_w \Phi^{-1}$) indicates water pathways and traps in unfrozen-aquifersice-free area, while increased water ~~contents~~ saturations between ice-rich permafrost could indicate aquitards and/or thawing permafrost in late summer. Note the different horizontal and vertical scales of the figures for the different profiles.

1235



1240 Fig. 9: Topographic positions of aquifers-water pathways and ice-rich permafrost based on observed hydrological structures in the
 1245 4PM along the geophysical profiles (cf. Fig.8). The spatial distribution of ice-rich permafrost, high water content, and interpreted
water pathways in the subsurface indicate interrelations with, thermokarst ponds, aquifers and interpreted water pathways
indicate interrelations with the ridge and furrows topography and thermokarst ponds at the surface of Dos Lenguas. The dotted
 lines show the depth of the basal layers at both front slopes, which roughly corresponds to the thickness of ice-rich permafrost in
 the tongues.

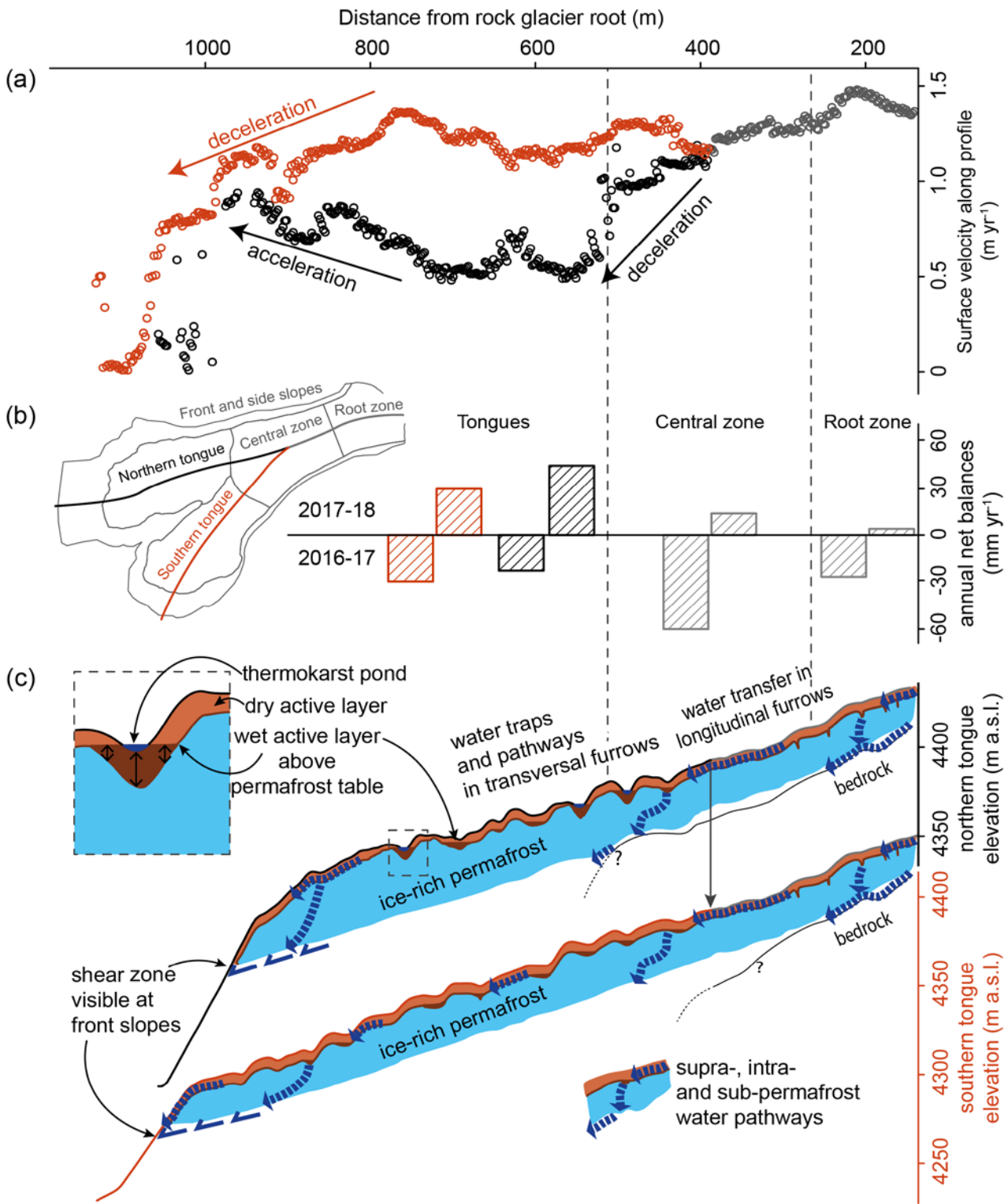


Fig. 10: (a) Spatial interrelation of horizontal surface velocities along the central flow line, (b) negative and positive interannual storage changes (net balance) in 2016–17 and 2017–18, respectively, and (c) longitudinal sketch profiles (not to scale) along the central flowline topographies (scaled) of the northern (black) and southern tongue (red) including potential internal hydrologic structure with water traps and pathways in the active layer, as well as potential intra- and sub-permafrost drainage pathways. Volumetric changes due to seasonal freezing and thawing at the interface of an ice-rich permafrost table and a wet active layer base could be locally enhanced by increased water [contents](#) where melt water is trapped in and along furrows e.g. thermokarst ponds (see inset).

1250